

**Functional renormalization group and the field theory of disordered elastic systems**

Pierre Le Doussal

*CNRS–Laboratoire de Physique Théorique de l’Ecole Normale Supérieure, 24 rue Lhomond, 75005 Paris, France*

Kay Jörg Wiese

*Kavli Institute of Theoretical Physics, University of California at Santa Barbara, Santa Barbara, California 93106-4030, USA*

Pascal Chauve

*CNRS–Laboratoire de Physique des Solides, Université de Paris–Sud, Bâtiment 510, 91405 Orsay, France*

(Received 23 June 2003; published 25 February 2004)

We study elastic systems, such as interfaces or lattices, pinned by quenched disorder. To escape triviality as a result of “dimensional reduction,” we use the functional renormalization group. Difficulties arise in the calculation of the renormalization group functions beyond one-loop order. Even worse, observables such as the two-point correlation function exhibit the same problem already at one-loop order. These difficulties are due to the nonanalyticity of the renormalized disorder correlator at zero temperature, which is inherent to the physics beyond the Larkin length, characterized by many metastable states. As a result, two-loop diagrams, which involve derivatives of the disorder correlator at the nonanalytic point, are naively “ambiguous.” We examine several routes out of this dilemma, which lead to a unique renormalizable field theory at two-loop order. It is also the only theory consistent with the potentiality of the problem. The  $\beta$  function differs from previous work and the one at depinning by novel “anomalous terms.” For interfaces and random-bond disorder we find a roughness exponent  $\zeta = 0.208\,298\,04\epsilon + 0.006\,858\epsilon^2$ ,  $\epsilon = 4 - d$ . For random-field disorder we find  $\zeta = \epsilon/3$  and compute universal amplitudes to order  $O(\epsilon^2)$ . For periodic systems we evaluate the universal amplitude of the two-point function. We also clarify the dependence of universal amplitudes on the boundary conditions at large scale. All predictions are in good agreement with numerical and exact results and are an improvement over one loop. Finally we calculate higher correlation functions, which turn out to be equivalent to those at depinning to leading order in  $\epsilon$ .

DOI: 10.1103/PhysRevE.69.026112

PACS number(s): 64.60.–i

**I. INTRODUCTION**

Elastic objects pinned by quenched disorder are central to the physics of disordered systems. In the last decades a considerable amount of research has been devoted to them. From the theory side they are among the simplest, but still quite nontrivial, models of glasses with complex energy landscape and many metastable states. They are related to a remarkably broad set of problems, from subsequences of random permutations in mathematics [1–3] and random matrices [4,5] to growth models [6–14] and Burgers turbulence in physics [15,16], as well as directed polymers [6,17] and optimization problems such as sequence alignment in biology [18–20]. Foremost, they are very useful models for numerous experimental systems, each with its specific features in a variety of situations. Interfaces in magnets [21,22] experience either short-range [random-bond (RB)] or long-range [random-field (RF)] disorder. Charge density waves (CDW’s) [23] or the Bragg glass in superconductors [24–28] are periodic objects pinned by disorder. The contact line of liquid helium meniscus on a rough substrate is governed by long-range (LR) elasticity [29–31]. All these systems can be parametrized by an  $N$ -component height or displacement field  $u_x$ , where  $x$  denotes the  $d$ -dimensional internal coordinate of the elastic object (we will use  $u_q$  to denote Fourier components). An interface in the three-dimensional (3D) random-field Ising model has  $d=2$ ,  $N=1$ , a vortex lattice  $d=3$ ,  $N=2$ , a contact line  $d=1$ , and  $N=1$ . The so-called

directed polymer ( $d=1$ ) has been much studied [32] as it maps onto the Kardar-Parisi-Zhang growth model [6] for any  $N$ . The equilibrium problem is defined by the partition function  $\mathcal{Z} = \int \mathcal{D}[u] \exp(-\mathcal{H}[u]/T)$  associated with the Hamiltonian

$$\mathcal{H}[u] = \int d^d x \frac{1}{2} (\nabla u)^2 + V(u_x, x), \quad (1.1)$$

which is the sum of an elastic energy which tends to suppress fluctuations away from the perfectly ordered state  $u=0$  and a random potential which enhances them. The resulting roughness exponent  $\zeta$ ,

$$\overline{[u(x) - u(x')]^2} \sim |x - x'|^{2\zeta}, \quad (1.2)$$

is measured in experiments for systems at equilibrium ( $\zeta_{\text{eq}}$ ) or driven by a force  $f$ . Here and below  $\langle \cdots \rangle$  denote thermal averages and  $\overline{(\cdots)}$  disorder ones. In some cases, long-range elasticity appears, e.g., for the contact line by integrating out the bulk degrees of freedom [31], corresponding to  $q^2 \rightarrow |q|$  in the elastic energy. As will become clear later, the random potential can without loss of generality be a chosen Gaussian with second cumulant,

$$\overline{V(u, x) V(u', x')} = R(u - u') \delta^d(x - x'), \quad (1.3)$$

with various forms: Periodic systems are described by a periodic function  $R(u)$ , random-bond disorder by a short-range function, and random-field disorder of variance  $\sigma$  by  $R(u) \sim -\sigma|u|$  at large  $u$ . Although this paper is devoted to equilibrium statics, some comparison with dynamics will be made and it is thus useful to indicate the equation of motion

$$\eta \partial_t u_{xt} = c \nabla_x^2 u_{xt} + F(x, u_{xt}) + f, \quad (1.4)$$

with friction  $\eta$ . The pinning force is  $F(u, x) = -\partial_u V(u, x)$  of correlator  $\Delta(u) = -R''(u)$  in the bare model.

Despite some significant progress, the model (1.1) has mostly resisted analytical treatment, and one often has to rely on numerics. Apart from the case of the directed polymer in  $1+1$  dimensions ( $d=1, N=1$ ), where a set of exact and rigorous results was obtained [2,5,33–35], analytical methods are scarce. Two main analytical methods exist at present, both interesting, but also with severe limitations. The first one is the replica Gaussian variational method (GVM) [36]. It is a mean-field method, which can be justified for  $N=\infty$  and relies on spontaneous replica symmetry breaking (RSB) [37,38]. Although useful as an approximation, its validity at finite  $N$  remains unclear. Indeed, it seems now generally accepted that RSB does not occur for low  $d$  and  $N$ . The remaining so-called weak RSB in excitations [39–41] may not be different from a more conventional droplet picture. Another exactly solvable mean-field limit is the directed polymer on the Cayley tree, which also mimics  $N \rightarrow \infty$ , and there too it is not fully clear how to meaningfully expand around that limit [42–44]. The second main analytical method is the functional renormalization group (FRG), which attempts a dimensional expansion around  $d=4$  [26,27,45–47]. The hope there is to include fluctuations, neglected in the mean-field approaches. However, until now this method has only been developed to one loop, for good reasons, as we discuss below. Its consistency has never been checked or tested in any calculation beyond one loop (i.e., lowest order in  $\epsilon=4-d$ ). Thus contrarily to pure interacting elastic systems (such as, e.g., polymers) *there is at present no quantitative method, such as a renormalizable field theory, which would allow one to compute accurately all universal observables in these systems.*

The central reason for these difficulties is the existence of many metastable states (i.e., local extrema) in these systems. Although qualitative arguments show that they arise beyond the Larkin length [48], these are hard to capture by conventional field theory methods. The best illustration of that is the so-called dimensional reduction (DR) phenomenon, which renders naive perturbation theory useless [21,49–53] in pinned elastic systems as well as in a wider class of disordered models (e.g., random-field spin models). Indeed it is shown that to *any* order in the disorder at zero temperature  $T=0$ , any physical observable is found to be *identical* to its (trivial) average in a Gaussian random force (Larkin) model, e.g.,  $\zeta = (4-d)/2$  for RB disorder. Thus perturbation theory appears (naively) unable to help in situations where there are many metastable states. The two above mentioned methods (GVM and FRG) are presently the only known ways to *escape dimensional reduction* and to obtain nontrivial values

for  $\zeta$  (in two different limits, but consistent when they can be compared [26,27,47]). The mean-field method accounts for metastable states by RSB. This however may go further than needed since it implies a large number of pure states [i.e., low- (free-) energy states differing by  $O(T)$  in (free) energy]. The other method, the FRG, captures metastability through a nonanalytic action with a cusp singularity. Both the RSB and cusp arise dynamically—i.e. spontaneously—in the limits studied.

The one-loop FRG has had some success in describing pinned systems. It was noted by Fisher [46] within a Wilson scheme analysis of the interface problem in  $d=4-\epsilon$  that the coarse-grained disorder correlator becomes *nonanalytic* beyond the Larkin scale  $L_c$ , yielding large-scale results distinct from naive perturbation theory. Within this approach an infinite set of operators becomes relevant in  $d < 4$ , parametrized by the second cumulant  $R(u)$  of the random potential. Explicit solution of the one-loop FRG for  $R(u)$  gives several nontrivial attractive fixed points (FP's) to  $O(\epsilon)$  proposed in [46] to describe RB, RF disorder and, in [26,27], periodic systems such as CDW's or vortex lattices. All these fixed points exhibit a “cusp” singularity as  $R^{*''}(u) - R^{*''}(0) \sim |u|$  at small  $|u|$ . The cusp was interpreted in terms of shocks in the renormalized force [54], familiar from the study of Burgers turbulence (for  $d=1, N=1$ ). The dynamical FRG was also developed to one loop [55–57] to describe the depinning transition. The mere existence of a nonzero critical threshold force  $f_c \sim |\Delta'(0^+)| > 0$  is a direct consequence of the cusp [it vanishes for an analytic force correlator  $\Delta(u)$ ]. Extension to nonzero temperature  $T > 0$  suggested that the cusp is rounded within a thermal boundary layer  $u \sim TL^{-\theta}$ . This was interpreted to describe thermal activation and leads to a reasonable derivation of the celebrated creep law for activated motion [58,59].

In standard critical phenomena a successful one-loop calculation usually quickly opens the way for higher-loop computations, allowing for accurate calculation of universal observables and comparison with simulations and experiments and, eventually, a proof of renormalizability. In the present context, however, no such work has appeared in the last 15 years since the initial proposal of [46], a striking sign of the high difficulties which remain. Only recently a two-loop calculation was performed [60,61], but since this study is confined to an analytic  $R(u)$ , it only applies below the Larkin length and does not consistently address the true large-scale critical behavior. In fact, doubts were even raised [47] about the validity of the  $\epsilon$  expansion beyond order  $\epsilon$ .

It is thus crucial to construct a renormalizable field theory which describes statics and depinning of disordered elastic systems and which allows for a systematic expansion in  $\epsilon = 4-d$ . As long as this is not achieved, the physical meaning and validity of the one-loop approximation does not stand on solid ground and thus, legitimately, may itself be called into question. Indeed, despite its successes, the one-loop approach has obvious weaknesses. One example is that the FRG flow equations for the equilibrium statics and for depinning are identical, while it is clear that these are two vastly different physical phenomena, depinning being irreversible. Also, the detailed mechanism by which the system

escapes dimensional reduction in both cases is not really elucidated. Finally, there exists no convincing scheme to compute correlations, and in fact no calculation of higher than two-point correlations has been performed.

Another motivation to investigate the FRG is that it should apply to other disordered systems, such as random-field spin models and quantum elastic systems, where dimensional reduction also occurs and progress has been slow [45,62–67]. Insight into model (1.1) will thus certainly lead to progresses in a broader class of disordered systems.

In this paper we construct a renormalizable field theory for the statics of disordered elastic systems beyond one loop. The main difficulty is the nonanalytic nature of the theory (i.e., of the fixed-point effective action) at  $T=0$ . This makes it *a priori* quite different from conventional field theories for pure systems. We find that the two-loop diagrams are naively “ambiguous,” i.e., it is not obvious how to assign a value to them. We want to emphasize that this difficulty already exists at one loop; e.g., *even the simplest one-loop correction to the two-point function is naively “ambiguous.”* Thus it is not a mere curiosity, but a fundamental problem with the theory, “swept under the rug” in all previous studies, but which becomes unavoidable to confront at two-loop order. It originates from the metastability inherent in the problem. For the related theory of the depinning transition, we have shown in companion papers [68,69] how to surmount this problem and we constructed a two-loop renormalizable field theory *from first principles*. There, all ambiguities are naturally lifted using the known exact property that the manifold only moves forward in the slowly moving steady state. Unfortunately in the statics there is no such helpful property and the ambiguity problem is even more arduous. Here we examine the possible ways of curing these difficulties. We find that the natural physical requirements—i.e., that the theory should be (i) *renormalizable* (i.e., that a universal continuum limit exists independent of short-scale details), (ii) that the renormalized force should remain *potential*, and (iii) that no stronger singularity than the cusp in  $R''(u)$  should appear to two loop (i.e., *no “supercusp”*)—are rather restrictive and constrain possible choices. We then propose a theory which satisfies all these physical requirements and is consistent to two loops. The resulting  $\beta$  function differs from the one derived in previous studies [60,61] by novel static “anomalous terms.” These are different from the dynamical “anomalous terms” obtained in [68–70] showing that indeed depinning and statics differ at two loop, fulfilling another physical requirement.

We then study the fixed points describing several universality classes—i.e., the interface with RB and RF disorder, the random periodic problem, and the case of LR elasticity. We obtain the  $O(\epsilon^2)$  corrections to several universal quantities. The prediction for the roughness exponent  $\zeta$  for random-bond disorder has the correct sign and order of magnitude to notably improve the precision as compared to numerics in  $d=3,2$  and to match the exact result  $\zeta=2/3$  in  $d=1$ . For random-field disorder we find  $\zeta=\epsilon/3$ , which, for equilibrium, is likely to hold to all orders. By contrast, nontrivial corrections of order  $O(\epsilon^2)$  were found for depinning [68,69]. The amplitude, which in that case is a universal function of the random-field strength, is computed and it is found that

the two-loop result also improves the agreement as compared to the exact result known [71] for  $d=0$ . For the periodic CDW case we compare with the numerical simulations in  $d=3$  and obtain reasonable agreement. Some of the results of this paper were briefly described in a short version [68] and agree with a companion study using an exact RG [72,73].

Since the physical results also seem to favor this theory, we then look for better methods to justify the various assumptions. We found several methods which allow us to lift ambiguities and all yield consistent answers. A detailed discussion of these methods is given. In particular, we find that correlation functions can be unambiguously defined in the limit of a small background field which splits apart quasidegenerate states when they occur. This is very similar to what was found in a related study where we obtained the exact solution of the FRG in the large- $N$  limit [74]. Finally, the methods introduced here will be used and developed further to obtain a renormalizable theory to three loops and compute its  $\beta$  function in [75]. Let us mention that a first-principles method which avoids ambiguities is to study the system at  $T>0$ . However, this turns out to be highly involved. It is attempted via an exact RG in [72] and studied more recently in [76,77] where a field theory of thermal droplet excitation was constructed. A short account of our work has appeared in [68], and a short pedagogical introduction is given in [78,79].

The outline of this paper is as follows. In Sec. II we explain in a detailed and pedagogical way the perturbation theory and the power counting. In Sec. III we compute the one-loop (Sec. III A) and two-loop (Sec. III B) corrections to the disorder. The calculation of the repeated one-loop counterterm is given in Sec. III C. In Sec. III D we identify the values for ambiguous graphs. This yields a renormalizable theory with a finite  $\beta$  function, which is potential and free of a supercusp. The more systematic discussion of these ambiguities is postponed to Sec. V. We derive the  $\beta$  function and in Sec. IV present physical results, exponents, and universal amplitudes to  $O(\epsilon^2)$ . Some of these quantities are new and have not yet been tested numerically. In Sec. V we enumerate all the methods which aim at lifting ambiguities and explain in detail several of them, which gave consistent results. In Sec. VI we detail the proper definition and calculation of correlation functions. In Appendixes A and B we present two methods which seem promising, but *do not* work, in order to illustrate the difficulties of the problem. In Appendix F we present a summary of all one- and two-loop corrections including finite temperature. In Appendix D we give details of calculations for what we call the sloop elimination method.

The reader interested in the results can skip Secs. II and III and go directly to Sec. IV. The reader interested in a detailed discussion of the problems arising in this field theory should read Sec. V.

## II. MODEL AND PERTURBATION THEORY

### A. Replicated action and effective action

We study the static equilibrium problem using replicas—i.e., consider the partition sum in the presence of sources:

$$\mathcal{Z}[j] = \int \prod_a \mathcal{D}[u_a] \exp\left(-\mathcal{S}[u] + \int_x \sum_a j_x^a u_x^a\right), \quad (2.1)$$

from which all static observables can be obtained. The action  $\mathcal{S}$  and replicated Hamiltonian corresponding to Eq. (1.1) are

$$\begin{aligned} \mathcal{S}[u] &= \frac{\mathcal{H}[u]}{T} = \frac{1}{2T} \int_x \sum_a [(\nabla u_x^a)^2 + m^2 u_x^a] \\ &\quad - \frac{1}{2T^2} \int_x \sum_{ab} R(u_x^a - u_x^b). \end{aligned} \quad (2.2)$$

$a$  runs from 1 to  $n$  and the limit of zero number of replicas  $n=0$  is implicit everywhere. We have added a small mass which confines the interface inside a quadratic well and provides an infrared cutoff. We are interested in the large-scale limit  $m \rightarrow 0$ . We will denote

$$\int_q := \int \frac{d^d q}{(2\pi)^d}, \quad (2.3)$$

$$\int_x := \int d^d x. \quad (2.4)$$

For periodic systems the integration is over the first Brillouin zone. A short-scale UV cutoff is implied at  $q \sim \Lambda$ , but for actual calculations we find it more convenient to use dimensional regularization. We also consider the effective action functional  $\Gamma[u]$  associated with  $\mathcal{S}$ . It is, as we recall [80,81], the Legendre transform of the generating function of connected correlations  $\mathcal{W}[j] = \ln \mathcal{Z}[j]$ , thus defined by eliminating  $j$  in  $\Gamma[u] = ju - \mathcal{W}[j]$ ,  $\mathcal{W}[j] = u$ .

If we had chosen non-Gaussian disorder, additional terms with free sums over  $p$  replicas (called  $p$ -replica terms) corresponding to higher cumulants of disorder would be present in Eq. (2.2), together with a factor of  $1/T^p$ . These terms are generated in the perturbation expansion; i.e., they are present in  $\Gamma[u]$ . We do not include them in Eq. (2.2) because, as we will see below, these higher-disorder cumulants are not relevant within (conventional) power counting, so for now we ignore them. The temperature  $T$  appears explicitly in the replicated action (2.2), although we will focus on the  $T=0$  limit.

Because the disorder distribution is translation invariant, the disorder term in the above action is invariant under the so-called statistical tilt symmetry [17,82] (STS)—i.e., the shift  $u_x^a \rightarrow u_x^a + g_x$ . One implication of STS is that the one-replica replica part of the action [i.e., the first line of Eq. (2.2)] is uncorrected by disorder; i.e., it is the same in  $\Gamma[u]$  and  $\mathcal{S}[u]$  [83]. Since the elastic coefficient is not renormalized, we have set it to unity.

### B. Diagrammatics, definitions

We first study perturbation theory, its graphical representation, and power counting. Everywhere in the paper we denote the exact two-point correlation by  $C_{ab}(x-y)$ , i.e., in Fourier terms

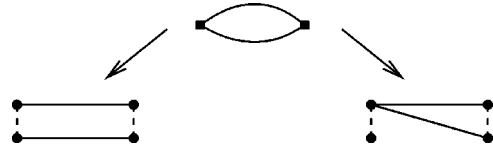


FIG. 1. Each diagram with unsplit vertices contains several diagrams with split vertices: here the one-loop unsplit diagram (top) generates three possible topologically distinct split diagrams, two (shown here, bottom) are two-replica terms, the third one—i.e., (a) in Fig. 2—is a three-replica term.

$$\langle u_q^a u_{q'}^b \rangle = (2\pi)^d \delta^d(q+q') C_{ab}(q), \quad (2.5)$$

while the free correlation function (from the elastic term) used for perturbation theory in the disorder is denoted by  $G_{ab}(x-y) = \delta_{ab} G(x-y)$  and reads, in Fourier representation,

$$\langle u_q^a u_{q'}^b \rangle_0 = (2\pi)^d \delta^d(q+q') G_{ab}(q), \quad (2.6)$$

$$G_{ab}(q) = \frac{T}{q^2 + m^2} \delta_{ab}, \quad (2.7)$$

which is represented graphically by a line

$$a \text{---} b = \frac{T \delta_{ab}}{q^2 + m^2}. \quad (2.8)$$

Each propagator thus carries one factor of  $G(q) = T/(q^2 + m^2)$ . Each disorder interaction vertex comes with a factor of  $1/T^2$  and gives one momentum conservation rule. Since each disorder vertex is a function, an arbitrary number of lines can come out of it.  $k$  lines coming out of a vertex result in  $k$  derivatives  $R^{(k)}$  after Wick contractions

$$\star = R^{(k)}. \quad (2.9)$$

Since each disorder vertex contains two replicas, it is sometimes convenient to use “split vertices” rather than “unsplit ones.” Thus we call “vertex” an unsplit vertex and we call a “point” the half of a vertex:

$$a \bullet \quad b \bullet = \sum_{ab} \frac{R(u_a - u_b)}{2T^2}. \quad (2.10)$$

Each unsplit diagram thus gives rise to several split diagrams, as illustrated in Fig. 1

One can define the number of connected components in a graph with split vertices. Since each propagator identifies two replicas, a  $p$ -replica term contains  $p$  connected components. When the two points of a vertex are connected, this vertex is said to be “saturated.” It gives a derivative evaluated at zero  $R^{(k)}(0)$ . Standard momentum loops are loops with respect to unsplit vertices, while we call “sloops” the loops with respect to points (in split diagrams). This is illustrated in Fig. 2 The momentum one- and two-loop diagrams which correct the disorder at  $T=0$  are shown in Fig. 3 (unsplit vertices). There are three types of two-loop graphs  $A, B,$

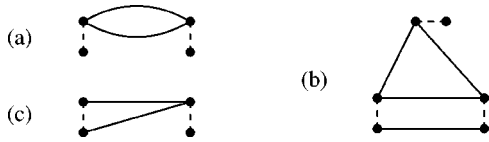


FIG. 2. Graphs (a) (a one-loop diagram) and (b) (a two-loop diagram) each contains three connected components. Since each contain one “sloop,” they are both three-replica terms proportional to  $T$ . The left vertex on diagram (c) is “saturated:” replica indices are constrained to be equal and thus the diagram does not depend on the left space point.

and  $C$ . Since they have two vertices (a factor  $R/T^2$  each) and three propagators (a factor of  $T$  each), graphs  $E$  and  $F$  lead to corrections to  $R$  proportional to temperature and will not be studied here (see, however, Appendix F).

It is important to distinguish between *fully saturated (FS) diagrams* and *functional diagrams*. The FS diagrams are those needed for a full average—e.g., a correlation function. There all fields are contracted and one is only left with the space dependence. These are the standard diagrams in more conventional polynomial field theories such as  $\phi^4$ . Then all vertices are evaluated at  $u=0$ , yielding products of derivatives  $R^{(k)}(0)$ . These are also the graphs which come in the standard expansion of  $\Gamma[u]$  in powers of  $u$  which generate the “proper” or “renormalized” vertices—i.e., the sum over all one-particle irreducible graphs with some external legs—from which all correlations can be obtained. Note that in the fully saturated diagrams there can be no free point: all points in a vertex have to be connected to some propagator (and to some external replica). Otherwise, there is a free replica sum yielding a factor of  $n$  and a vanishing contribution in the limit of  $n=0$ .

However, since we have to deal with a function  $R(u)$ , we will more often consider functional diagrams. A functional diagram still depends on the field  $u$ . It can depend on  $u$  at several points in space (multilocal term), as, for example,

$$\begin{array}{c} \bullet \\ \vdots \\ \text{---} \\ \bullet \end{array} \begin{array}{c} \bullet \\ \vdots \\ \text{---} \\ \bullet \end{array} \begin{array}{c} \bullet \\ \vdots \\ \text{---} \\ \bullet \end{array} \sim \sum_{abc} \frac{R'(u_x^a - u_x^b)}{2T^2} \frac{R'(u_y^a - u_y^c)}{2T^2} TG(x - y). \quad (2.11)$$

Such a graph with  $p$  connected components corresponds to a  $p$ -replica functional term. Or it can represent the projection of such a term onto a local part, as arises in the standard operator product expansion (OPE):

$$\begin{array}{c} \bullet \\ \vdots \\ \text{---} \\ \bullet \end{array} \begin{array}{c} \bullet \\ \vdots \\ \text{---} \\ \bullet \end{array} \sim \sum_{abc} \frac{R'(u_x^a - u_x^b)}{2T^2} \frac{R'(u_x^a - u_x^c)}{2T^2} T \int_y G(x - y). \quad (2.12)$$

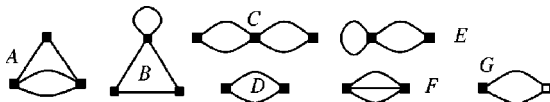


FIG. 3. Unsplit diagrams to one loop  $D$ , one loop with inserted one-loop counterterm  $G$ , and two-loop diagrams  $A$ ,  $B$ ,  $C$ ,  $E$ , and  $F$ .

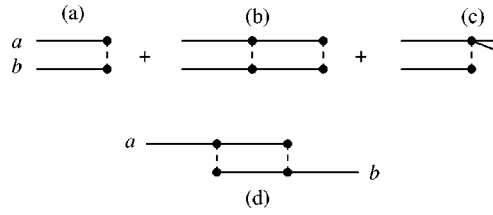


FIG. 4. Calculation of the two-point function for analytic  $R(u)$ . Due to DR, only the first diagram (a) survives. Diagrams (b) and (c) cancel because by shifting the line one gets a minus sign. Diagram (c) is proportional to  $R'''(0)^2$  and vanishes in an analytic theory. Similar cancellations occur to all orders.

Typically, using functional diagrams, we want to compute the effective action functional  $\Gamma[u]$  or its local part—i.e., its value for a spatially uniform mode  $u_x^a = u^a$ , which includes the corrections to disorder. Specifying the two replicas on each connected component, one example of a one-particle irreducible diagram producing corrections to disorder is

$$\begin{array}{c} \bullet \\ \vdots \\ \text{---} \\ \bullet \end{array} \begin{array}{c} \bullet \\ \vdots \\ \text{---} \\ \bullet \end{array} \sim \frac{T^2}{T^4} R''(u^a - u^b) R''(u^a - u^b) \int_q G(q)^2. \quad (2.13)$$

The complete analysis of these corrections will be made in Sec. III. Finally, note that functional diagrams may contain saturated vertices, whose space and field dependence disappears [such as (c) in Fig. 2] and that the limit  $n \rightarrow 0$  does not produce constraints. An example is the calculation of  $\Gamma[u]$  since one can always attach additional external legs to any point by taking a derivative with respect to the field  $u$ .

**C. Dimensional reduction**

If we consider fully saturated diagrams and analytic  $R(u)$ , we find trivial results. This is because at  $T=0$  the model exhibits the property of DR [21,49–53] both in the statics and dynamics. Its “naive” perturbation theory, obtained by taking for the disorder correlator  $R(u)$  an *analytic function* of  $u$ , has a triviality property. As is easy to show using the above diagrammatic rules (see a typical cancellation due to the “mounting” construction in Fig. 4: see also Appendix D in Ref. [72]), the perturbative expansion of any correlation function  $\langle \Pi_i u_{x_i}^{a_i} \rangle_S$  (of any *analytic* observable) in the derivatives  $R^{(k)}(0)$  yields to all orders the same result as that obtained from the Gaussian theory setting  $R(u) \equiv R''(0)u^2/2$  (the so-called Larkin random-force model). The two-point function thus reads, to all orders,

$$C(q)_{ab}^{\text{DR}} = \frac{-R''(0)}{(q^2 + m^2)^2} \quad (2.14)$$

(at  $T=0$  correlations are independent of the replica indices  $a_i$ ). This dimensional reduction results in a roughness exponent  $\zeta = (4 - d)/2$ , which is well known to be incorrect. One physical reason is that this  $T=0$  perturbation theory amounts to solving in perturbation the zero-force equation

$$(-\nabla^2 + m^2)u + F(x, u) = 0. \quad (2.15)$$

This, whenever more than one solution exists (which certainly happens for small  $m$ ), is clearly not identical to finding

the lowest-energy configuration.<sup>1</sup> Curing this problem within the field theory, is highly nontrivial. Coarse graining within the FRG up to a scale at which the renormalized disorder correlator  $R(u)$  becomes *nonanalytic* (which includes some of the physics of multiple extrema) is one possible route, although understanding exactly how this cures the problem within the field theory is a difficult open problem.

It is important to note that dimensional reduction is not the end of perturbation theory, since saturated diagrams remain nontrivial at finite temperature, so one way out is to study  $T > 0$ . This is not the route chosen here: instead, we will attempt to work at  $T = 0$  with a nonanalytic action and focus on functional diagrams which remain nontrivial.

#### D. Power counting

Let us now consider power counting. Let us recall the conventional analysis within, e.g., the Wilson scheme [46,47]. The elastic term is invariant under  $x \rightarrow bx$ ,  $u \rightarrow b^\zeta u$ , and  $T \rightarrow b^\theta T$ , with  $\theta = d - 2 + 2\zeta$ . Here  $\zeta$  is for now undetermined. Under this transformation the disorder function  $R$  is multiplied by  $b^{d-2\theta} = b^{4-d+2\zeta}$ . It becomes relevant for  $d < 4$ , provided  $\zeta < (4-d)/2$ , which is physically expected [for instance, in the random periodic case,  $\zeta = 0$  is the only possible choice and for other cases  $\zeta = O(\epsilon)$ ]. The re-scaled dimensionless temperature term scales as  $-m\partial_m \tilde{T} = -\theta \tilde{T}$  (see below) and is formally irrelevant near four dimension. In the end  $\zeta$  will be fixed by the disorder distribution at the fixed point.

To be more precise, we want to determine in the field-theoretic framework the necessary counterterms to render the theory UV finite as  $d \rightarrow 4$ . The study of superficial divergences usually involves examining the irreducible vertex functions (IVF):

$$\Gamma_{u \dots u}(q_i) = \prod_{i=1}^{E_u} \frac{\delta}{\delta u_{q_i}} \Gamma[u] \Big|_{u=0}, \quad (2.16)$$

with  $E_u$  external fields  $u$  (at momenta  $q_i$ ,  $i = 1, \dots, E_u$ ). The perturbation expansion of a given IVF to any given order in the disorder is represented by a set of one-particle irreducible (1PI) graphs (in unsplit diagrammatics). Being the derivative of the effective action, they are the important physical objects since all averages of products of fields  $u$  can be expressed as tree diagrams of the IVF. Finiteness of the IVF thus implies finiteness of all such averages.

However, since  $\Gamma[u]$  is nonanalytic in some directions (e.g., for a uniform mode  $u_x^a = u^a$ ), derivatives such as Eq. (2.16) may not exist at  $q = 0$ , and we have to be more general

<sup>1</sup>One can easily see that the DR result (2.14) arises if one averages over multiple solutions  $u_\alpha$  with some random weights  $W_\alpha \sim |\det[\nabla^2 + m^2 + F'_u(x, u_\alpha)]|$  (then using the representation of the delta function  $\exp\{i \int_x \tilde{u} [(-\nabla^2 + m^2)u + F(x, u)]\}$  and averaging over disorder using Eq. (1.3)). Summing over multiple solutions  $u_\alpha$  requires instead to include the crucial weight  $\exp[-\beta H(u_\alpha)]$  in order to select the true ground state.

and consider *functional diagrams*. The (disorder part of the) effective action is the sum of  $k$ -replica terms, denoted  $\Gamma_k[u]$ :

$$\Gamma[u] = \sum_{k \geq 2} T^{-k} \Gamma_k[u]. \quad (2.17)$$

Each  $\Gamma_k[u]$  is the sum over 1PI graphs with  $k$  connected components (using split vertices) and itself depends on  $T$  as

$$\Gamma_k[u] = \sum_{l \geq 0} T^l \Gamma_{k,l}[u], \quad (2.18)$$

where  $l$  is the number of sloops. Thus at  $T = 0$  there are no sloops and  $\Gamma_k[u] = \Gamma_{k,l=0}[u]$  is the sum over 1 PI *tree* graphs with  $k$  connected components (trees in replica space, not position space).

Let us compute the superficial degree of UV divergence  $\delta$  of a functional graph entering the expansion of the local part of the effective action. We denote  $v$  the number of unsplit disorder vertices,  $I$  the number of internal lines (propagators),  $L$  the number of loops, and  $l$  the number of sloops. One has the relations

$$2v + l = k + I, \quad (2.19)$$

$$v + L = 1 + I. \quad (2.20)$$

The total factors of  $T$  are  $T^{l-2v} = T^{l-k}$ . At  $T = 0$  ( $l = 0$ ) the superficial degree of UV divergence is thus

$$\delta = dL - 2I = d - k(d-2) + (d-4)v. \quad (2.21)$$

Thus in  $d = 4$  the only graphs with positive superficial degrees of divergence are for  $k = 1$  (quadratic  $\sim \Lambda^2$ ) and  $k = 2$  (logarithmic divergence). Here  $k = 1$  corresponds to a constant in the free energy. Because of STS, all single-replica terms are uncorrected and there is no wave-function renormalization in this model.

Thus to renormalize the  $T = 0$  theory we need *a priori* to look only at graphs with  $p = 2$  connected components, which by definition are those correcting the second cumulant  $R(u)$ , compute their divergent parts, and construct the proper counterterm to the function  $R(u)$ . As mentioned above, higher cumulants are irrelevant by power counting and are superficially UV finite. The graphs which contribute to the two-replica part  $\Gamma_2[u]$  have  $L$  loops with  $L = 1 + v + l$ . At zero temperature,  $l = 0$ : thus,  $L = 1 + v$ . The loop expansion thus corresponds to the expansion in power of  $R(u)$  and, as we will see below, to an  $\epsilon$  expansion. More generally, using the above relation one, has, schematically,

$$\Gamma_{k,l}[u] = \sum_{L \geq \max(1, 2+l-k)} \partial_u^{(4L-4+2k-2l)} R^{(L-1+k-l)}, \quad (2.22)$$

where the number of internal lines gives the total number of derivatives acting on an argument  $u$  of the functions  $R$ . For instance, the two-replica part at  $T = 0$  is a sum over  $L$ -loop graphs of the type

$$\Gamma_{k=2,l=0}[u] = \sum_{L \geq 1} \partial_u^{4L} R^{L+1}. \quad (2.23)$$

If one now considers  $T > 0$ , one finds that  $\delta = d - k(d-2) + (d-4)v + (d-2)l$ . Each additional power of  $T$  yields an additional quadratic divergence, more generally a factor of  $T\Lambda^{d-2}$ . Thus to obtain a theory where observables are finite as  $\Lambda \rightarrow \infty$  one must start from a model where the initial temperature scales with the UV cutoff as

$$T = \hat{T} \Lambda^{2-d}. \quad (2.24)$$

This is similar to  $\phi^4$  theory where it is known that a  $\phi^6$  term can be present and yields a finite UV limit (i.e., does not spoil renormalizability) only if it has the form  $g_6 \phi^6 / \Lambda^{d-2}$ . Such a term, with precisely this cutoff dependence, is in fact usually present in the starting bare model—e.g., in lattice spin models. It then produces only a finite shift to  $g_4$  without changing universal properties.<sup>2</sup> Here each factor of  $\hat{T}$  comes with a factor of  $\Lambda^{2-d}$  which compensates the UV divergence from the graph. Thus the finite- $T$  theory may also be renormalizable. Computing the resulting shift in  $R(u)$  to order  $R^2$  by resumming the diagrams  $E$  and  $F$  of Fig. 3 and all similar diagrams to any number of loops has not been attempted here (see, however, Appendix F). The “finite shift” here is, however, much less innocuous than in  $\phi^4$  theory since it smoothes the cusp. The effects of a nonzero temperature are explored in [74,76,77,84].

One can use the freedom to rescale  $u$  by  $m^{-\zeta}$ . The dimensionless temperature  $\tilde{T} = Tm^\theta$  is then defined. The disorder term in  $\Gamma[u]$  is then as in Eq. (2.2) with  $R(u)$  replaced by  $m^{\epsilon-4\zeta} \tilde{R}(um^\zeta)$  in terms of a dimensionless rescaled function  $\tilde{R}$  of a dimensionless rescaled argument. This will be further discussed below.

### III. RENORMALIZATION PROGRAM

In this section we compute the effective action to two-loop order at  $T=0$ . We are only interested in the part which contains UV divergences as  $d \rightarrow 4$ . We know from the analysis of the last section that we only need to consider the local  $k=2$  two-replica part—i.e., the corrections to  $R(u)$ . These  $L=1$  and  $L=2$  loop corrections contain  $v=L+1$  vertices. Higher  $v$  yields a higher number of replicas.

#### A. One-loop corrections to disorder

To one loop at  $T=0$  there is only one unsplit diagram  $v=2$ , corresponding to two split diagrams (a) and (b) as indicated in Fig. 5. Both come with a combinatorial factor of  $1/2!$  from Taylor-expanding the exponential function and  $1/2$  from the action. (a) has a combinatoric factor of 2 and (b) of 4. Together, they add up to the one-loop correction to disorder:

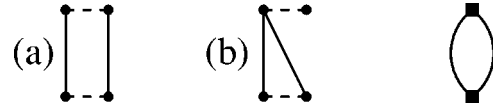


FIG. 5. The two one-loop diagrams with split vertices and the corresponding diagram with standard (i.e., unsplit) vertices.

$$\delta^1 R(u) = \left[ \frac{1}{2} R''(u)^2 - R''(0) R''(u) \right] I_1, \quad (3.1)$$

$$\begin{aligned} I_1^m = I_1 &:= \int_q \frac{1}{(q^2 + m^2)^2} \\ &= \Gamma \left( 2 - \frac{d}{2} \right) m^{-\epsilon} \int_q e^{-q^2} \\ &= \frac{1}{(4\pi)^{d/2}} \Gamma \left( 2 - \frac{d}{2} \right) m^{-\epsilon} \\ &= O \left( \frac{1}{\epsilon} \right). \end{aligned} \quad (3.2)$$

Note that (b) has a saturated vertex, hence the factor  $R''(0)$ . This does not lead to ambiguities in the one-loop  $\beta$  function, since the FRG to one loop yields a discontinuity only in the third derivative and  $R''(u)$  remains continuous.

#### B. Two-loop corrections to disorder

There are only three graphs correcting disorder at  $T=0$  with  $L=2$  loops and  $v=3$  vertices. They are denoted  $A$ ,  $B$ , and  $C$  (see Fig. 6), and we will examine each of them.

We begin our analysis with class  $A$ .

##### 1. Class A

The possible diagrams with split vertices of type  $A$  are diagrams (a)–(f) given in Fig. 7. The resulting correction to  $R(u)$  is written as

$$\begin{aligned} \delta^2 R(u) &= \frac{1}{3!} \frac{2}{2^3} 3(2^3) \sum (a+b+c+d+e+f) \\ &= \sum (a+b+c+d+e+f), \end{aligned} \quad (3.3)$$

where the combinatorial factors are  $1/3!$  from the Taylor expansion of the exponential function,  $2/2^3$  from the explicit factors of  $1/2$  in the interaction, a factor of 3 to chose the vertex at the top of the hat, and a factor of 2 for the possible two choices in each of the vertices. Furthermore, below some additional combinatorial factors are given: a factor of 2 for

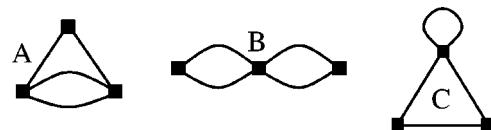


FIG. 6. The three possible two-loop unsplit graphs correcting disorder at  $T=0$ .

<sup>2</sup>We thank E. Brezin for a discussion on this point.

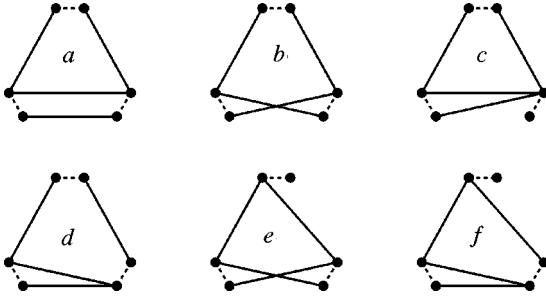


FIG. 7. Graphs at two-loop order in the form of a hat (class A in Sec. III B 1) contributing to two-replica terms.

generic graphs and 1 if it has the mirror symmetry with respect to the vertical axis. Each diagram symbol denotes the diagram including the symmetry factor. The first two graphs are

$$a = -R''(0)R'''(u)^2 I_A, \quad (3.4)$$

$$b = R''(u)R'''(u)^2 I_A. \quad (3.5)$$

To obtain the sign one can choose an ‘‘orientation’’ in each vertex ( $u_a - u_b$ ); the final result does not depend on the choice. The minus sign in  $a$  comes because the two legs enter on opposite points in the top vertex. Define the two-loop momentum integral (see Appendix A in Ref. [69])

$$I_A := \int_{q_1} \int_{q_2} \frac{1}{q_1^2 + m^2} \frac{1}{q_2^2 + m^2} \frac{1}{[(q_1 + q_2)^2 + m^2]^2} \\ = \left( \frac{1}{2\epsilon^2} + \frac{1}{4\epsilon} + O(\epsilon^2) \right) (\epsilon I_1)^2. \quad (3.6)$$

Graphs  $a$  and  $b$  are nonambiguous. They are the only contributions in an analytic theory. The other graphs are

$$c = 2\lambda_c R'''(0)R''(0)R'''(u)I_A, \quad (3.7)$$

$$d = 2\lambda_d R'''(0)R''(u)R'''(u)I_A, \quad (3.8)$$

$$e = -\lambda_e (R'''(0+))^2 R''(u)I_A, \quad (3.9)$$

$$f = 2\lambda_f R'''(0)^2 R''(u)I_A, \quad (3.10)$$

and vanish if  $R(u)$  is analytic [since then  $R'''(0)=0$ ], but *a priori* should be considered when  $R(u)$  is nonanalytic. We have indicated their ‘‘natural’’ sign and amplitude (e.g., symmetry factor setting  $\lambda_i=1$ ), but have introduced factors  $\lambda_i$  to recall that they are *ambiguous*: since  $R'''(0^+) = -R'''(0^-)$ , one is confronted with a choice each time one saturates a vertex and there is no obvious way to choose the sign at this stage. We recall that we have defined *saturated* vertices as vertices evaluated at  $u=0$ , while *unsaturated* vertices still contain  $u$  and do not lead to ambiguities.

At this stage we will not discuss in detail how to give a definite values to these contributions to disorder. This will be done in Sec. V. We will just use the most reasonable assumptions, which will be reevaluated and justified later. A natural step is to set

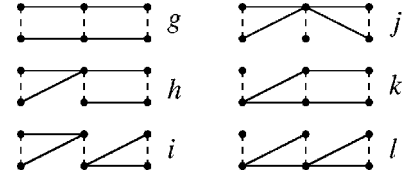


FIG. 8. Two-loop diagrams of class B.

$$c = d = 0, \quad (3.11)$$

since these graphs cannot correct  $R(u)$  as they are *odd* functions of  $u$ , which yields no contribution when inserted into the action  $\sum_{ab} R(u_a - u_b)$ .

## 2. Class B

We now turn to graphs of type *B* (bubble diagrams),  $g-l$  represented in Fig. 8. We use the same convention as in Eq. (3.3) and start with the combinatorics. There are three ways to choose the vertex in the middle. Upon splitting the vertices, for  $i$  and  $j$  there are only two choices at the middle vertex, whereas for  $g$  there are four choices. There are also four choices for  $h$ ,  $k$ , and  $l$ . There one must also choose the rightmost vertex, leading to an extra factor of 2. The final result is

$$g = \frac{1}{2} R''(u)^2 R'''(u) I_1^2, \quad (3.12)$$

$$h = -R''(u)R'''(u)R''(0) I_1^2, \quad (3.13)$$

$$i = j = \frac{1}{4} R'''(u)R''(0)^2 I_1^2, \quad (3.14)$$

$$k = -\lambda_k R''(u)R''(0)R'''(0) I_1^2, \quad (3.15)$$

$$l = \lambda_l R''(u)R''(0)R'''(0) I_1^2. \quad (3.16)$$

Only  $k$  and  $l$  are ambiguous, but it is also natural to set

$$k + l = 0, \quad (3.17)$$

which we do for now and discuss later.

## 3. Class C

Diagrams  $m$ ,  $n$ ,  $p$ , and  $q$  of class *C* are represented in Fig. 9:

$$m = c_1 \lambda_m R''(0)R'''(0)R''(u) I_t I_T, \quad (3.18)$$

$$n = -c_1 \lambda_n R''(0)R'''(0)R''(u) I_t I_T, \quad (3.19)$$

$$p = c_2 \lambda_p R'''(0)R''(u)^2 I_t I_T, \quad (3.20)$$

$$q = -c_2 \lambda_q R'''(0)R''(u)^2 I_t I_T, \quad (3.21)$$

with

$$I_t = \int \frac{1}{q^2 + m^2}, \quad (3.22)$$



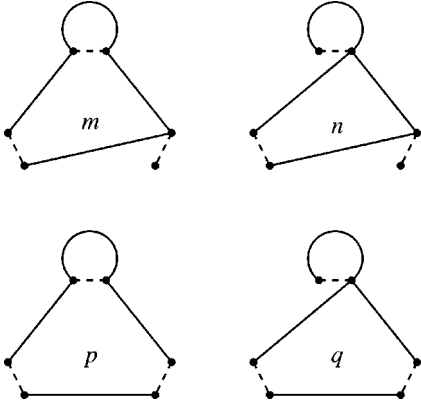


FIG. 9. Two-loop diagrams of class C.

$$I_T = \int_q \frac{1}{(q^2 + m^2)^3}. \quad (3.23)$$

There it is natural to assume

$$m + n = 0, \quad (3.24)$$

$$p + q = 0, \quad (3.25)$$

which we do for now and discuss it later. This leaves no correction to disorder from graphs C, as is the case for depinning [69]. This is fortunate, since the integral  $I_t$  has a quadratic UV divergence in  $d=4$ , while  $I_T$  is UV finite. Physically, it is unlikely that these could enter physical observables as the tadpole divergence can usually be eliminated by proper field reordering (normal ordering) or vacuum subtraction.

To summarize, for the equilibrium statics at  $T=0$  in perturbation of  $R \equiv R(u)$ , the contributions to the disorder to one and two loops—i.e., the corresponding terms in the effective action  $\Gamma[u, \hat{u}]$ —are

$$\delta^1 R(u) = \left[ \frac{1}{2} R''(u)^2 - R''(0) R''(u) \right] I_1, \quad (3.26)$$

$$\begin{aligned} \delta^2 R(u) = & \{ R'''(u)^2 [R''(u) - R''(0)] \} I_A \\ & + \frac{1}{2} \{ [R''(u) - R''(0)]^2 R'''(u) \} I_1^2 \\ & - \lambda R'''(0^+) R''(u) I_A. \end{aligned} \quad (3.27)$$

We have allowed for a yet undetermined constant  $\lambda = \lambda_e - 2\lambda_f$ . We now show that requiring renormalizability allows us to fix  $\lambda$ .

### C. Renormalization method to two loops and calculation of counterterms

Let us now recall the method, also used in our study of depinning [69], to renormalize a theory where the interaction is not a single coupling constant, but a whole function, the disorder correlator  $R(u)$ . We denote by  $R_0$  the bare disorder—this is the object in which perturbation theory is

carried out—i.e., one considers the bare action (2.2) with  $R \rightarrow R_0$ . We denote here by  $R$  the renormalized dimensionless disorder; i.e., the corresponding term in the effective action  $\Gamma[u]$  is  $m^\epsilon R$  (i.e., the local two-replica part of  $\Gamma[u]$ ). Symbolically, we can write

$$\mathcal{S}[u] \leftrightarrow R_0, \quad (3.28)$$

$$\Gamma[u] \leftrightarrow m^\epsilon R. \quad (3.29)$$

We define the dimensionless symmetric bilinear one-loop and trilinear two-loop functions [see Eqs. (3.26) and (3.27)] such that

$$\delta^{(1)}(R, R) = m^\epsilon \delta^1 R, \quad (3.30)$$

$$\delta^{(2)}(R, R, R) = m^\epsilon \delta^2 R. \quad (3.31)$$

They can be extended to a nonequal argument using  $f(x, y) := \frac{1}{2}[f(x+y, x+y) - f(x, x) - f(y, y)]$  and a similar expression for the trilinear function. Whenever possible, we will use the shorthand notation  $\delta^{(1)}(R) = \delta^{(1)}(R, R)$  and  $\delta^{(2)}(R) = \delta^{(2)}(R, R, R)$ . The expression of  $R$  obtained perturbatively in powers of  $R_0$  at two-loop order reads

$$R = m^{-\epsilon} R_0 + \delta^{(1)}(m^{-\epsilon} R_0) + \delta^{(2)}(m^{-\epsilon} R_0) + O(R_0^4). \quad (3.32)$$

It contains terms of order  $1/\epsilon$  and  $1/\epsilon^2$ . This is sufficient to calculate the RG functions at this order. In principle, one has to keep the finite part of the one-loop terms, but we will work in a scheme where these terms are exactly 0 by normalizing all diagrams by the one-loop diagram. Inverting Eq. (3.32) yields

$$R_0 = m^\epsilon [R - \delta^{(1)}(R) - \delta^{(2)}(R) + \delta^{(1,1)}(R) + \dots], \quad (3.33)$$

where  $\delta^{(1,1)}(R)$  is the one-loop repeated counterterm:

$$\delta^{(1,1)}(R) = 2 \delta^{(1)}(R, \delta^{(1)}(R, R)). \quad (3.34)$$

The  $\beta$  function is by definition the derivative of  $R$  at fixed  $R_0$ . It reads

$$\begin{aligned} -m \partial_m R|_{R_0} &= \epsilon [m^{-\epsilon} R_0 + 2 \delta^{(1)}(m^{-\epsilon} R_0) + 3 \delta^{(2)}(m^{-\epsilon} R_0) + \dots]. \end{aligned} \quad (3.35)$$

Using the inversion formula (3.33), the  $\beta$  function can be written in terms of the renormalized disorder  $R$ :

$$-m \partial_m R|_{R_0} = \epsilon [R + \delta^{(1)}(R) + 2 \delta^{(2)}(R) - \delta^{(1,1)}(R) + \dots]. \quad (3.36)$$

In order to proceed, let us calculate the repeated one-loop counterterm  $\delta^{(1,1)}(R)$ . We start from the one-loop counterterm (3.26), which has the bilinear form

$$\delta^{(1)}(f, g) = -\frac{1}{2} [f''(u)g''(u) - f''(0)g''(u) - f''(u)g''(0)] \tilde{I}_1, \quad (3.37)$$

with the dimensionless integral  $\tilde{I}_1 := I_1|_{m=1}$ ; we will use the same convention for  $\tilde{I}_A := I_A|_{m=1}$ . Thus  $\delta^{(1,1)}(R)$  reads

$$\begin{aligned} \delta^{(1,1)}(R(u)) &= 2 \delta^{(1)}(R, \delta^{(1)}(R)) = \{ [R''(u) - R''(0)] R'''(u)^2 \\ &\quad + [R''(u) - R''(0)]^2 R'''(u) \\ &\quad - R'''(0^+)^2 R''(u) \} \tilde{I}_1^2. \end{aligned} \quad (3.38)$$

In the course of the calculation the only possible ambiguity could come from

$$\begin{aligned} g''(0) &= \left[ \frac{1}{2} R''(u)^2 - R''(0) R''(u) \right] \Big|_{u \rightarrow 0} \\ &= \{ R'''(u)^2 - R'''(u) [R''(u) - R''(0)] \} \Big|_{u \rightarrow 0} \\ &= R'''(0^+)^2, \end{aligned} \quad (3.39)$$

but there is *no ambiguity* since the function  $R'''(u)^2$  is continuous at  $u=0$  with value  $R'''(0^+)^2 = R'''(0^-)^2$ . This is exactly the same calculation as is done to one loop when computing the nontrivial fixed point for the pinning force correlator  $\Delta(u) = -R''(u)$  yielding  $0 = (\epsilon - 2\zeta) \tilde{\Delta}(0) - \Delta'(0^+)^2$ . Thus there is no doubt that the graph  $G$  with the one-loop counterterm inserted in a one-loop diagram is *non-ambiguous*.

#### D. Final function, renormalizability, and potentiality

The two-loop  $\beta$  function (3.36) then becomes, with the help of Eq. (3.38),

$$\begin{aligned} -m \partial_m R(u) &= \epsilon R(u) + \left[ \frac{1}{2} R''(u)^2 - R''(0) R''(u) \right] (\epsilon \tilde{I}_1) \\ &\quad + \{ [R''(u) - R''(0)] R'''(u)^2 \} \epsilon (2\tilde{I}_A - \tilde{I}_1^2) \\ &\quad - [R'''(0^+)]^2 R''(u) \epsilon (2\lambda \tilde{I}_A - \tilde{I}_1^2). \end{aligned} \quad (3.40)$$

The first result is that, apart from the last ‘‘anomalous’’ term, the  $1/\epsilon^2$  terms cancel in the corrections to disorder. In the terms coming from graphs  $A$  this works because, as we recall,  $\tilde{I}_A = [1/2\epsilon^2 + 1/4\epsilon^2 + O(\epsilon^2)] (\epsilon \tilde{I}_1)^2$  so that the combination  $\epsilon(2\tilde{I}_A - \tilde{I}_1^2)$  is finite. Graphs  $B$  cancel completely since we have chosen as counterterm the full one-loop graph. So for an analytic theory the above  $\beta$  function would be finite. This however is incomplete, since the flow of such a  $\beta$  function leads to a nonanalytic  $R(u)$  above the Larkin scale.

Thus we must consider the last, ‘‘anomalous’’ term in Eq. (3.40). It clearly appears that the only value of  $\lambda$  compatible with the cancellation of the  $1/\epsilon^2$  poles is

$$\lambda = 1, \quad (3.41)$$

leading to a finite  $\beta$  function. Thus the requirement that the theory be renormalizable (i.e., yield universal large-scale re-

sults independent of the short scale details) fixes the value  $\lambda = 1$ . Note that the cancellation of the graphs  $B$  also works thanks to Eq. (3.17).

It is interesting to compare with what happens at depinning. There the cancellation of the  $1/\epsilon^2$  terms in the anomalous part is more complicated, but automatic. It requires a consistent evaluation of all anomalous nonanalytic diagrams. In the depinning theory the cancellation was unusual: a nontrivial bubble diagram (called  $i_3$  in [69]) was crucial in achieving the cancellation. In the statics the two-loop bubble diagrams of type  $B$  appear to be simply the square of the one-loop ones, which is the usual situation. This however is clearly a consequence of Eq. (3.17), so the previous experience with depinning indicates that care is required and we will discuss some justification for Eq. (3.17) below.

In the search for a fixed point it is convenient to write the  $\beta$  function for the rescaled function  $\tilde{R}(u)$  defined through

$$R(u) = \frac{1}{\epsilon \tilde{I}_1} m^{-4\zeta} \tilde{R}(um^\zeta), \quad (3.42)$$

which amounts to rescaling the fields  $u$  by  $m^\zeta$ . Note that this is a simple field rescaling and different from standard wavefunction renormalization, since as mentioned above there is none in this theory due to STS. We have also included the one-loop integral factor to simplify notation and further calculations (equivalently it can be absorbed in the normalization of momentum or space integrals). With this, the  $\beta$  function takes the simple form

$$\begin{aligned} -m \partial_m \tilde{R}(u) &= (\epsilon - 4\zeta) \tilde{R}(u) + \zeta u \tilde{R}'(u) \\ &\quad + \left[ \frac{1}{2} \tilde{R}''(u)^2 - \tilde{R}''(0) \tilde{R}''(u) \right] \\ &\quad + \frac{1}{2} X \{ [\tilde{R}''(u) - \tilde{R}''(0)] \tilde{R}'''(u)^2 \} \\ &\quad - \frac{\lambda}{2} X [\tilde{R}'''(0^+)]^2 \tilde{R}''(u), \end{aligned} \quad (3.43)$$

$$\lambda = 1, \quad X = 1. \quad (3.44)$$

We have left a  $\lambda$  for future use, but its value in the theory we study here is set to 1. Also for convenience we have introduced

$$X = \frac{2\epsilon(2I_A - I_1^2)}{(\epsilon I_1)^2}, \quad (3.45)$$

which is  $X = 1 + O(\epsilon)$  in the  $\epsilon$  expansion studied here, but has a different value for LR elasticity; see below. In fact, it is shown in Appendix E that  $\lim_{\epsilon \rightarrow 0} X$  is independent of the particular infrared cutoff procedure (here a massive scheme). Although the global rescaling factor of  $\tilde{R}, \epsilon \tilde{I}_1$ , has  $O(\epsilon)$  corrections which depend on the infrared cutoff chosen, the FRG equation above does not depend on it. Note that the

above equation remains true in fixed dimension, with the appropriate value for  $X$ , up to terms of order  $\tilde{R}^4$ .

We will see that the value  $\lambda=1$  in Eq. (3.43) has other highly desirable properties. First, this value is *the only one* which guarantees that the nonanalyticity in  $\tilde{R}(u)$  does not become *more severe* at two loops than it is at one loop. Let us take one derivative of Eq. (3.43) and take  $u \rightarrow 0^+$ . One finds

$$-m \partial_m \tilde{R}'(0^+) = (\epsilon - 3\zeta) \tilde{R}'(0^+) + \frac{1}{2} (1 - \lambda) \tilde{R}'''(0^+)^3. \quad (3.46)$$

Thus, if  $\lambda \neq 1$ , the cusp in  $\tilde{R}''$  and the resulting finite value of  $R'''(0^+)$  immediately creates a cusp in  $\tilde{R}'$ . The singularity has become worse. We call this a supercusp. It must be avoided in the statics (see also discussion in Sec. V). Interestingly it *does occur in the driven dynamics*, where it is a physical signature of irreversibility.

Indeed, this property is intimately related to another highly desirable property of the statics: *potentiality*. This property is more conveniently described by considering the flow equation for the (rescaled) *correlator of the pinning force*  $\tilde{\Delta}(u) = -\tilde{R}''(u)$ , the second derivative of Eq. (3.43):

$$\begin{aligned} -m \partial_m \tilde{\Delta}(u) &= (\epsilon - 2\zeta) \tilde{\Delta}(u) + \zeta u \tilde{\Delta}'(u) \\ &\quad - \frac{1}{2} \{[\Delta(u)^2 - \tilde{\Delta}(0)]^2\}'' \\ &\quad + \frac{1}{2} \{[\tilde{\Delta}(u) - \tilde{\Delta}(0)] \tilde{\Delta}'(u)^2\}'' \\ &\quad - \frac{\lambda}{2} [\tilde{\Delta}'(0^+)]^2 \tilde{\Delta}''(u). \end{aligned} \quad (3.47)$$

Formally, this equation could have been obtained directly from a study of the dynamical field theory. Such an equation was indeed obtained at depinning, but with a different value of  $\lambda$ :

$$\lambda_{\text{dep}} = -1, \quad (3.48)$$

which shows that statics and dynamics differ not at one, but at two loops. Integrating the equation for  $\Delta(u)$  once yields a nonzero fixed point value for  $\int \Delta(u)$  unless  $\lambda = 1$ . Potentiality, on the other hand, requires that the force remain the derivative of a potential and that, for short-range disorder (e.g., RB for interface), one must have  $\int \Delta(u) = 0$ . While violating potentiality is desirable at depinning where irreversibility is expected, this would be physically incorrect in the statics and thus again points to the value  $\lambda = 1$  as the physically correct one.

Thus we will for now assume that this is the correct theory of the statics and explore its consequences in the next section. In Sec. V we will provide better justifications and explain our understanding of the tantalizing problem of ambiguous diagrammatics in the nonanalytic theory of pinned disordered systems. Especially we will present methods

which satisfy all the above constraints of renormalizability, absence of a supercusp, and potentiality up to three-loop order [75].

#### IV. ANALYSIS OF FIXED POINTS AND PHYSICAL RESULTS

The FRG equation derived above describes several different physical situations and admits a small number of fixed-point functions  $R^*(u)$  describing a few universality classes. The fixed point associated with a periodic disorder correlator describes single-component periodic systems (such as charge density waves). The fixed point associated with a short-range (exponentially decaying) correlator  $\tilde{R}(u)$  describes a class of systems with so-called random-bond disorder. There is also a family of fixed points associated with long-range—i.e., algebraic—correlations. This includes, as one particular example, random-field disorder, which will be discussed separately.

We now give the results for these fixed points, first for short-range elasticity, then for LR elasticity, and compare with available numerical and exact results. The most important quantity to compute is the roughness exponent  $\zeta$ . Since we have shown that  $X$  in Eq. (3.43) is universal to dominant order, this proves universality of  $\zeta$  to the order in  $\epsilon$  studied here [i.e.,  $O(\epsilon^2)$ ]. For LR disorder and for periodic fixed points we can also compute the universal amplitudes for the correlation function of displacements and discuss their dependence on large-scale boundary conditions. Anticipating a bit, let us summarize the general result that we use in that case, which is derived in Sec. VI. The  $T=0$  disorder-averaged two-point function for  $q \rightarrow 0$ ,  $q/m$  fixed, reads for any dimension  $d$ , in Fourier representation,

$$\overline{u_q u_{q'}} = (2\pi)^d \delta^d(q + q') C(q), \quad (4.1)$$

$$C(q) = C(q=0) F_d(q/m), \quad (4.2)$$

$$C(q=0) = \tilde{c}(d) m^{-d-2\zeta}. \quad (4.3)$$

The amplitude  $\tilde{c}(d)$  is given by the relation (exact to all orders in the present scheme)

$$\tilde{c}(d) = - \frac{1}{(\epsilon \tilde{I}_1)} \tilde{R}^{*''}(0). \quad (4.4)$$

It is found to be universal only for long-range and periodic disorder. The scaling function, computed in Sec. VI for SR and LR elasticity, is always universal (independent of short-scale details) and satisfies  $F_d(0) = 1$  and

$$F_d(z) \sim B z^{-(d+2\zeta)} \quad \text{for } z \rightarrow \infty, \quad (4.5)$$

$$B = 1 + b\epsilon + O(\epsilon^2), \quad (4.6)$$

where  $b$  is computed in Sec. VI. This gives us all we need for a calculation to  $O(\epsilon^2)$  of the universal amplitude, e.g., for the propagator in the massless limit  $m \ll q$ :

$$C(q) = c(d)q^{-(d+2\zeta)}, \quad (4.7)$$

$$c(d) = \tilde{c}(d)[1 + b\epsilon + O(\epsilon^2)]. \quad (4.8)$$

The result for  $C(q=0)$  in the presence of a mass is also interesting since it gives the fluctuations of the center-of-mass coordinate for an interface physically confined in a quadratic well. Although that situation would be interesting to study numerically, most numerical results are for finite-size systems of volume  $L^d$  (and  $m \rightarrow 0$ ). We thus also define, in that case,

$$C_L(q) = c'(d)q^{-(d+2\zeta)}g_d(gL), \quad (4.9)$$

with  $\lim_{z \rightarrow \infty} g_d(z) = 1$ . For *periodic* boundary conditions,  $q = 2\pi n/L$ ,  $n \in \mathbb{Z}^d$  and  $n \neq 0$ . The prime indicates that the value of this amplitude depends on the large-scale boundary conditions: i.e., it depends on whether, e.g., a mass is used or periodic boundary conditions as an infrared cutoff. The ratio, computed in Sec. VI for short-range elasticity,

$$\frac{c'(d)}{c(d)} = 1 - 1.46935\zeta + O(\epsilon^2), \quad (4.10)$$

is unity only for periodic disorder, in which case the amplitude is independent of both large- and small-scale details.

Before studying the different fixed points, let us mention an important property, valid under all conditions: If  $\tilde{R}(u)$  is a solution of Eq. (3.43), then

$$\hat{R}(u) := \kappa^4 \tilde{R}(u/\kappa) \quad (4.11)$$

is also a solution (for  $\kappa$  a constant independent of  $m$ ). We can use this property to fix  $\tilde{R}(0)$  or  $\tilde{R}''(0)$  in the case of nonperiodic disorder. (For periodic disorder the solution is unique, since the period is fixed.)

#### A. Nonperiodic systems: Random-bond disorder

Let us now look for a solution of our two-loop FRG equation which decays exponentially fast at infinity as expected for SR random-bond disorder. To this aim, we have to solve order by order in  $\epsilon$  the fixed-point equation (3.43) numerically. Making the ansatz

$$\tilde{R}(u) = \epsilon r_1(u) + \epsilon^2 r_2(u) + \dots, \quad (4.12)$$

$$\zeta = \epsilon \zeta_1 + \epsilon^2 \zeta_2 + \dots, \quad (4.13)$$

the partial differential equation to be solved at leading order is

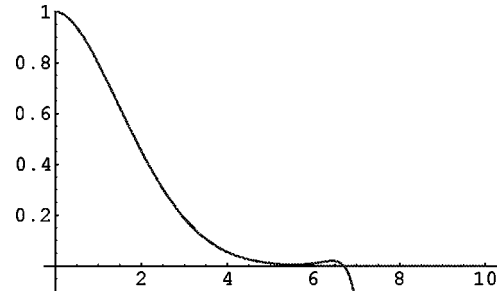


FIG. 10. The fixed-point function  $r_1(u)$  at one-loop order. We have plotted a numerical solution (red, converging to 0 at large  $u$ ) as well as the Taylor expansion (4.16) about 0 up to order 25 (blue, converging up to  $u=5$ ).

$$0 = (1 - 4\zeta_1)r_1(u) + \zeta_1 u r_1'(u) + \frac{1}{2} r_1''(u)^2 - r_1''(u)r_1''(0),$$

$$1 = r_1(0), \quad (4.14)$$

where we have used our freedom to normalize  $\tilde{R}(0) := \epsilon$ . Equation (4.14) has a solution for any  $\zeta_1$ , but only for one specific value of  $\zeta_1$  does this solution decay exponentially fast to 0, without crossing the axis: see Fig. 10. The strategy is thus the following: One guesses  $\zeta_1$  and then integrates Eq. (4.14) from 0 to infinity. In practice, however, there are numerical problems for small  $u$ . One strategy, which we have adopted here and which works very well, is to use the value of  $\zeta_1$  to generate a Taylor expansion about 0. This Taylor expansion is then evaluated at 0.5, where the numerical integration of Eq. (4.14) is started, both forwards to infinity (which in practice is chosen to be 25) and backwards to 0. This enables us to control the accuracy of both the Taylor expansion and the numerical integration. The result for the best value

$$\zeta_1 = 0.20829806(3) \quad (4.15)$$

is given in Fig. 10. (Note that in [46] only the first four digits were given.) On this scale, Taylor expansion and numerical integration are indistinguishable. The error estimate on the last digit comes from moving the starting point of the numerical integration (which was 0.5 above) up to 1, which allows for a crude estimate of the error. We also reproduce the Taylor expansion up to order 25 below:

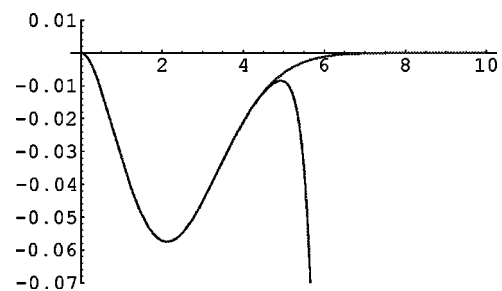


FIG. 11. Fixed-point function  $r_2(u)$  at two-loop order. We have plotted a numerical solution (red, converging to 0 for large  $u$ ) as well as the Taylor expansion (4.20) about 0 up to order 25 (blue, converging up to  $u=5$ ).

TABLE I. First column: exponents obtained by setting  $\epsilon=4-d$  in the one-loop result. Second column: exponents obtained by setting  $\epsilon=4-d$  in the two-loop result. Third column: errors bars are estimated as half the two-loop contribution. Fourth column: improved estimates using the exact result  $\zeta_{\text{eq}}=2/3$  in  $d=1$  (see text).

$\zeta_{\text{eq}}$	One loop	Two loop	Estimate	Improved estimate	Simulation and exact
$d=3$	0.208	0.215	$0.215 \pm 0.004$	0.214	$0.22 \times 0.01$ [85]
$d=2$	0.417	0.444	$0.444 \pm 0.015$	0.438	$0.41 \pm 0.01$ [85]
$d=1$	0.625	0.687	$0.687 \pm 0.03$	2/3	2/3 [86]

$$\begin{aligned}
r_1(u) = & 1 - 0.288797u^2 + 0.0967487u^3 - 0.0109959u^4 + 0.000197282u^5 + 0.0000162077u^6 + 1.37054 \times 10^{-6}u^7 \\
& + 1.06127 \times 10^{-7}u^8 + 5.84538 \times 10^{-9}u^9 - 1.50021 \times 10^{-10}u^{10} - 1.19821 \times 10^{-10}u^{11} - 2.52931 \times 10^{-11}u^{12} \\
& - 3.93584 \times 10^{-12}u^{13} - 4.90717 \times 10^{-13}u^{14} - 4.49154 \times 10^{-14}u^{15} - 1.21758 \times 10^{-15}u^{16} + 6.77579 \times 10^{-16}u^{17} \\
& + 2.11465 \times 10^{-16}u^{18} + 4.19348 \times 10^{-17}u^{19} + 6.49482 \times 10^{-18}u^{20} + 7.78044 \times 10^{-19}u^{21} + 5.52691 \times 10^{-20}u^{22} \\
& - 4.37557 \times 10^{-21}u^{23} - 2.72231 \times 10^{-21}u^{24} - 6.74331 \times 10^{-22}u^{25} + O(u^{26}).
\end{aligned} \tag{4.16}$$

At second order in  $\epsilon$ , we have to solve

$$\begin{aligned}
0 = & r_2(u) - 4\zeta_2 r_1(u) - 4\zeta_1 r_2(u) + u\zeta_2 r_1'(u) + u\zeta_1 r_2'(u) + r_1''(u)r_2''(u) - r_1''(0)r_2''(u) - r_1''(u)r_2''(0) + \frac{1}{2}[r_1''(u) - r_1''(0)]r_1'''(u)^2 \\
& - \frac{1}{2}r_1''(u)r_1'''(0^+)^2,
\end{aligned} \tag{4.17}$$

$$0 = r_2(0), \tag{4.18}$$

where the last equation reflects our choice of  $\tilde{R}(0) = \epsilon$ . Note that to solve the two-loop order equation, one has to feed in the solution at one-loop order, both the Taylor expansion about 0 and the numerically obtained solution for larger  $u$ . Again,  $\zeta_2$  is determined from the condition that the solution decay at infinity. Following the same procedure as at one-loop order, we find

$$\zeta_2 = 0.006858(1). \tag{4.19}$$

The function  $r_2$  is plotted in Fig. 11. The Taylor expansion up to order 25 about 0 reads

$$\begin{aligned}
r_2(u) = & -0.0604942u^2 + 0.0345276u^3 - 0.00628098u^4 + 0.000239628u^5 + 0.000019823u^6 + 1.42202 \times 10^{-6}u^7 + 5.17941 \\
& \times 10^{-8}u^8 - 8.64456 \times 10^{-9}u^9 - 2.72755 \times 10^{-9}u^{10} - 4.78607 \times 10^{-10}u^{11} - 6.23531 \times 10^{-11}u^{12} - 5.49541 \times 10^{-12}u^{13} \\
& - 8.78473 \times 10^{-15}u^{14} + 1.30232 \times 10^{-13}u^{15} + 3.60568 \times 10^{-14}u^{16} + 6.7239 \times 10^{-15}u^{17} + 9.51299 \times 10^{-16}u^{18} \\
& + 9.06111 \times 10^{-17}u^{19} - 9.06201 \times 10^{-20}u^{20} - 2.59561 \times 10^{-18}u^{21} - 7.67911 \times 10^{-19}u^{22} - 1.53922 \times 10^{-19}u^{23} \\
& - 2.36569 \times 10^{-20}u^{24} - 4.42973 \times 10^{-21}u^{25} + O(u^{26}).
\end{aligned} \tag{4.20}$$

One observes that  $\zeta_{\text{SR}}$  is necessarily bounded from above by  $\epsilon/4$  as no SR solution can cross this value (to any order) without exploding. This reflects the exact bound for SR disorder,  $\theta < d/2$ , which simply means that optimization of energy must lower energy fluctuations compared to a simple sum of random numbers. Equality is obtained for the trivial constant eigenmode  $\tilde{R}(u) = \tilde{R}(0)$  corresponding to  $\zeta = \epsilon/4$ , associated with the fluctuation of the zero mode of the random potential.

We can now discuss our results for the roughness exponent. These are summarized in Table I and compared to nu-

merical simulations in  $d=3,2$  and the exact result for the directed polymer in  $d=1$ . A first observation is that the corrections compared to the one-loop result have the correct sign and, further, that they improve the precision of the one-loop result. Given the difficulties associated with this theory, this is a significant achievement. Second, the error bars given in Table I are estimated as half the two-loop contribution, which should not be taken too literally, as it is difficult to obtain a good precision from only two terms of the series and no currently available information about the large order behavior of this novel  $\epsilon$  expansion. Third, one may try to im-

prove the precision using the exact result  $\zeta=2/3$  in  $d=1$ . Estimating the third-order correction in the three possible Padé approximations in order to match  $\zeta=2/3$  for  $\epsilon=3$ , we obtain consistently the values quoted in the fourth column of Table I. We hope that these predictions can be tested in higher-precision numerics soon.

**B. Nonperiodic systems: Random-field disorder**

Let us first recall that at the level of the *bare* model the static random-field disorder correlator obeys  $\tilde{R}(u) \sim -\tilde{\sigma}|u|$  at large  $|u|$  [46,72], where  $\tilde{\sigma}=(\epsilon\tilde{T}_1)\sigma$  is proportional to the amplitude of the random field.

If one studies the large- $u$  behavior in the FRG equation (3.43), one clearly sees that the nonlinear terms do not contribute: thus, one has

$$-m\partial_m\tilde{\sigma}=(\epsilon-3\zeta)\tilde{\sigma}. \tag{4.21}$$

Thus for a RF fixed point to exist, the  $O(\epsilon^2)$  correction to  $\zeta$  has to vanish:

$$\zeta_{\text{RF}}=\epsilon/3. \tag{4.22}$$

This will presumably hold to all orders. Indeed, it is clear that if there is a similar  $\beta$  function to any order, since each  $R$  carries at least two derivatives and at least one must be evaluated at  $u \neq 0$ , the sum of all nonlinear terms to a given *finite* order decreases at least as  $R''(u) \sim 1/u$ . (This does not strictly exclude that summing up all orders may yield a slower decay, although it appears far fetched and does not occur in the nonperturbative large- $N$  limit.) The above value of  $\zeta$  ensures that  $m^\epsilon R(u) \sim -\sigma|u|$  in the effective action—i.e., nonrenormalization of  $\sigma$ .

Note that this argument based on long-range large- $u$  behavior is *a priori* valid for any  $\lambda$ . Since it is made on the  $R$  equation (no such, argument can be made on the equation for  $\Delta$ ), it uses the property of potentiality. However, from Eq. (3.46) with  $\zeta=\epsilon/3$  one sees that  $\lambda \neq 1$  is incompatible with the existence of a fixed point, even a fixed point with a supercusp. Thus the only way to satisfy potentiality for the static random-field problem seems to have  $\sigma$  unrenormalized,  $\zeta=\epsilon/3$  and  $\lambda=1$  (the previous discussion of potentiality in Sec. III D assumed short-range disorder).

This must be contrasted with the theory of depinning, where we found that

$$\zeta_{\text{dep}}=\frac{\epsilon}{3}(1+0.143\ 31\epsilon) \tag{4.23}$$

following from  $\lambda_{\text{dep}}=-1$  in Eq. (3.47). Since in that case the RG flow is nonpotential, it is clear that no similar argument as above exists to protect the value  $\zeta=\epsilon/3$ . (The force correlator is short range.) The conjecture of [57] thus appears rather unphysical in that respect.

**1. Fixed-point function**

We first study the fixed-point equation for

$$\tilde{\Delta}(u)=-\tilde{R}''(u)=\frac{\epsilon}{3}y(u), \tag{4.24}$$

$$y(0)=1, \tag{4.25}$$

and later use the rescaling freedom to tune the solution to the correct value of  $\sigma$  at large scale  $u$ .

The two-loop FRG equation (3.47) becomes ( $\lambda=1$ )

$$0=(uy)'-\frac{1}{2}[(y-1)^2]'' + \frac{\epsilon}{3}\left[\frac{1}{2}[y'^2(y-1)]''-\frac{1}{2}y'(0^+)^2y''\right]. \tag{4.26}$$

One can then integrate once with respect to  $u$ :

$$0=uy-y'(y-1)+\frac{\epsilon}{3}\left[\frac{1}{2}[y'^2(y-1)]'-\frac{1}{2}y'(0^+)^2y'\right]. \tag{4.27}$$

There is no integration constant here because the second line precisely vanishes at  $u=0^+$  (absence of a supercusp).

The one-loop solution involves the first line only. Dividing by  $y$  and integrating over  $u$  yields

$$\frac{u^2}{2}=y_1-1-\ln y_1, \tag{4.28}$$

i.e., an implicit equation for  $y$ , which defines  $y=y_1(u)$ . It satisfies

$$y_1(0)=1, \quad y_1'(0^+)=-1, \\ y_1''(0^+)=\frac{2}{3}, \quad y_1'''(0^+)=-\frac{1}{6}. \tag{4.29}$$

We can put the two-loop solution under a similar form. Making the ansatz

$$\frac{u^2}{2}=y-1-\ln y-\frac{\epsilon}{3}F(y), \tag{4.30}$$

one obtains

$$F(y(\bar{u}))=\frac{1}{2}\int_0^{\bar{u}}\frac{du}{y}[y'^2(y-1)-y]'. \tag{4.31}$$

At this order, one can replace  $y$  by  $y_1$ —i.e., use  $uy=y'(y-1)$  to eliminate  $y'$ . This gives, changing variables from  $u$  to  $y$ ,

$$F(\bar{y})=\frac{1}{2}\int_1^{\bar{y}}dy\frac{1}{y}\frac{d}{dy}\left(\frac{y^2[u(y)]^2}{y-1}-y\right). \tag{4.32}$$

The last term in the brackets is easily integrated. For the remaining terms, we integrate by part and use Eq. (4.30) to replace  $u^2/2$  by  $y-1-\ln y$ :

$$F(\bar{y}) = \int_1^{\bar{y}} dy \frac{y-1-\ln y}{y-1} + \frac{\bar{y}(\bar{y}-1-\ln \bar{y})}{\bar{y}-1} - \frac{1}{2} \ln \bar{y}. \quad (4.33)$$

This yields the final result

$$F(y) = 2y - 1 + \frac{y \ln y}{1-y} - \frac{1}{2} \ln y + \text{Li}_2(1-y), \quad (4.34)$$

$$\text{Li}_2(z) := \int_z^0 dt \frac{\ln(1-t)}{t} = \sum_{k=1}^{\infty} \frac{z^k}{k^2}. \quad (4.35)$$

We find that

$$F(y) = \frac{2}{3}(y-1)^2 - \frac{13}{36}(y-1)^3 + O((y-1)^4) \quad (4.36)$$

has a quadratic behavior around  $y=1$ , similar to the one-loop result, and corrects the value of the cusp.

**2. Universal amplitude**

Since we know the exact fixed-point function up to a scale factor, we can now fix the scale by fitting the exact large- $|u|$  behavior to  $R(u) \sim -\sigma|u|$  where  $\sigma$  is the amplitude of the random field. The general fixed-point solution reads

$$\tilde{\Delta}(u) = \frac{\epsilon}{3} \xi^2 y(u/\xi), \quad (4.37)$$

where  $\xi$  can be related to  $\sigma$  as

$$\tilde{\sigma} = \int_0^{\infty} du \tilde{\Delta}(u) = \frac{\epsilon}{3} \xi^3 I_y. \quad (4.38)$$

We need

$$I_y = \int_0^{\infty} du y(u) = \int_0^1 dy y(u) = \gamma_1 + \epsilon \gamma_2, \quad (4.39)$$

$$\gamma_1 = \int_0^1 dy \sqrt{2(y-1-\ln y)} = 0.775\,304\,245\,188, \quad (4.40)$$

$$\gamma_2 = - \int_0^1 dy \frac{F(y)}{3\sqrt{2(y-1-\ln y)}} = -0.139\,455\,24. \quad (4.41)$$

One can now express

$$\tilde{\Delta}^*(0) = \frac{\epsilon}{3} \xi^2 = \frac{\epsilon}{3} \left( \frac{3\tilde{\sigma}}{\epsilon} \right)^{2/3} I_y^{-2/3} \quad (4.42)$$

and thus compute, using Eq. (4.4), the universal amplitude (4.3) associated with the mode  $q=0$  in the presence of a confining mass:

$$\begin{aligned} \tilde{c}(d) &= \sigma^{2/3} \left( \frac{\epsilon}{3} \right)^{1/3} (\gamma_1 + \epsilon \gamma_2)^{-2/3} (\epsilon \tilde{I}_1)^{-1/3} \\ &= \left( \frac{\epsilon}{3} \right)^{1/3} (\gamma_1 + \epsilon \gamma_2)^{-2/3} \left[ \frac{\epsilon \Gamma\left(\frac{\epsilon}{2}\right)}{(4\pi)^{d/2}} \right]^{-1/3} \sigma^{2/3}, \end{aligned} \quad (4.43)$$

where one has restored the factors  $\epsilon \tilde{I}_1$  absorbed in  $\tilde{\Delta}$  and  $\tilde{\sigma}$ . Expanding all factors in a series of  $\epsilon$ , one finds

$$\tilde{c}(d) = \epsilon^{1/3} [3.524\,59 - 0.725\,079\epsilon + O(\epsilon^2)] \sigma^{2/3}. \quad (4.44)$$

The lowest order was obtained in Ref. [72], and we have obtained here the next-order corrections. It is interesting to compare our result with the exact result in  $d=0$ , which is [71]

$$\tilde{c}(d=0) = 1.054\,238\,565\,19 \dots \sigma^{2/3}. \quad (4.45)$$

While the simple extrapolation setting  $\epsilon=4$  of Eq. (4.44) to one loop  $\tilde{c}(d=0) = 5.59\sigma^{2/3}$  is very far off, to two loop it gives  $\tilde{c}(d=0) = 0.99\sigma^{2/3}$ , surprisingly close to the exact result. It was noted in Ref. [72] that extrapolation of the one-loop result could be considerably improved by not expanding Eq. (4.43) in  $\epsilon$ , but instead directly setting  $\epsilon=4$  [(with  $\gamma_2=0$ ) in Eq. (4.43)]. That gives  $\tilde{c}_1(d=0) = 0.821\sigma^{2/3}$ , an underestimate already reasonably close from the exact result. We extend this procedure to two loop by truncating the  $\epsilon$  expansion of  $I_y^{-2/3}$  to second order in Eq. (4.43) and then set  $\epsilon=4$ . This yields  $\tilde{c}_2(d=0) = 1.22\sigma^{2/3}$ , and the exact result is then halfway between  $\tilde{c}_1(d=0)$  and  $\tilde{c}_2(d=0)$ . To summarize, our two-loop corrections (4.44) have the correct sign and order of magnitude to improve the agreement with the exact result in  $d=0$ .

The universal amplitude for the massless case (4.7) (or  $q \gg m$ ) is obtained from Eq. (4.8) with  $b = -1/3$  from Sec. VI as

$$\begin{aligned} c(d) &= \tilde{c}(d) \left[ 1 - \frac{1}{3} \epsilon + O(\epsilon^2) \right] \\ &= \epsilon^{1/3} [3.524\,59 - 1.899\,94\epsilon + O(\epsilon^2)] \sigma^{2/3}, \end{aligned} \quad (4.46)$$

and writing  $c(d) = \tilde{c}(d)/(1 + \frac{1}{3}\epsilon)$  should provide a reasonable extrapolation to low dimensions. Finally, we recall that for random-field disorder, this coefficient is different for different large-scale boundary conditions. The result for periodic boundary conditions can be obtained from formula (4.10).

In Ref. [72], the one-loop result was compared to the result of the GVM. It is instructive to pursue this comparison to two loops. We get, from [72],

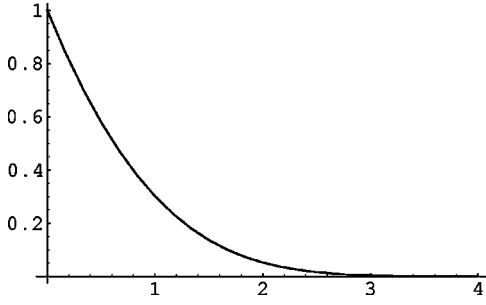


FIG. 12. Fixed-point function  $y_1(u)$  at one-loop order for non-periodic disorder.

$$\begin{aligned} \tilde{c}_{\text{GVM}}(d) &= \left(2 \frac{\epsilon}{\pi}\right)^{1/3} \left[ \frac{\epsilon \Gamma\left(\frac{\epsilon}{2}\right)}{(4\pi)^{d/2}} \right]^{-1/3} \frac{1}{1 - \frac{\epsilon}{12}} \sigma^{2/3} \\ &= \epsilon^{1/3} [3.69054 - 0.894223\epsilon + O(\epsilon^2)] \sigma^{2/3}, \end{aligned} \quad (4.47)$$

$$\begin{aligned} \frac{c_{\text{GVM}}(d)}{\tilde{c}_{\text{GVM}}(d)} &= \left(1 - \frac{\epsilon - 2\zeta}{2}\right) \left(1 - \frac{\epsilon - 2\zeta}{4}\right) \frac{\pi(\epsilon - 2\zeta)/2}{\sin[\pi(\epsilon - 2\zeta)/2]} \\ &= 1 - \frac{\epsilon}{4} + O(\epsilon^2), \end{aligned} \quad (4.48)$$

where in the last line we have inserted  $\zeta = \epsilon/3$  and performed the  $\epsilon$  expansion. Thus one finds, quite generally, that  $b_{\text{var}} = 3b/4$ . As noted in [72], to one loop the FRG and GVM give rather close amplitudes (differing by about 5%). We see here that to two loop—i.e., next order in  $\epsilon$ —the difference increases. Finally,

$$c_{\text{GVM}}(d) = \epsilon^{1/3} [3.69054 - 1.81686\epsilon + O(\epsilon^2)] \sigma^{2/3}$$

and the coefficient remains rather close to the one Eq. (4.46).

### C. Generic long-range fixed points

There is a family of fixed points such that

$$\tilde{R}(u) \sim |u|^{2(1-\gamma)}, \quad (4.49)$$

associated with

$$\zeta = \frac{\epsilon}{2(1+\gamma)}. \quad (4.50)$$

These fixed points were found for infinite  $N$  in any  $d$  in Refs. [36,74] (we use the same notation). They were studied to first order in  $\epsilon$  for any  $N$  in [47] and argued to be stable only for  $\gamma < \gamma^*(d)$ , the value of the crossover to short range identified in [47] as  $\zeta_{\text{SR}} = \zeta_{\text{LR}}(\gamma^*(d))$ .

Here we have not studied these fixed points in detail, but we note that the two-loop corrections do not change  $\zeta$ , by the same discussion as for the random-field case  $\gamma = 1/2$ . They will, however, affect the amplitudes (see Fig. 12).

## D. Periodic systems

### 1. Fixed-point function

For periodic  $R(u)$  such as, e.g., CDW's, there is another fixed point of Eq. (3.43). It is sufficient to study the case where the period is set to unity; all other cases are easily obtained using the reparametrization invariance of Eq. (4.11). No rescaling is possible in that direction, and thus the roughness exponent is

$$\zeta = 0. \quad (4.51)$$

The fixed-point function is then periodic and can in the interval  $[0,1]$  be expanded in a Taylor series in  $u(1-u)$ . Even more, the ansatz

$$\tilde{R}(u) = (a_1\epsilon + a_2\epsilon^2 + \dots) + (b_1\epsilon + b_2\epsilon^2 + \dots)u^2(1-u)^2 \quad (4.52)$$

allows us to satisfy the fixed-point equation (3.43) to order  $\epsilon^2$  and will presumably work to all orders. For a more general case of this, see Ref. [70].

To gain insight into the more general case, let us write the fixed point for Eq. (3.43) with arbitrary  $\lambda$ :

$$\begin{aligned} \tilde{R}^*(u) &= \frac{\epsilon}{2592} + (3-2\lambda) \frac{\epsilon^2}{7776} + (\lambda-1) \frac{\epsilon^2}{432} u(1-u) \\ &\quad - \left( \frac{\epsilon}{72} + \frac{\epsilon^2}{108} \right) u^2(1-u)^2. \end{aligned} \quad (4.53)$$

One can see in this solution that  $\lambda = 1$  is the only value which avoids the appearance at two loops of the supercusp—i.e., a cusp in the potential correlator  $\tilde{R}(u)$  rather than in the force correlator  $\tilde{\Delta}(u)$ .

The same discussion can be made on the the flow equation of  $\tilde{\Delta}(u)$  by taking two derivatives of Eq. (3.43). One finds that there is *a priori* an unstable direction corresponding to a uniform shift in  $\tilde{\Delta}(u) \rightarrow \tilde{\Delta}(u) + cst$ . While this is natural in, e.g., depinning, it is here forbidden by the potential nature of the problem which requires

$$\int_0^1 du \Delta(u) = 0, \quad (4.54)$$

since in a potential environment, the integral of the force over one period must vanish. This is indeed satisfied for the fixed point for  $\tilde{\Delta}(u)$ ,

$$\begin{aligned} \tilde{\Delta}^*(u) &= -\tilde{R}^{*\prime\prime}(u) = \frac{\epsilon}{36} + \frac{\epsilon^2}{54} \left(1 + \frac{\lambda-1}{4}\right) \\ &\quad - \left(\frac{\epsilon}{6} + \frac{\epsilon^2}{9}\right) u(1-u), \end{aligned} \quad (4.55)$$

only if  $\lambda = 1$ :

$$\int_0^1 du \tilde{\Delta}^*(u) = \frac{\epsilon^2}{216} (\lambda-1). \quad (4.56)$$

The values for depinning are obtained by setting  $\lambda = -1$ : in that case, the problem becomes nonpotential at large scales.



## 2. Universal amplitude

This fixed point implies for the amplitude of the zero mode in the presence of an harmonic well, defined in Eq. (4.3), using Eq. (4.4):

$$\begin{aligned} \bar{c}(d) &= \frac{(4\pi)^{d/2}}{\epsilon \Gamma\left(\frac{\epsilon}{2}\right)} \left( \frac{\epsilon}{36} + \frac{\epsilon^2}{54} + O(\epsilon^2) \right) \\ &= 2.193\,25\epsilon - 0.680\,427\epsilon^2 + O(\epsilon^3). \end{aligned} \quad (4.57)$$

In the other limit  $m \ll q$  one obtains the amplitude (using  $b = -1$  from Sec. VI)

$$\begin{aligned} c(d) &= \frac{(4\pi)^{d/2}}{\epsilon \Gamma\left(\frac{\epsilon}{2}\right)} \left( \frac{\epsilon}{36} - \frac{\epsilon^2}{108} + O(\epsilon^3) \right) \\ &= 2.193\,25\epsilon - 2.873\,67\epsilon^2 + O(\epsilon^3). \end{aligned} \quad (4.58)$$

Note that we prove in Sec. VI that this amplitude is *independent* of large-scale boundary conditions and is thus identical for, e.g., periodic boundary conditions and in presence of a mass. As can be seen from Eq. (4.10), this is a consequence of  $\zeta$  being zero.

This can be compared to the GVM method [26,27]:

$$\begin{aligned} c_{\text{GVM}}(d) &= (4-d)2^{d-3}\pi^{d/2-2}\Gamma\left(\frac{d}{2}\right) \\ &= 2\epsilon - 2.9538\epsilon^2 + O(\epsilon^3), \end{aligned} \quad (4.60)$$

$$(4.61)$$

with coefficients surprisingly close to the  $\epsilon$  expansion.

It is interesting to compare predictions in  $d=3$ . We recall that we are studying a problem where the period is unity, the general case being obtained by a trivial rescaling in  $u$ . Since Eq. (4.59) has a poor behavior [and so does Eq. (4.61), which resums into Eq. (4.60)], it is better to use instead Eq. (4.58). It was indeed noted in [26,27] that the improved one-loop prediction  $c_1(d=3)$  obtained by setting  $\epsilon=1$  and ignoring the  $\epsilon^2/108$  term in Eq. (4.58) yields a value rather close to the prediction of the GVM:

$$c_1(d=3) = 2\pi/9 = 0.6981, \quad (4.62)$$

$$c_{\text{GVM}}(d=3) = 1/2. \quad (4.63)$$

Including the two-loop  $\epsilon^2/108$  term now gives  $c_2(d=3) = 0.4654$  and  $c_2(d=3) = 0.5235$  for the two Padé approximations, respectively. This type of extrapolation makes the GVM and FRG predictions get closer when including the two-loop corrections. On the other hand, comparison of Eqs. (4.59) and (4.61) suggests that  $c(d) > c_{\text{GVM}}(d)$ .

This is in reasonable agreement with the numerical results of Middleton *et al.* [87]. They obtained good evidence for the existence of the Bragg glass (i.e., its stability with respect to topological defects predicted in [26,27]). They measure directly the correlation (4.7) and obtain strong evidence for the behavior (4.58) (as well as the correct correction to scaling behavior) with

$$2c(d=3) \approx 1.04 \quad (4.64)$$

[their amplitude  $A$  is twice our  $c(d)$ ], which lies in between the GVM and one-loop FRG. [More precisely two different discretizations gave  $2c(d=3) = 1.01 \pm 0.04$  and  $2c(d=3) = 1.08 \pm 0.05$ .]

Another interesting observable is the slow growth of displacements characteristic of the Bragg glass:

$$\overline{(u_x - u_0)^2} = \tilde{A}_d \ln|x| \quad (4.65)$$

at large  $x$ . Performing the momentum integral from Eq. (4.7), one obtains

$$\begin{aligned} \tilde{A}_d &= \frac{4}{(4\pi)^{d/2}\Gamma(d/2)} c(d) \\ &= \frac{4 \sin(\pi\epsilon/2)}{\pi\epsilon \left(1 - \frac{\epsilon}{2}\right)} \left[ \frac{\epsilon}{36} - \frac{\epsilon^2}{108} + O(\epsilon^3) \right]. \end{aligned} \quad (4.66)$$

If one expands each factor in  $\epsilon$ , it yields

$$\tilde{A}_d = \frac{\epsilon}{18} + \frac{\epsilon^2}{108} + O(\epsilon^3). \quad (4.67)$$

For comparison, the GVM gives

$$\tilde{A}_{d,\text{GVM}} = \frac{\epsilon}{2\pi^2}. \quad (4.68)$$

Here extrapolation directly setting  $\epsilon=1$  in Eq. (4.67) looks possible and yields  $\tilde{A}_3 = 0.0556$  to one loop, increasing to  $\tilde{A}_3 = 0.0648$  to two loops. On the other hand, setting  $\epsilon=1$  in Eq. (4.66) yields instead  $\tilde{A}_3 = 0.0707$  to one loop, decreasing to  $\tilde{A}_3 = 0.047$  at two loops. The GVM gives the result  $\tilde{A}_{3,\text{GVM}} = 0.0507$ .

Another interesting observable is

$$\overline{w^2} = B_d \ln L, \quad (4.69)$$

$$w^2 = \frac{1}{L^d} \int_x u_x^2 - \left( \frac{1}{L^d} \int_x u_x \right)^2, \quad (4.70)$$

where  $L$  is the linear system size. In Ref. [87] it was assumed that  $B_d = \tilde{A}_d/2$ ; thus, in  $d=3$ ,  $B_3 = c(3)/(2\pi^2)$ , yielding a value of  $c(d)$  consistent with the direct measurement of this quantity.<sup>3</sup> This was also done in [88] where it was deduced

<sup>3</sup>One can also comment on their result for the extremal excursions  $\Delta H = u_{\max} - u_{\min}$ . If  $u$  were a *Gaussian* variable with the same two-point correlator, the exact result for extrema of logarithmically correlated Gaussian variables predicted in [102] yields  $\Delta H = \bar{b} \ln L - \bar{c} \ln(\ln L) + \bar{a}$  where  $\bar{b} = 4\sqrt{3b/2}$ ,  $c = 2\gamma\sqrt{b/6}$ ,  $\gamma = 3/2$ , and  $\bar{a}$  a fluctuating constant of order  $O(1)$  (in their notation  $b$  is our  $B_d$ ). Inserting the value obtained numerically in [87] for  $b$  yields  $\bar{b} = 0.795$  and  $\bar{c} = 0.20$ . This is in reasonable agreement with the measured values  $\bar{b} \approx 0.73$  quoted in [87]. Since deviations from Gaussian are not expected to be large, this agreement could probably be improved by using the above form of finite-size corrections (as was done in [102] for a one-dimensional version where much larger sizes had to be considered) rather than the simpler form used in [87].

from a measurement of  $B_d$  that  $0.98 < 2c(d=3) < 1.11$ .<sup>4</sup> Although this is a reasonable approximation, it is not exact. Indeed, the quantity  $B_d$ , contrary to  $c(d)$ , depends on the (large-scale) boundary conditions. It is of course universal, since it does not depend on small-scale details. Its value can be computed, e.g., for periodic boundary conditions and pinned zero mode, and depends on the whole finite-size scaling function (4.9) computed in Sec. VI:

$$\overline{w^2} = c(d) \sum_{q \neq 0} q^{-(d+2\zeta)} g_d(qL). \quad (4.71)$$

As shown recently,  $w^2$  fluctuates from sample to sample and the full distribution  $P(w^2)$  averaged over disorder realizations was computed for the depinning problem [89,90].

### E. Long-range elasticity

Let us now consider the case of long-range elasticity. There are physical systems where the elastic energy does not scale with the square of the wave vector  $q$  as  $E_{\text{elastic}} \sim q^2$ , but as  $E_{\text{elastic}} \sim |q|^\alpha$ . In this situation, the upper critical dimension is  $d_c = 2\alpha$  and we define

$$\epsilon := 2\alpha - d. \quad (4.72)$$

The most interesting case, *a priori* relevant to model a contact line, is  $\alpha = 1$ ; thus,  $d_c = 2$ . For calculational convenience, we choose the elastic energy to be

$$E_{\text{elastic}} \sim (q^2 + m^2)^{\alpha/2}. \quad (4.73)$$

This changes the free correlation to

$$G_{ab}(q) = \delta_{ab} \frac{T}{(q^2 + m^2)^{\alpha/2}}. \quad (4.74)$$

The energy exponent in that case is

$$\theta = \alpha - d + 2\zeta. \quad (4.75)$$

The changes are very similar to the case of Ref. [69], so we summarize them here only briefly. The  $\beta$  function is still given by Eq. (3.40), but with the integrals replaced by

$$I_1^{(\alpha)} = \int_q \frac{1}{(q^2 + m^2)^\alpha} = m^{-\epsilon} \frac{\Gamma(\epsilon/2)}{\Gamma(\alpha)} \int_q e^{-q^2}, \quad (4.76)$$

$$I_A^{(\alpha)} = \int_{q_1, q_2} \frac{1}{(q_1^2 + m^2)^{\alpha/2} (q_2^2 + m^2)^\alpha [(q_1 + q_2)^2 + m^2]^{\alpha/2}}, \quad (4.77)$$

and thus the  $\beta$  function is given by Eq. (3.43) with

$$X \rightarrow X^{(\alpha)} := \frac{2\epsilon [2I_A^{(\alpha)} - (I_1^{(\alpha)})^2]}{(\epsilon I_1^{(\alpha)})^2} = \int_0^1 \frac{dt}{t} \frac{1 + t^{\alpha/2} - (1+t)^{\alpha/2}}{(1+t)^{\alpha/2}} + \psi(\alpha) - \psi\left(\frac{\alpha}{2}\right) + O(\epsilon). \quad (4.78)$$

(See Appendix F of Ref. [69].) And of course the relation (3.42) between  $R$  and  $\tilde{R}$  is identical except that  $\epsilon \tilde{I}_1$  must be replaced by  $\epsilon \tilde{I}_1^{(\alpha)}$ . Since  $X^{(\alpha)}$  is finite, the  $\beta$  function is finite; this is of course necessary for the theory to be renormalizable. For the cases of interest,  $\alpha = 1$  and  $\alpha = 2$ , we find

$$X^{(2)} = 1, \quad (4.79)$$

$$X^{(1)} = 4 \ln 2. \quad (4.80)$$

The exponent  $\zeta$  (as a function of  $\epsilon$ ) and the fixed-point function are thus changed only at two loops.

Let us now give the results in the cases of interest

<sup>4</sup>They also measure the decay of the correlation of  $\exp(2i\pi u)$ , which, within a Gaussian approximation for the distribution of  $u$ , yields the decay  $L^{-A_d}$ , with the Bragg glass exponent  $A_d = 2\pi^2 \tilde{A}_d$ .

#### 1. Random-bond disorder

The solution of Eq. (3.43) with  $X \rightarrow X^{(\alpha)}$  can be written, to second order in  $\epsilon$ , as

$$\tilde{R}(u) = \epsilon r_1(u) + \epsilon^2 X^{(\alpha)} r_2(u) + \dots, \quad (4.81)$$

$$\zeta = \epsilon \zeta_1 + \epsilon^2 X^{(\alpha)} \zeta_2 + \dots, \quad (4.82)$$

since Eq. (4.17) for  $r_2(u)$  is linear. Thus one has, for any  $\alpha$ ,

$$\zeta = 0.208\,298\,06(3)\epsilon + 0.006\,858(1)X^{(\alpha)}\epsilon^2 + O(\epsilon^3). \quad (4.83)$$

For the case of most interest,  $\alpha = 1$ ,  $X^{(1)} = 4 \ln 2$ , one finds

$$\zeta = 0.208\,298\,06(3)\epsilon + 0.019\,0114(3)\epsilon^2,$$

$$\epsilon = 2 - d, \quad (4.84)$$

and  $\theta = 2\zeta$ .

It would thus be interesting to perform numerical simulations in  $d=1$  for the directed polymer with LR elasticity. This would be another nontrivial test of the two-loop corrections. The one-loop prediction is  $\zeta = 0.208$ , significantly smaller than the roughness for SR elasticity  $\zeta = 2/3$ . The naive two-loop result is (setting  $\epsilon = 1$ )  $\zeta \approx 0.227 \pm 0.01$ . Error bars are estimated by half the difference between the one- and two-loop results. Note that the bound  $\theta < d/2$  implies  $\zeta < 1/4$  in  $d=1$ , already rather close to the two-loop result.

### 2. Random-field disorder

The exponent is still

$$\zeta = \frac{\epsilon}{3} \quad (4.85)$$

and was indeed measured in experiments on an equilibrium contact line [30]. It would be of interest to measure the universal distributions there, such as the one defined in [89,90].

The fixed-point function is given by Eqs. (4.30) and (4.34) upon replacing  $F(y) \rightarrow X^{(\alpha)}F(y)$ . The amplitude of the zero mode in a well  $c(d)$  is now given by

$$\bar{c}(d) = \sigma^{2/3} \left( \frac{\epsilon}{3} \right)^{1/3} (\gamma_1 + \epsilon X^{(\alpha)} \gamma_2)^{-2/3} (\epsilon \bar{\Gamma}_1^{(\alpha)})^{-1/3} \quad (4.86)$$

and the amplitude of the massless propagator

$$c(d) = \bar{c}(d)(1 + b_\alpha \epsilon). \quad (4.87)$$

where  $b_\alpha$  is given in Eq. (6.14) setting  $\zeta_1 = 1/3$ .

### 3. Periodic disorder

The fixed point becomes

$$\bar{\Delta}^*(u) = -\bar{R}^{*''}(u) = \frac{\epsilon}{36} + \frac{\epsilon^2}{54} X^{(\alpha)} - \left( \frac{\epsilon}{6} + \frac{\epsilon^2}{9} X^{(\alpha)} \right) u(1-u). \quad (4.88)$$

For the periodic case, the universal amplitude reads

$$\bar{c}(d) = \Gamma(\alpha) \frac{(4\pi)^{d/2}}{\epsilon \Gamma\left(\frac{\epsilon}{2}\right)} \left( \frac{\epsilon}{36} + \frac{\epsilon^2}{54} X^{(\alpha)} + O(\epsilon^3) \right) \quad (4.89)$$

and

$$c(d) = \bar{c}(d)(1 + b_\alpha \epsilon). \quad (4.90)$$

Setting  $\zeta_1 = 0$  in Eq. (6.14) yields

$$\bar{A}_d = \frac{4}{(4\pi)^{d/2} \Gamma(d/2)} c(d). \quad (4.91)$$

Using  $\epsilon = 2\alpha - d$ , this gives

$$\bar{A}_d = \frac{1}{18} \epsilon + \frac{4X^{(\alpha)} + 3[\gamma + \psi(\alpha)] + 6b_\alpha}{108} \epsilon^2, \quad (4.92)$$

which in the case of  $\alpha = 1$  takes the simple form

$$\bar{A}_1 = \frac{1}{18} \epsilon + \frac{16 \ln 2 + 6b_\alpha}{108} \epsilon^2. \quad (4.93)$$

## V. LIFTING AMBIGUITIES IN NONANALYTIC THEORY

### A. Summary of possible methods

As we have seen above, ambiguities arise in computing the effective action at the level of two-loop diagrams if one uses a nonanalytic action. One can see that these arise even at the one-loop level for correlations (see below Sec. VI). To resolve this issue, our strategy has been to use physics as a guide and require the theory to be renormalizable, potential, and without a supercusp. This pointed to a specific assignment of values to the ‘‘anomalous’’ graphs. The physical properties of the ensuing theory, studied in the previous section, were found to be quite reasonable. Of course, one would like to have a better, more detailed justification of the used ‘‘prescription.’’ Although we do not know at present of a derivation of this theory from first principles, we have developed a set of observations and a number of rather natural and compelling ‘‘rules’’ which all lead to the same theory. We describe below our successful efforts in that direction as well as some unsuccessful ones, which illustrate the difficulty of the problem.

A number of approaches can be explored to lift the ambiguities in the nonanalytic theory. We here give a list; some of the methods will be detailed in the forthcoming sections.

(1) *Nonzero temperature.* At  $T > 0$  previous Wilson one-loop FRG analysis [58,59,67,72] found that the effective action *remains analytic* in a boundary layer  $u \sim \bar{T}$ . However, since the rescaled temperature (2.24) flows to zero as  $\bar{T} \sim m^\theta$  as  $m \rightarrow 0$  (temperature being formally irrelevant), all (even) derivatives of  $R(u)$  higher than second grow unboundedly as  $m \rightarrow 0$ —for instance,  $R^{(4)}(0) \sim R^{(4)}(0^+)/\bar{T}$  (in terms of the zero-temperature fixed-point function). On a *qualitative* level one can thus see how finite- $T$  diagrams such as  $E$  in Fig. 3 yielding

$$\sim TR^{(4)}(0)R''(u) \rightarrow R^{(4)}(0^+)R''(u) \quad (5.1)$$

can build up ‘‘anomalous’’ terms in the  $\beta$  function, hence confirming what is found here [72]. However, correctly and quantitatively accounting for higher loops is a nontrivial problem as stronger blowups in  $1/\bar{T}^k$  seem to arise. In fact, each new loop brings two derivatives and a propagator, hence an additional factor  $1/\bar{T}$ . Despite some recent progress, a quantitative finite-temperature approach which would reproduce and justify the present  $\epsilon$  expansion has proved dif-

difficult [76,77]. Not only for technical reasons, as methods using exact RG were found to be appropriate, but also for physical reasons, as an extension to nonzero  $T$  must also handle low-lying thermal excitations in the system (e.g., droplets). A theory from first principles at  $T>0$  is thus presently not available and will not be further addressed here. All other methods use a *nonanalytic action*.

(2) *Exact RG*. Exact RG methods directly at  $T=0$  have been studied to one loop [72,91] and two loops [73,92]. Although it does yield interesting insights into the way to handle ambiguities (see below) and confirm the present results, it suffers from basically the same problems as described here.

(3) *Direct evaluation of nonanalytic averages*. In this approach one attempts a direct evaluation of nonanalytic averages (e.g., in fully saturated diagrams). For instance, expanding at each vertex the disorder  $R(u_a^x - u_b^x)$  in powers of  $|u_a^x - u_b^x|$  using the proper nonanalytic Taylor expansion,

$$R''(u) = R''(0) + R'''(0^+) |u| + R'''(0^+) u^2 + \dots, \quad (5.2)$$

one can try to compute directly all averages in vertex functions and correlations. After performing a few Wick contractions one typically ends up with averages involving sign functions or delta functions. These can be computed *in principle* using the free Gaussian measure: for instance, using formulas such as

$$\langle \text{sgn}(u) \text{sgn}(v) \rangle_0 = \frac{2}{\pi} \arcsin \left( \frac{\langle uv \rangle_0}{\sqrt{\langle uu \rangle_0 \langle vv \rangle_0}} \right). \quad (5.3)$$

Although promising at first sight, the results are disappointing. Averages over the thermal measure involve many changes of signs which destroy all interesting divergences, indicating that some physics is missing. The method, briefly described in Appendix B, is thus not developed further. A dynamical version of this method, which is similar in spirit [68,69], did work for depinning, although there it simply identified with another method used below, the background field (which, for depinning, is  $u_{xt} \rightarrow vt + u_{xt}$ ; see below).

(4) *Calculation of  $\Gamma(u)$  with excluded vertices and symmetrization*. A valid, general, and useful observation (not limited to this method) is that if one uses the *excluded vertex*

$$\frac{1}{2T^2} \sum_{a \neq b} R(u_a - u_b), \quad (5.4)$$

then all Wick contractions can be performed *without ambiguities*. The excluded vertex is as good as the nonexcluded one since one can always add a constant  $-nR(0)$  to the action of the model (2.2). Thus one can compute *without any ambiguity* the effective action  $\Gamma(u)$  for an “off-diagonal” field configuration,

$$u_x^a \text{ such that } u_x^a \neq u_x^b \text{ for all } a \neq b, \quad (5.5)$$

since then no vertex is ever evaluated at  $u=0$ . The drawback is that one ends up with expressions containing terms such as

$$\sum_{a \neq b, a \neq c} R''(u_a - u_b) R'''(u_a - u_b) R'''(u_b - u_c), \quad (5.6)$$

which superficially looks like a three-replica term, but due to the exclusions, may in fact contain a two-replica part, which can in principle be recovered from the above by adding appropriate diagonal terms, using that  $p$ -replica parts are properly defined as *free replica sums*, e.g., from a cumulant expansion. The two-replica part of Eq. (5.6) thus naively is

$$\begin{aligned} & - \sum_{ac} R''(0) R'''(0) R'''(u_a - u_c) \\ & + \sum_{ab} R''(u_a - u_b) R'''(u_a - u_b) R'''(0), \end{aligned} \quad (5.7)$$

and one is again faced with the problem of assigning a value to  $R'''(0)$ . The calculation with excluded vertices thus yields a sum of  $p$ -replica terms with  $p \geq 2$ , and to project them onto the needed two-replica part, one may need to continue these expressions to coinciding arguments  $u^a = u^b$ .

The symmetrization method attempts to do that in the most “natural” way. Using the permutation symmetry over replicas and the hypothesis of no supercusp yields a rather systematic method of continuation. Surprisingly, it fails to yield a renormalizable theory at two loops. We identified some difference with methods which do work, but the precise reason for the failure in terms of continuity properties remains unclear. It may thus be that there is a way to make this method work, but we have not found it. Being interesting in spirit, this method is reported in some details in Appendix A.

If one renounces to the projection onto two-replica terms, one can, in a certain sense, obtain renormalizability properties. This generates an infinite number of different replica sums and seems to be not promising, too. It is described in Appendix F.

We now come to methods which were found to work and which will be described in detail in the next section. In all of them one performs the Wick contractions in some given order (the order hopefully does not matter) and uses at each stage some properties. The fact that one can order the Wick contractions stems from the identity, which we recall, for any set of mutually correlated Gaussian variables  $u_i$ ,

$$\langle u_i W(u) \rangle = \sum_j \langle u_i u_j \rangle \langle \partial_{u_j} W(u) \rangle, \quad (5.8)$$

under very little analyticity assumption for  $W(u)$ , which can even be a distribution. At each stage one can either use excluded or nonexcluded vertices as is found more convenient.

(5) *Elimination of sloops*. We found another method, which seems rather compelling, to determine the two-replica part of terms such as Eq. (5.6). It starts, as the previous one, by computing (unambiguously) diagrams with the excluded vertices. Then instead of symmetrization, one uses identities derived from the fact that diagrams with free replica sums and which contain sloops cannot appear in a  $T=0$  theory and can thus be set to zero. Further contracting such diagrams

generates a set of identities, which, remarkably, is sufficient to obtain unambiguously the two-replica projection without any further assumption. It works very nicely and produces a renormalizable theory, as we have checked up to three loops. In some sense, it uses in a nontrivial way the constraint that we are working with a true  $T=0$  theory. This method is detailed below.

(6) *Background field method.* This method is similar to method number 3 except that the vertex  $R(u)$  at point  $x$  is evaluated at the field  $u_x^a = u^a + \delta u_x^a$ , then expanded in  $\delta u_x^a$ , which then are contracted in some order. This amounts to compute the effective action in presence of a uniform background field which satisfies Eq. (5.5). Thanks to this uniform background and upon some rather weak assumptions, the ambiguities seem to disappear. The method is explained below.

(7) *Recursive construction.* An efficient method is to construct diagrams recursively. The idea is to identify in a first step parts of the diagram, which can be computed without ambiguity. This is in general the one-loop chain diagram (3.1). In a second step, one treats the already calculated subdiagrams as effective vertices. In general, these vertices have the same analyticity properties—namely, are derivable twice—and then have a cusp. (Compare  $R(u)$  with  $[R''(u) - R''(0)]R'''(u)^2 - R''(u)R'''(0)^2$ .) By construction, this method ensures renormalizability, at least as long as there is only one possible path. However, it is not more general than the demand of renormalizability diagram by diagram, discussed below.

(8) *Renormalizability diagram by diagram.* In Sec. III we have used a *global* renormalizability requirement: The one-loop repeated counterterm being nonambiguous, one could fix all ambiguities of the divergent two-loop corrections. However, as will be discussed in [75], this global constraint appears insufficient at three loops to fix all ambiguities. Fortunately, one notes that renormalizability even gives a stronger constraint—namely, *renormalizability diagram by diagram*. The idea goes back to formal proofs of perturbative renormalizability in field theory; see, e.g., [93–100]. These methods define a subtraction operator  $\mathbf{R}$ . Graphically, it can be constructed by drawing a box around each subdivergence, which leads to a “forest” or “hest” of subdiagrams (the counterterms in the usual language), which have to be subtracted, rendering the diagram “finite.” The advantage of this procedure is that it explicitly assigns all counterterms to a given diagram, which finally yields a proof of perturbative renormalizability. If we demand that this proof go through for the *functional* renormalization group, the counterterms must necessarily have the same functional dependence on  $R(u)$  as the diagram itself. In general, the counterterms are less ambiguous, and this procedure can thus be used to lift ambiguities in the calculation of the diagram itself. By construction this procedure is very similar to the recursive construction discussed under point (7).

It has some limitations though. Indeed, if one applies this procedure to the three-loop calculation, one finds that it renders unique all but one ambiguous diagram—namely,



which has no subdivergence: thus, there are no counterterms, which could lift the ambiguities. Thus this diagram must be computed directly and we found that it can be obtained unambiguously by the sloop elimination method [75].

(9) *Reparametrization invariance.* From standard field theory, one knows that renormalization group functions are not unique, but depend on the renormalization scheme. Only critical exponents are unique. This is reflected in the freedom to reparametrize the coupling constant  $g$  according  $g \rightarrow \tilde{g}(g)$  where  $\tilde{g}(g)$  is a smooth function, which has to be invertible in the domain of validity of the RG  $\beta$  function.

Here we have chosen a scheme—namely, defining  $R(u)$  from the exact zero-momentum effective action—using dimensional regularization and a mass. One could explore the freedom in performing reparametrization. In the functional RG framework, reparametrizations are also functional, of the form

$$R(u) \rightarrow \hat{R}(u) = \hat{R}[R](u). \tag{5.10}$$

Of course, the new function  $\hat{R}(u)$  does not have the same meaning as  $R(u)$ . Perturbatively, this reads

$$R(u) \rightarrow \hat{R}(u) = R(u) + B(R, R)(u) + O(R^3), \tag{5.11}$$

where  $B(R, R)$  is a functional of  $R$ . For consistency, one has to demand that  $B(R, R)$  has the same analyticity properties as  $R$ , at least at the fixed point  $\tilde{R} = \tilde{R}^*$ ; i.e.,  $B(R, R)$  should as  $R$  be twice differentiable and then have a cusp. A specifically useful candidate is the one-loop counterterm  $B(R, R) = \delta^{(1,1)}R$ . One can convince oneself that by choosing the correct amplitude, one can eliminate all contributions of class  $A$ , in favor of contributions of class  $B$ . Details can be found in [75].

Apart from methods (3) and (4), which did not work for reasons which remain to be better understood, methods (2) and (5)–(9) were all found to give consistent results, making us confident that the resulting theory is sufficiently constrained by general arguments (such as renormalizability) to be uniquely identified. Let us now turn to actual calculations using these methods.

## B. Calculation using the sloop elimination method

### 1. Unambiguous diagrammatics

Let us redo the calculation of Sec. III B using *excluded vertices*. From now on we use sometimes the shorthand notation

$$u^{ab} = u^a - u^b, \quad u_x^{ab} = u_x^a - u_x^b,$$

$$R_{ab} = R(u^a - u^b), \quad R_{ab}^{(p)} = R^{(p)}(u^a - u^b), \tag{5.12}$$

whenever confusion is not possible.

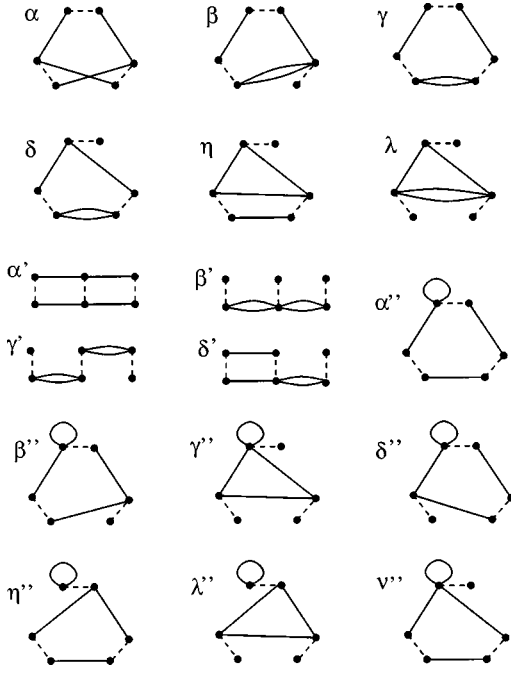


FIG. 13. Two-loop diagrams corresponding to Larkin's hat (top) and banana (bottom). The graph  $\alpha$  is a one-replica term,  $\beta$ ,  $\gamma$ ,  $\delta$ , and  $\eta$  are improper three-replica terms, and  $\lambda$  is an improper four-replica term.

The resulting diagrammatics looks very different from the usual unexcluded one. When making all four Wick contractions of the two-loop diagrams  $A$ ,  $B$ , and  $C$  in Fig. 6 between three unsplit vertices one now excludes all diagrams with saturated vertices, but instead has to allow for more than two connected components and for sloops. The splitted excluded diagrams corresponding to classes  $A$ ,  $B$ , and  $C$  are given in Fig. 13. There is an additional multiplicative coefficient  $1/(m_1!m_2!m_3!m_4!)$  in the combinatorics for each pair of unsplit vertices (say,  $ab$  and  $cd$ ) linked by an internal line where  $m_1$  propagators link  $ac$ ,  $m_2$  link  $ad$ ,  $m_3$  link  $bc$ , and  $m_4$  link  $bd$ . (This is equivalent to assigning a color to each propagator.)

Let us denote by  $\delta\Gamma = (-1/2T^2)\delta_A^{(2)}R$  the two-loop contribution of all diagrams of class  $A$  to the effective action. One finds

$$\begin{aligned} \delta_A^{(2)}R = & \left[ \sum_{a \neq b} R''_{ab} (R'''_{ab})^2 + \sum_{a \neq b, a \neq c} R''_{ab} R'''_{ab} R'''_{ac} \right. \\ & - \frac{1}{2} \sum_{a \neq b, a \neq c, b \neq c} R''_{ab} R'''_{ac} R'''_{bc} + \frac{3}{2} \sum_{a \neq b, a \neq c} R''_{ab} (R'''_{ac})^2 \\ & \left. + \frac{1}{2} \sum_{a \neq b, a \neq c, a \neq d} R''_{ab} R'''_{ac} R'''_{ad} \right] I_A \end{aligned} \quad (5.13)$$

coming, respectively, and in the same order from graphs  $\alpha$ ,  $\beta, \gamma, \delta + \eta$  (they are equal), and  $\lambda$  in Fig. 13. The only graph common to excluded and free-sum diagrammatics is  $\alpha$ , which is a graph  $b$  of Fig. 7, since all the other graphs in Fig. 7 have saturated vertices.

Similarly, the graphs of class  $B$  give a total contribution

$$\begin{aligned} \delta_B^{(2)}R = & \left[ \frac{1}{2} \sum_{a \neq b} R'''_{ab} R''_{ab} R''_{ab} + \frac{1}{4} \sum_{a \neq b, a \neq c, a \neq d} R'''_{ab} R''_{ac} R''_{ad} \right. \\ & + \frac{1}{4} \sum_{a \neq b, a \neq c, b \neq d} R'''_{ab} R''_{ac} R''_{bd} \\ & \left. + \sum_{a \neq b, a \neq c} R'''_{ab} R''_{ab} R''_{ac} \right] I_1^2 \end{aligned} \quad (5.14)$$

coming, respectively, and in the same order from graphs  $\alpha'$ ,  $\beta'$ ,  $\gamma'$ , and  $\delta'$  in Fig. 13. Again, the only graph common to excluded and free-sum diagrammatics is  $\alpha'$ , which is a graph  $g$  of Fig. 8, since all the other graphs in Fig. 8 have saturated vertices.

The contribution  $\delta_C^{(2)}R$  of the diagrams of class  $C$  is given in Appendix C. Note that adding a tadpole does not alter the structure of the summations in the excluded-replica formalism, since a tadpole can never identify indices on different vertices. This indicates that class  $C$  does not contain a two-replica contribution, but starts with a three-replica contribution (times  $T$ ). This is explained in more detail in Appendix D.

One can first check that when  $R(u)$  is *analytic* one recovers correctly the same result as Eq. (3.27) setting the last (anomalous) term to zero. Adding and subtracting the excluded terms in Eq. (5.13) to build free replica sums [using  $R'''(0) = 0$  in that case] or, equivalently, lifting all exclusions but replacing everywhere

$$R_{ab}^{(p)} \rightarrow R_{ab}^{(p)} (1 - \delta_{ab}) \quad (5.15)$$

and then expanding and selecting the two-replica part, one finds the contributions

$$\begin{aligned} \alpha & \rightarrow R''(u) R'''(u)^2, \\ \gamma & \rightarrow \frac{1}{2} R''(0) R'''(u)^2, \\ \delta + \eta & \rightarrow -\frac{3}{2} R''(0) R'''(u)^2, \\ \beta & \rightarrow 0, \\ \lambda & \rightarrow 0. \end{aligned} \quad (5.16)$$

Similarly in Eq. (5.14) one obtains

$$\begin{aligned} \alpha' & \rightarrow \frac{1}{2} R'''(u) R''(u)^2, \\ \beta' \rightarrow \gamma' & \rightarrow \frac{1}{2} R'''(0) R''(0) R''(u) + \frac{1}{4} R''(0)^2 R'''(u), \\ \delta' & \rightarrow -R'''(0) R''(0) R''(u) - R''(0) R'''(u) R''(u). \end{aligned} \quad (5.17)$$

We now want to perform the same projection for a nonanalytic  $R(u)$ .

### 2. Sloop elimination method

The idea of the method is very simple. Let us consider the one-loop functional diagram (a) in Fig. 2 which contains a sloop. It is a three-replica term proportional to the temperature. In a  $T=0$  theory such a diagram should not appear, so it can be identically set to zero:

$$W := \frac{1}{T^2} \sum_{abc} R''(u_x^{ab}) R''(u_y^{ac}) \equiv 0. \quad (5.18)$$

It is multiplied by  $G(x-y)^2$ , which we have not written. We will also omit global multiplicative numerical factors. Projecting such terms to zero at any stage of further contractions is very natural in our present calculation (and also, e.g., in the exact RG approach, where terms are constructed recursively and such forbidden terms must be projected out). It is valid only when (i) the summations over replicas are free and (ii) the term inside the sum is nonambiguous. These conditions are met for any diagram with sloops, provided the vertices have at most two derivatives. (One can in fact start from vertices which either have no derivative or exactly two.)

Let us illustrate the procedure on an example. We want to contract  $W$  with a third vertex  $R$  at point  $z$ ; i.e., we first write the product

$$W \frac{1}{T^2} \sum_{de} R_{de} = \frac{1}{T^4} \sum_{a \neq b, a \neq c, de} R''_{ab} R''_{ac} R_{de} \equiv 0, \quad (5.19)$$

where implicitly here and in the following the vertices are at points  $x, y, z$  in that order. We will contract the third vertex twice, once with the first and once with the second—i.e., look at the term proportional to  $G(x-y)^2 G(x-z) G(y-z)$ . Note that since we will contract each vertex, we are always allowed to introduce excluded sums (clearly the diagonal terms  $a=b$ ,  $a=c$ , or  $d=e$  give zero, since  $R_{ab}$  and its two lowest derivatives at  $a=b$  are field-independent constants). Performing the first correction, i.e., inserting  $(\delta_{ad} - \delta_{ae} - \delta_{bd} + \delta_{be})$  multiplied by the exclusion factors  $(1 - \delta_{ab})(1 - \delta_{ac})(1 - \delta_{de})$  yields (up to a global factor of 2)

$$\frac{1}{T^3} \left[ \sum_{a \neq b, a \neq c, a \neq e} R'''_{ab} R''_{ac} R'_{ae} - \sum_{a \neq b, a \neq c, b \neq e} R'''_{ab} R''_{ac} R'_{be} \right] \equiv 0. \quad (5.20)$$

Similarly, the second contraction then yields (up to a global factor of 4)

$$\begin{aligned} & \frac{1}{T^2} \left[ \frac{1}{2} \sum_{a \neq b, a \neq c, a \neq e} R'''_{ab} R'''_{ac} R''_{ae} + \sum_{a \neq b, a \neq c} R'''_{ab} R'''_{ac} R''_{ac} \right. \\ & + \frac{1}{2} \sum_{a \neq b, b \neq e} R'''_{ab} R'''_{ab} R''_{ae} \\ & \left. - \frac{1}{2} \sum_{a \neq b, a \neq c, b \neq c} R'''_{ab} R'''_{ac} R''_{bc} \right] \equiv 0. \quad (5.21) \end{aligned}$$

This nontrivial identity tells us that the sum of all terms (or diagrams) generated upon contractions of diagram (a) of Fig. 2 [i.e., the one-loop sloop diagram equivalent to term  $W$  in Eq. (5.18)] with other vertices must vanish. Stated differently, a sloop, as well as the sum of all its descendents, vanishes. Note that this is *not* true for each single term, but only for the sum.

A property that we request from a proper  $p$ -replica term is that upon one self-contraction it give a  $(p-1)$ -replica term. It may also give  $T$  times a  $p$ -replica term (a sloop), but this is zero at  $T=0$ , so we can continue to contract. Thus we have generated several nontrivial projection identities. The starting one is that the two-replica part of Eq. (5.18) is zero, since Eq. (5.18) is a proper three-replica term. Thus Eq. (5.19), prior to the exclusions, is a legitimate five-replica term, and its four-replica part is zero. Upon contracting once we obtain that the three-replica part of Eq. (5.20) is zero. The final contraction tells us that the two-replica part of Eq. (5.21) is zero. This is what is meant by the symbol “ $\equiv$ ” above and the last identity is the one we now use.

Indeed, compare Eq. (5.21) with Eq. (5.13). One notices that all terms apart from the first term in Eq. (5.13) appear in Eq. (5.21) and with the same relative coefficients, apart from the third one of Eq. (5.13). Thus one can use Eq. (5.21) to simplify Eq. (5.13):

$$\delta_A^{(2)}(R) = \left[ \sum_{a \neq b} R''_{ab} (R'''_{ab})^2 + \sum_{a \neq b, a \neq c} R''_{ab} (R'''_{ac})^2 \right] I_A. \quad (5.22)$$

The function  $R'''(u)^2$ , which appears in the last term, is continuous at  $u=0$ . It is thus obvious how to rewrite this expression using free summations and extract the two-replica part:

$$\delta_A^{(2)} R(u) = [(R''(u) - R''(0)) R'''(u)^2 - R'''(0^+)^2 R''(u)] I_A, \quad (5.23)$$

which coincides with the contribution of diagrams  $A$  in Eq. (3.27) with  $\lambda=1$ .

We can write diagrammatically the subtraction that has been performed

$$\delta_A^{(2)} R = \text{Diagram 1} - \text{Diagram 2}, \quad (5.24)$$

where the loop with the dashed line represents the subdiagram with the sloop—i.e., the term (5.18) (with in fact the same global coefficient). The idea is of course that subtracting sloops is allowed since they formally vanish.

There are other possible identities, which are descendents of other sloops. For instance, a triangular sloop gives, by a similar calculation,

$$\begin{aligned} & \text{Diagram 3} = R''(0) \sum_{a \neq b} (R'''_{ab})^2 + \sum_{a \neq b, a \neq c} R''(0) R'''_{ab} R'''_{ac} \\ & + \sum_{a \neq b, b \neq c} R'''_{bc} (R'''_{ab})^2 + \sum_{a \neq c, b \neq c, c \neq d} R'''_{ac} R'''_{bc} R'''_{cd}. \quad (5.25) \end{aligned}$$

This however does not prove useful to simplify  $\delta_A^{(2)} R$ .

Since the above method generates a large number of identities, one can wonder whether they are all compatible. We

have checked a large number of examples (see the three-loop calculations in [75]) and found no contradictions, although we have not attempted a general proof.

The diagrams *B* and *C* are computed in Appendix D. One finds, by the same procedure,

$$\delta_B R = \frac{1}{2} R'''(u) [R''(u) - R''(0)]^2, \quad (5.26)$$

$$\delta_C R = 0, \quad (5.27)$$

confirming our earlier results in Secs. III B 2 and III B 3.

### C. Background method

In the background method, one computes  $\Gamma[u]$  to two loops for a uniform background  $u$  such that  $u_{ab} \neq 0$  for any  $a \neq b$ . We start from

$$\langle \mathcal{S}[u + v_x]^3 \rangle_{1PI}, \quad (5.28)$$

Taylor expand in  $v_x$ , and contract all the  $v$  fields, keeping only 1PI diagrams. This is certainly a correct formula for the uniform (i.e., zero-momentum) effective action.

Then one needs the small  $|u|$  expansion of derivatives of  $R$ —i.e., Eq. (5.2)—as well as

$$R'''(u) = R''(0^+) \operatorname{sgn}(u) + R''''(0^+) u + \dots, \quad (5.29)$$

$$R''''(u) = 2R''''(0^+) \delta(u) + R''''(0^+) + \dots. \quad (5.30)$$

Let us start from

$$\sum_{abcdef} R(u_{ab} + v_x^{ab}) R(u_{cd} + v_y^{cd}) R(u_{ef} + v_z^{ef}).$$

We expand in  $v$ , and of course in diagrams *A* one must handle terms involving  $R'''(0)$  and in diagrams *B* terms proportional to  $R''''(0)$ . Let us start with diagrams *A*, which come from the following term in the Taylor expansion:

$$\sum_{abcdef} R'''(u_{ab}) R'''(u_{cd}) R''(u_{ef}) \langle (v_x^{ab})^3 (v_y^{cd})^3 (v_z^{ef})^2 \rangle. \quad (5.31)$$

Here and in the following, we will drop all combinatorial factors. Note that the expectation values vanish at coinciding replicas, so there is no need to specify the values of  $R'''(u_{ab})$  at  $a = b$ . Let us perform the first  $xy$  contraction

$$\sum_{abcef} R'''(u_{ab}) R'''(u_{ad}) R''(u_{ef}) \langle (v_x^{ab})^2 (v_y^{ad})^2 (v_z^{ef})^2 \rangle.$$

If we now perform a second  $xy$  contraction, there is a  $\delta_{aa}$  term which is a sloop and thus should be discarded. The  $\delta_{ad} + \delta_{ba}$  terms build saturated vertices. However, the corresponding expectation values contain

$$R'''(u_{ad}) \langle (v_y^{ad}) \dots \rangle |_{d \rightarrow a} = 0, \quad (5.32)$$

which is reasonably set to zero. Thus the first two contractions have been performed with no ambiguity, leading to

$$\sum_{abef} R'''(u_{ab}) R'''(u_{ab}) R''(u_{ef}) \langle (v_x^{ab}) (v_y^{ab}) (v_z^{ef})^2 \rangle. \quad (5.33)$$

This term is no more ambiguous. Expanding as in Eq. (5.29), the potentially ambiguous part is

$$R'''(0^+)^2 \sum_{abef} R''(u_{ef}) \langle (v_x^{ab}) (v_y^{ab}) (v_z^{ef})^2 \rangle, \quad (5.34)$$

clearly free of any ambiguity. It yields the result (5.23). The question arises as to whether the result may depend on the order. We found that when first contracting  $xy$  and  $xz$ , one reproduces the result (5.23). However, when one first contracts  $xy$  and  $yz$  (in any order) one encounters a problem, if one wants to contract  $yz$  again. The intermediate result after the first two contractions is

$$\sum_{abef} R'''(u_{ab}) R'''(u_{ad}) R''(u_{af}) \langle (v_x^{ab}) (v_y^{ad}) (v_z^{af}) \rangle. \quad (5.35)$$

The next contraction between  $xy$  contains one term with a single  $R'''_{aa}$ . One would like to argue that this term can be set to 0. Following this procedure, however, leads to problems. We therefore adopt the rule that whenever one arrives at a single  $R'''_{aa}$ , one has to stop and search for a different path. Note that this equivalently applies to the recursive constructions method. In two-loop order, one can always find a path, which is unambiguous. It seems to fail at three-loop order; at least we have not yet been able to calculate



$$(5.36)$$

using any other than the sloop elimination method. Whether some refinement of the background method can be constructed there is an open question.

For diagrams of class *B* one expands as

$$\sum_{abcdef} R''(u_{ab}) R'''(u_{cd}) R''(u_{ef}) \langle (v_x^{ab})^2 (v_y^{cd})^4 (v_z^{ef})^2 \rangle.$$

Again, no need to attribute a value to  $R'''(u_{cd})$  for  $c = d$  since the summand vanishes there. Contract  $xy$ :

$$\sum_{abdef} R''(u_{ab}) R'''(u_{ad}) R''(u_{ef}) \langle (v_x^{ab}) (v_y^{ad})^3 (v_z^{ef})^2 \rangle. \quad (5.37)$$

Contracting  $yz$ , one gets

$$\sum_{abf} R''(u_{ab}) R'''(u_{ad}) \times \langle (v_x^{ab}) (v_y^{ad})^2 [R''(u_{af}) v_z^{af} - R''(u_{df}) v_z^{df}] \rangle.$$

Contracting next  $xy$ , the danger is the term  $\delta_{ad}$ , yielding a saturated vertex in the middle. But, again, if one takes



$$R'''(u_{ad})\langle(v_y^{ad})\cdots\rangle|_{d\rightarrow a}=0, \quad (5.38)$$

then one gets unambiguously

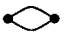
$$\sum_{ab} R''(u_{ab})R'''(u_{ab})\langle(v_y^{ab})(R''(u_{af})v_z^{af}-R''(u_{bf})v_z^{bf})\rangle.$$

The rest is straightforward. The background method thus seems to work properly at two-loop order.

**D. Renormalizability, diagram by diagram**

In Sec. V A we have stated that renormalization diagram by diagram gives a method to lift the ambiguity of a given diagram, as long as it has sufficient subdivergences. This method is inspired by formal proofs of perturbative renormalizability; the reader may consult [93–100] for more details. The key ingredient is the subtraction operator **S**, which acts on the effective action—i.e., all terms generated in perturbation theory which contribute to the renormalized *R* and which subtract the divergences at a scale  $\mu$ . At one-loop order, the renormalized disorder  $R_m$  at scale  $m$  is symbolically (with  $R_0$  the bare disorder)

$$R_m = [R_0 + (R_0'')^2 \text{diagram} + \dots],$$

where of course the integral  depends on  $m$ . The operator **S** rewrites this as a function of the *renormalized* disorder  $R_\mu$  at scale  $\mu$ :

$$R_m = \mathbf{S} [R_0 + (R_0'')^2 \text{diagram} + \dots] := R_\mu + (R_\mu'')^2 \left( \text{diagram} - \boxed{\text{diagram}} + \dots \right). \quad (5.39)$$

Here the boxed diagram is defined as

$$\boxed{\text{diagram}} = \text{diagram} \Big|_\mu. \quad (5.40)$$

The idea behind this construction is that at any order in perturbation theory, any observable in the renormalized theory can be written as perturbative expansion in the *bare* diagrams, to which one applies **S**. Here **S** reorganizes the perturbative expansion in terms of the *renormalized* diagrams. The action of **S** is to subtract divergencies, which graphically is denoted by drawing a box around each divergent diagram or subdiagram, and to repeat this procedure recursively inside each box. The second line of Eq. (5.39) is manifestly finite, since it contains the diagram at scale  $m$  minus the diagram at scale  $\mu$ . This is easily interpreted as the one-loop contribution to the  $\beta$  function.

The power of this method is not revealed before two-loop order. Let us give the contribution from the hat diagram (class A):

$$\delta R_A^{(2)} = \text{hat diagram} R_0''(R_0''')^2 \quad (5.41)$$

Using **S**, this is rewritten as

$$\delta R_A^{(2)} = \mathbf{S} \left[ R_0''(R_0''')^2 \text{hat diagram} \right] = R''(R''')^2 \left[ \text{hat diagram} - \boxed{\text{hat diagram}} - \boxed{\text{diagram}} + \boxed{\boxed{\text{diagram}}} \right] \quad (5.42)$$


Note that not only the global divergence is subtracted, but also the subdivergence in the bottom loop, and finally the divergence which remains, after having subtracted the latter (last term). Note the factor of  $1 = (-1)^2$  in front of the last diagram, which comes with the two (nested) boxes.

Let us halt the discussion of the formal subtraction operator at this point and not prove that the procedure renders all expectation values finite; this task is beyond the scope of this article, although it is not difficult to prove, e.g., along the lines of [99], once the question of the ambiguities of a diagram is settled. However, let us discuss what the subtraction procedure can contribute to the clarification of the ambiguities.

In standard field theory, the main problem to handle is the cancellation of divergences, whereas the combinatorics of the vertices is usually straightforward. This means that the sum of the integrals, represented by the diagrams in the brackets on the right-hand side of Eq. (5.42), is finite. This ensures of course renormalizability, subject to the condition

that all diagrams have the same functional dependence on  $R$ . Here the factor  $R''(R''')^2$  should more completely read

$$[R''(u) - R'(0)]R'''(u)^2 - R''(u)R'''(0^+)^2. \quad (5.43)$$

For the first term, there was no problem. However, we have seen that the last term was more difficult to obtain. If we demand *renormalizability diagram by diagram*, all diagrams have to give the *same* factor (5.43). Thus, if *at least one of them* can be calculated without ambiguity, we have an unambiguous procedure to calculate *all of them*. We now demonstrate that  is unambiguous. To this aim, we detail on the subtraction operator **S**, whose action is represented by the box. This box tells us to calculate the divergent part of the subdiagram in the box and to replace everything in the box by the counterterm, which here is

$$\boxed{\text{diagram}} = I_1^\mu (R''(u)^2 - 2R''(u)R''(0)). \quad (5.44)$$

In a second step, one has to calculate the remaining diagram, which is obtained by treating the box as a point—i.e., as a local vertex. The idea is, of course, that the subdivergence comes from parts of the integral, where the distances in the box are *much* smaller than all remaining distances, such that this replacement is justified. Graphically this can be written as

$$\text{Diagram} = I_1^\mu \times \text{Diagram} \quad (5.45)$$

Remains to calculate the rightmost term—i.e., to calculate the one-loop diagram—from one vertex  $R(u)$  and a second vertex  $V(u) := R''(u)^2 - 2R''(u)R''(0)$ . The result is a straightforward generalization of Eq. (3.1):

$$\text{Diagram} = I_1 \left[ R''(u)V''(u) - R''(0)V''(u) - R''(0)V''(0) \right] \quad (5.46)$$

We need

$$V''(u) = R'''(u)^2 + \dots \quad (5.47)$$

The omitted terms are proportional to  $R'''R''$  and contribute to class  $B$ . We could have avoided their appearance altogether, but this would have rendered the notation unnecessarily heavy. The term which contributes to Eq. (5.46) is  $V''(u) = R'''(u)^2$ . It has the same analyticity properties as  $R''(u)$  and especially can unambiguously be continued to  $u = 0$ —i.e.,  $V''(0) = R'''(0^+)^2$ . Expression (5.46) becomes

$$\text{Diagram} = I_1 \left[ R''(u)R'''(u)^2 - R''(0)R'''(u)^2 - R''(u)R'''(0^+)^2 \right] \quad (5.48)$$

without any ambiguity.<sup>5</sup>

To summarize, using ideas of perturbative renormalizability diagram by diagram, we have been able to compute unambiguously one of the terms in Eq. (5.42) and can use this information to make the functional dependence of the whole expression unambiguous. If we were to chose any other prescription, a proof of perturbative renormalizability is doomed to fail, a scenario which we vehemently reject.

<sup>5</sup>The same procedure can be applied to the dynamics at the depinning transition. Care has to be taken there, since it exists an additional one-loop counterterm, which is an asymmetric function with a vanishing integral. The repeated counterterm at two-loop order (integrated over all positions) therefore also vanishes; however, it gives a nonzero contribution both to classes  $A$  and  $B$  (chains and hat diagrams), of which the sum vanishes. In order to ensure finiteness diagram by diagram, these contributions may not be neglected. This is discussed in [69].

### E. Recursive construction

This method is very similar in spirit to the one of Sec. VD. There we had first calculated a subdiagram and then treated the result as a new effective vertex. This procedure can be made a prescription, which ensures renormalizability and potentiality, since the one-loop diagram ensures the latter. Only at three-loop order does a new diagram (5.36) appear which cannot be handled that way, but the procedure, which is otherwise very economic, can handle again most diagrams at three-loop order, using the new three-loop diagram (5.36).

## VI. CORRELATION FUNCTIONS

Here we address the issue of the calculation of correlation functions. We note that it has not been examined in detail in previous works on the  $T=0$  FRG. Usually correlations are obtained from tree diagrams using the proper or renormalized vertices from the polynomial expansion of the effective action. Thus in a standard theory one could check at this stage that correlation functions are rendered finite by the above counterterms, compute them, and obtain a universal answer. In a more conventional theory that would be more or less automatic.

Here, as we point out, it is not so easy. Indeed, as we show below, if one tries to compute even the simplest two-point correlation at nonzero momentum, one finds ambiguities already at one loop. This is because the effective action (the counterterm) is nonanalytic.

Again, the requirement of renormalizability and independence of short-scale details guide us toward a proper definition of the correlation functions that we can compute. Interestingly, this definition is very similar as the one obtained from an exact solution in the large- $N$  limit in [74]. Let us illustrate this in the two-point function and, at the same time, derive the (finite-size) scaling function for any elasticity (not done in [69]) for massive and finite-size schemes.

### A. Two-point function

We want to compute the two-point correlation function at  $T=0$ . In Fourier representation it is given by Eq. (4.1) with

$$C(q) = [\Gamma^{(2)}(q)]_{ab}^{-1} \quad (6.1)$$

in terms of the quadratic part of the effective action, which reads, at any  $T$ ,

$$\Gamma^{(2)}(q)_{ab} = \frac{q^2 + m^2}{T} \delta_{ab} + \Gamma_{\text{OD}}^{(2)}(q), \quad (6.2)$$

$$\Gamma_{\text{OD}}^{(2)}(q=0) := m \epsilon \frac{R''(0)}{T^2}; \quad (6.3)$$

i.e., by construction here  $R''(0)$  gives the exact off-diagonal element of the quadratic part of the effective action. Inverting the replica matrix gives the relation, exact to all orders,

$$C(q=0) = -m^\epsilon \frac{R''(0)}{m^4} = -\frac{1}{\epsilon \tilde{I}_1} (\tilde{R}'')^*(0) m^{-d+2\zeta}. \quad (6.4)$$

$R(u)$  is exactly the function entering the  $\beta$  function [in the rescaled form  $\tilde{R}(u)$ ]. In the second line we have inserted the fixed-point form, which thus gives exactly the  $q=0$  correlations in the small- $m$  limit (i.e., up to subdominant terms in  $1/m$ ) which are bounded because of the small confining mass.

### 1. Calculation of scaling function

We now compute  $C(q)$  for arbitrary but small wave vector  $q$  and to one loop—i.e., to next order in  $\epsilon$ . One expects the scaling from (4.2) and that the scaling function is independent of the short-scale UV details (i.e., universal), if the theory is renormalizable. It satisfies  $F(0)=1$  and, from scaling, should satisfy  $F(z) \sim B/z^{d+2\zeta}$  at large  $z$ . In  $d=4$  one has  $F_4(z) = 1/(1+z^2)^2$  and we want to obtain the scaling function to the next order—i.e., identify  $b$  in  $B=1+b\epsilon + O(\epsilon^2)$ .

Let us use straight perturbation theory with  $R_0$ , defined as in Sec. III C, including the one-loop diagrams. This amounts to attaching two external legs to the one-loop diagrams in Fig. 5 and using a nonanalytic<sup>6</sup>  $R_0$ . Our result is

$$\begin{aligned} (q^2+m^2)^2 C(q) &= -T^2 \Gamma^{(2)}(q=0) \\ &= -R_0''(0) - R_0'''(0^+)^2 I(q), \\ I(q) &= \int_p \frac{1}{(p^2+m^2)[(p+q)^2+m^2]}. \end{aligned} \quad (6.5)$$

There is, however, an ambiguity in this calculation: i.e., again it is not obvious, *a priori*, how to interpret the  $R_0'''(0^+)^2$  which appear. If one computes the one-loop correction using Eq. (5.2), one must evaluate

$$R_0'''(0^+)^2 \left\langle u_x^a u_y^b \int_{zt} \sum_{cd} |u_z^c - u_t^d| |u_t^c - u_z^d| \right\rangle G(z-t)^2. \quad (6.6)$$

One notes that at the very special point  $z=t$  there is no ambiguity, as the interaction term is analytic to this order. Then performing the average amounts to take two derivatives  $\partial_{u_a} \partial_{u_b}$  of

<sup>6</sup>A subtle point in that construction is that if one defines  $R_0$  perturbatively from  $R$  to a given order, then  $R_0$  is not the original bare action (which is analytic); thus, there is no contradiction in  $R_0$  being non analytic. In a sense, introducing  $R_0$  is just a trick commonly used in field theory to express a closed equation for the flow of  $R$  to the same order. The (perturbative) exact RG method introduced in [103] does that automatically without the need to introduce  $R_0$ .

$$\sum_{cd} R_0''(u_c - u_d)^2 = R_0'''(0^+)^2 |u_c - u_d|^2 + O(u^3),$$

which, to this order, is analytic. In this case this is exactly the same calculation as for the repeated one-loop counterterm. However, the full expression (6.6) integrated over  $z, t$  is, itself, ambiguous. Interestingly, this simple ambiguity already to one loop has never been discussed previously.

Let us first show that *renormalizability* fixes the form to be the one written in Eq. (6.5). Indeed, let us reexpress Eq. (6.5) in terms of the renormalized dimensionless disorder in Eqs. (3.33) and (3.26):

$$R_0''(0) = m^\epsilon R''(0) - R'''(0^+)^2 m^2 \epsilon I(0). \quad (6.7)$$

As discussed in Sec. III C, no ambiguity arises when taking two derivatives of Eq. (3.33) at  $u=0^+$ ; i.e., the one-loop counterterm is unambiguous. This gives

$$(q^2+m^2)^2 C(q) = -m^\epsilon \{R''(0) + R'''(0^+)^2 m^\epsilon [I(q) - I(0)]\}.$$

Thus the substitution (6.7) acts as a counterterm which exactly subtracts the divergence, as it should. The result is finite, as required by renormalizability, only with the above choice (6.5). Stated differently, the  $q=0$  calculation of Eq. (6.5) fixes the ambiguity. We show below that the methods described in the previous section also allow us to obtain this result unambiguously. Before that, let us pursue the calculation of the scaling function.

Upon using Eq. (3.42) and the fixed-point equation, we obtain

$$F_d\left(\frac{q}{m}\right) = \frac{m^4}{(q^2+m^2)^2} \left[ 1 - (\epsilon - 2\zeta) \frac{1}{\epsilon \tilde{I}_1} m^\epsilon [I(q) - I(0)] \right]. \quad (6.8)$$

Apart from the dependence on  $\zeta$ , the calculation of the scaling function is very similar to the one given in [69]. We perform here a more general calculation which also contains the case of elasticity of arbitrary range

$$q^2 + m^2 \rightarrow (q^2 + m^2)^{\alpha/2}, \quad (6.9)$$

and expand in  $\epsilon = 2\alpha - d$ . Using that, in that case

$$\begin{aligned}
 I(q) &= \frac{1}{\Gamma\left(\frac{\alpha}{2}\right)^2} \int_p \int_{s,t>0} (st)^{\alpha/2-1} e^{-s(p+q/2)^2-t(p-q/2)^2-(s+t)m^2} \\
 &= \frac{1}{\Gamma\left(\frac{\alpha}{2}\right)^2} \int_p e^{-p^2} \int_{s,t>0} (st)^{\alpha/2-1} (s+t)^{-d/2} e^{-q^2 st/(s+t)-(s+t)m^2} \\
 &= \frac{1}{\Gamma\left(\frac{\alpha}{2}\right)^2} \int_p e^{-p^2} m^{-\epsilon} \Gamma\left(\frac{\epsilon}{2}\right) \int_{t>0} t^{\alpha/2-1} (1+t)^{-d/2} \left[ (1+t) + \frac{t}{1+t} \frac{q^2}{m^2} \right]^{-\epsilon/2}. \tag{6.10}
 \end{aligned}$$

Defining the one-loop value of  $\zeta/\epsilon = \zeta_1 + O(\epsilon)$ , we obtain, to the same accuracy, the scaling function in the form ( $z = |q|/m$ )

$$\begin{aligned}
 F_d(z) &= \frac{1}{(1+z^2)^\alpha} \left\{ 1 - (1-2\zeta_1) \frac{\Gamma(\alpha)}{\Gamma\left(\frac{\alpha}{2}\right)^2} \int_0^\infty dt t^{\alpha/2-1} (1+t)^{-\alpha} \left[ \left( 1 + \frac{tz^2}{(1+t)^2} \right)^{-\epsilon/2} - 1 \right] \right\} \\
 &= \frac{1}{(1+z^2)^\alpha} \left\{ 1 + \frac{\epsilon}{2} (1-2\zeta_1) \frac{\Gamma(\alpha)}{\Gamma\left(\frac{\alpha}{2}\right)^2} \int_0^1 ds [s(1-s)]^{\alpha/2-1} \ln[1+s(1-s)z^2] \right\}. \tag{6.11}
 \end{aligned}$$

[We have used the variable transformation  $s = 1/(1+t)$ .] To obtain  $b$ , we need the large- $z$  behavior of the scaling function

$$F_d(z) \xrightarrow{z \rightarrow \infty} \frac{1}{z^{2\alpha}} \left\{ 1 + (\epsilon - 2\zeta) \left[ \ln z + \psi\left(\frac{\alpha}{2}\right) - \psi(\alpha) \right] \right\}. \tag{6.12}$$

We want to match, at large  $z$ ,

$$\begin{aligned}
 F_d(z) &= \frac{1}{z^{2\alpha}} [1 + b\epsilon + O(\epsilon^2)] z^{\epsilon-2\zeta} \\
 &= \frac{1}{z^{2\alpha}} [1 + (\epsilon - 2\zeta) \ln z + b\epsilon + O(\epsilon^2)]. \tag{6.13}
 \end{aligned}$$

The above result yields

$$\begin{aligned}
 b &= b_\alpha = (1-2\zeta_1) \left[ \psi\left(\frac{\alpha}{2}\right) - \psi(\alpha) \right] \\
 &= \begin{cases} -2(1-2\zeta_1) \ln 2 & \text{for } \alpha = 1, \\ -(1-2\zeta_1) & \text{for } \alpha = 2. \end{cases} \tag{6.14}
 \end{aligned}$$

### 2. Lifting the ambiguity

Let us now present two additional methods to lift the ambiguity in the one-loop correction to the two-point function and recover Eq. (6.5).

In the background method of Sec. VC one performs this calculation in presence of a background field—i.e., considering that the field  $u_x^a$  has a uniform background expectation value:

$$u_x^a = u^a + v_x^a, \tag{6.15}$$

with  $u_a \neq u_b$  for all  $a \neq b$  and contracting the  $v_x^a$ . Then at  $T = 0$  the sign of any  $u_a - u_b$  is determined, and the above ambiguity in Eq. (6.6) is lifted (contracting further the  $v_x^a$  yields extra factors of  $T$  and thus is not needed here). Using the background method is physically natural as it amounts to compute correlations by adding a small external field which splits the degeneracies between ground states whenever they occur, as was also found in [74]. On the other hand, performing the calculation in the absence of a background field, in perturbation theory, directly of the nonanalytic action yields a different result, detailed in Appendix B, which appears to be inconsistent. It presumably only captures correlations within a single well.

The second method is sloop elimination. We want to compute contractions of

$$\frac{1}{8T^4} u_x^a u_y^a \sum_{cdef} R(u_z^c - u_z^d) R(u_w^e - u_w^f), \tag{6.16}$$

where the two disorder are at points  $z$  and  $w$ , respectively. Let us restrict our attention to the part proportional to  $G_{xz} G_{zw}^2 G_{wy}$ , which gives the  $q$ -dependent part of the two-point function. Since  $a$  is fixed, we need to extract the “0-replica part” of the expression after contractions (which will necessarily involve excluded vertices). Starting by contracting twice the two  $R$ ’s, we get

$$\frac{1}{4T^2} \left[ \sum_{c \neq d} R''(u_z^c - u_z^d) R''(u_w^c - u_w^d) + \sum_{c \neq d, c \neq e} R''(u_z^c - u_z^d) R''(u_w^c - u_w^e) \right]. \quad (6.17)$$

Subtracting the sloop  $W$  from Eq. (5.18) gives (up to terms which do not depend on both  $w$  and  $z$ , and which thus disappear after the two remaining contractions)

$$\frac{1}{4T^2} \sum_{c \neq d} R''(u_z^c - u_z^d) R''(u_w^c - u_w^d). \quad (6.18)$$

Contracting the external  $u$ 's with Eq. (6.18), we obtain (restoring the correlation functions)

$$\int_{z,w} G_{wx} G_{wy} G_{xy}^2 \sum_{a \neq b} (R''_{ab})^2. \quad (6.19)$$

The excluded sum can be rewritten as the sum minus the term with coinciding indices. Only the latter is a 0-replica term, which gives the desired result

$$-R'''(0^+)^2 \int_{z,w} G_{xz} G_{zw}^2 G_{wy}. \quad (6.20)$$

This result can also be obtained writing directly the graphs with excluded vertices and eliminating the descendants of the sloop.

### 3. Massless finite-size system with periodic boundary conditions

The FRG method described here can also be applied to a system of finite size, with, e.g., periodic boundary conditions  $u(0) = u(L)$ , and zero mass, which are of interest for numerical simulations. The momentum integrals in all diagrams are then replaced by discrete sums with  $q = 2\pi n/L$ ,  $n \in \mathbb{Z}^d$ . One must, however, be careful in specifying the mode  $q = 0$ , i.e.,  $\langle u \rangle = (1/L^d) \int_x u_x$ . The simplest choice is to constrain  $\langle u \rangle = 0$  in each disorder configuration, which we do for now. Since the zero mode is forbidden to fluctuate, sums over momentum in each internal line exclude  $q = 0$ .

One then finds that the two-loop FRG equation remains identical to Eq. (3.43), the only changes being that (1)  $-m\partial_m \tilde{R}$  has to be replaced by  $L\partial_L \tilde{R}$ , (2)  $m \rightarrow 1/L$  in the definition of the rescaled disorder, and (3) the one-loop integral  $I_1 = \int_k [1/(k^2 + m^2)^2]$  entering into the definition of the rescaled disorder has to be replaced by its homologue for periodic boundary conditions,

$$I_1 \rightarrow I'_1 = L^{-d} \sum_{n \in \mathbb{Z}^d, n \neq 0} \frac{1}{(2\pi/L)^4 (n^2)^2}, \quad (6.21)$$

used below.

Here and below we use a prime to distinguish the different IR schemes. As we have seen,  $X$  is, to dominant order, independent of the IR cutoff procedure.

Thus we can now compute the two-point function. Following the same procedure as above, we find

$$C(q) = \frac{1}{q^4} L^{2\zeta - \epsilon} \frac{-(\tilde{R}'')^*(0)}{\epsilon \tilde{I}'_1} \times \left[ 1 - (\epsilon - 2\zeta) \frac{1}{\epsilon \tilde{I}'_1} [\tilde{I}'(q) - \tilde{I}'(0)] \right], \quad (6.22)$$

with  $\tilde{I}'(0) = \tilde{I}'_1$  and, for  $q = 2\pi n/L$ ,

$$\tilde{I}'(q) = \sum_{m \in \mathbb{Z}^d, m \neq 0, n+m \neq 0} \frac{1}{(2\pi)^4 m^2 (n+m)^2}. \quad (6.23)$$

Thus one finds the finite-size scaling function [defined in Eq. (4.9)]

$$\begin{aligned} c'(d) g_d(qL) &= q^{d+2\zeta} C(q) \\ &= (qL)^{2\zeta - \epsilon} \frac{-(\tilde{R}'')^*(0)}{\epsilon \tilde{I}'_1} \\ &\quad \times \left[ 1 - (\epsilon - 2\zeta) \frac{1}{\epsilon \tilde{I}'_1} [\tilde{I}'(q) - \tilde{I}'(0)] \right] \end{aligned} \quad (6.24)$$

as a function of  $qL = 2\pi n$ . The asymptotic behavior is

$$\left[ 1 - (\epsilon - 2\zeta) \frac{1}{\epsilon \tilde{I}'_1} [\tilde{I}'(q) - \tilde{I}'(0)] \right] \xrightarrow{q \rightarrow \infty} [1 + b' \epsilon + (\epsilon - 2\zeta) \ln(qL)], \quad (6.25)$$

which defines  $b'$ . The corresponding equation (6.13), when regularizing with a mass, holds. Taking the difference between the two equations yields

$$(b - b')\epsilon = \lim_{q \rightarrow \infty} \frac{\epsilon - 2\zeta}{\epsilon} \left[ \frac{\tilde{I}'(q)}{\tilde{I}'(0)} - \frac{\tilde{I}(q)}{\tilde{I}(0)} \right], \quad (6.26)$$

where  $\tilde{I}(q) := I(q)|_{m=1}$ . To leading order in  $1/\epsilon$ ,  $\tilde{I}'(q) = \tilde{I}'(0) = \tilde{I}(q) = \tilde{I}(0)$ , such that this difference takes the simpler form

$$(b - b')\epsilon = \frac{\epsilon - 2\zeta}{\epsilon \tilde{I}(0)} \times \{ \lim_{q \rightarrow \infty} [\tilde{I}'(q) - \tilde{I}(q)] + [\tilde{I}(0) - \tilde{I}'(0)] \} + O(\epsilon^2). \quad (6.27)$$

Now observe that for large  $q$  the first integral can be bounded by

$$|\tilde{I}'(q) - \tilde{I}(q)| < \frac{\text{const}}{Lq}, \quad (6.28)$$

which is obtained by estimating the maximal difference of integral and discrete sum in each cell (defined by the discreteness of the sum) and then integrating. The difference  $\tilde{I}(0) - \tilde{I}'(0)$  is finite and can be evaluated in  $d=4$  dimensions. We need the formulas

$$\int_0^\infty ds s e^{-s(n^2 + \tau)} = \frac{1}{(n^2 + \tau)^2}, \quad (6.29)$$

$$\int_{-\infty}^\infty dn e^{-sn^2} = \sqrt{\frac{\pi}{s}}, \quad (6.30)$$

$$\sum_{n \in \mathbb{Z}} e^{-sn^2} = \Theta_{3,0}(e^{-s}), \quad (6.31)$$

where  $\Theta_{3,0}(t)$  is the elliptic  $\Theta$  function. This allows to write sum and integral as

$$\sum_{n \in \mathbb{Z}^4, n \neq 0} \frac{1}{(n^2)^2} = \int_0^\infty ds s \{ [\Theta_{3,0}(e^{-s})]^4 - 1 \}, \quad (6.32)$$

$$\int d^4n \frac{1}{(n^2 + 1)^2} = \int_0^\infty ds s \frac{\pi^2}{s^2} e^{-s}. \quad (6.33)$$

The difference in question is integrated numerically:

$$\begin{aligned} \tilde{I}(0) - \tilde{I}'(0) &= \frac{1}{(2\pi)^4} \int_0^\infty ds s \left[ \frac{\pi^2}{s^2} e^{-s} - [\Theta_{3,0}(e^{-s})]^4 + 1 \right] \\ &= -\frac{14.5019}{(2\pi)^4} = -0.009\,304\,79. \end{aligned} \quad (6.34)$$

We thus arrive at  $[\epsilon \tilde{I}(0) = 1/(8\pi^2) + O(\epsilon)]$

$$b' - b = \frac{14.5019}{(2\pi)^4} \frac{1 - 2\zeta_1}{\epsilon \tilde{I}(0)} = 0.734\,676(1 - 2\zeta_1). \quad (6.35)$$

Since the FRG equation and fixed-point value  $(\tilde{R}'')^*(0)$  is universal to two loops, the final result for the amplitude ratio between periodic and massive boundary conditions is

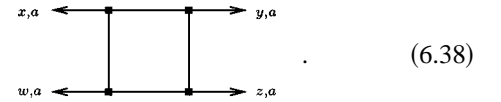
$$\begin{aligned} \frac{c'(d)}{c(d)} &= 1 - 2\zeta \frac{\tilde{I}'(0) - \tilde{I}(0)}{\epsilon \tilde{I}(0)} + O(\epsilon^2) \\ &= 1 - 1.469\,35\zeta + O(\epsilon^2). \end{aligned} \quad (6.36)$$

### B. Four-point functions and higher

Let us now show how to compute higher correlation functions with no ambiguity using the sloop method. Let us illustrate the method on, e.g., the four-point function

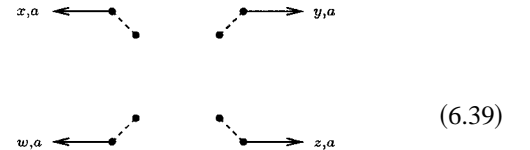
$$\langle u^a(w) u^a(x) u^a(y) u^a(z) \rangle^c. \quad (6.37)$$

The following class of diagrams contributes:



An arrow indicates contraction towards an external field, with position and replica index as indicated. The combinatorial factors are  $1/4!$  from the four  $R$ 's;  $1/2^4$ , the prefactor of the  $R$ 's,  $4!$  the possibilities to connect the  $u$ 's to the  $R$ 's; 3 for the ways to make the loop of  $R$ 's. When contracting first the  $u$ 's, there is another  $2^4$  for the possibilities, to attach the  $u$ 's to the two replicas of  $R$ . Therefore only the factor of 3 remains, which is the combinatorial factor for ordering four points on an unoriented ring.

We start by contracting the four  $u$ 's with four  $R$ 's, schematically,



and then we perform the four other contractions. Since exclusions at each vertex can be introduced early on, the number of possibilities is not too high and one easily obtains

$$\begin{aligned} F := & 5R_{ab}'''^4 + 4R_{ab}'''^3 R_{ac}''' + 2R_{ab}'''^2 R_{ac}'''^2 + 4R_{ab}''' R_{ac}''' R_{ad}'''^2 \\ & + R_{ab}''' R_{ac}''' R_{ad}''' R_{ae}''' , \end{aligned} \quad (6.40)$$

where all terms have to be summed over with excluded replicas at each vertices. Due to the factors of  $R_{ab}'''$  with an odd power, it is not trivial how to project this expression onto the space of 0-replica terms to yield the desired expectation value (as in the previous section  $a$  is fixed and thus no free replica sum should remain in the final result).

To perform this projection we will first simplify the above expression using sloops. There are a number of possible sloops which can be subtracted. The first one is obtained by starting from



$$(6.41)$$

It reads

$$S_1 := R_{ab}^{m4} + R_{ab}^{m3} R_{ac}^{m3} R_{ad}^{m3} R_{ae}^{m3} \equiv 0. \quad (6.42)$$

The next sloop is

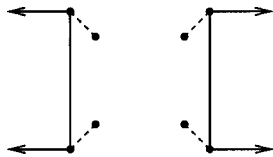


$$(6.43)$$

generating

$$S_2 := R_{ab}^{m4} + 2R_{ab}^{m3} R_{ac}^{m3} + R_{ab}^{m2} R_{ac}^{m2} + 3R_{ab}^{m3} R_{ac}^{m3} R_{ad}^{m2} + R_{ab}^{m3} R_{ac}^{m3} R_{ad}^{m3} R_{ae}^{m3} \equiv 0. \quad (6.44)$$

The last needed sloop is



$$(6.45)$$

leading to

$$S_3 := R_{ab}^{m2} R_{ac}^{m2} + 2R_{ab}^{m3} R_{ac}^{m2} R_{ad}^{m3} + R_{ab}^{m3} R_{ac}^{m3} R_{ad}^{m3} R_{ae}^{m3} \equiv 0. \quad (6.46)$$

The simplest combination out of  $F$ ,  $S_1$ ,  $S_2$ , and  $S_3$  is

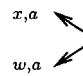
$$F - 2S_2 + S_3 = 3R_{ab}^{m4} + R_{ab}^{m2} R_{ac}^{m2}. \quad (6.47)$$

This expression is unambiguous because only squares of  $R^m(u)$  appear and it is easily projected onto the 0-replica part

$$-2R^m(0^+)^4, \quad (6.48)$$

e.g., one can replace  $R_{ab}^{m3} \rightarrow (1 - \delta_{ab})R_{ab}^{m3}$  in Eq. (6.47) and use free summations.

Other possible contributions are given in Fig. 14. However, none of these diagrams contributes. The reason is that they are all descendants of a sloop. We start by noting that



$$\sim \sum_b R_{ab}^{m2} \quad (6.49)$$

is a true one-replica term—i.e., a sloop. When constructing a diagram in Fig. 14, each of the terms in the excluded replica formalism is proportional to Eq. (6.49), thus descendant of a sloop. This means that to any order in perturbation theory, at  $T=0$ , no diagram contributes to a connected expectation value (of a single replica), which has two lines parting from one  $R$  towards external points.

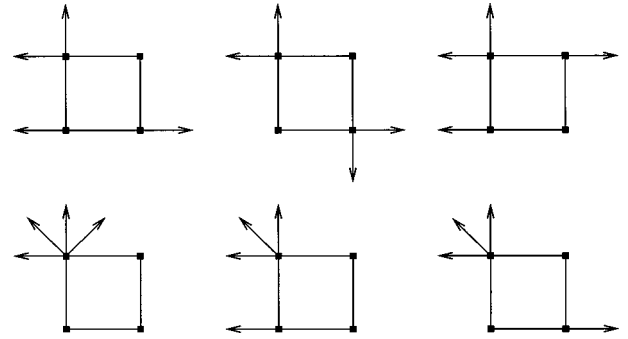


FIG. 14. Other possible contributions to the connected four-point function. They all are higher replica terms and thus do not contribute. Arrows indicate contraction towards external points.

Thus the leading contribution in  $R$  to the connected four-point function, as determined by the sloop method, is the one-loop diagram

$$\begin{aligned} & \langle u^a(w)u^a(x)u^a(y)u^a(z) \rangle^c \\ &= -2R^m(0^+)^4 \int_{rstu} G_{rs} G_{st} G_{tu} G_{ur} (G_{wr} G_{xs} G_{yt} G_{zu} \\ & \quad + G_{ws} G_{xr} G_{yt} G_{zu} + G_{wr} G_{xt} G_{ys} G_{zu}). \end{aligned} \quad (6.50)$$

If one expressed this result in terms of the force correlator  $R^m(0^+)^4 = \Delta^m(0^+)^4$ , we thus find that this expression is formally *identical* to the one that we obtained for the same four-point function at the  $T=0$  quasistatic depinning threshold [Eq. (5.4) in [90]]. This is quite remarkable given that the method of calculation there—i.e., via the nonanalytic dynamical field theory—is very different. Of course, the two physical situations are different and here one must insert the fixed-point value for  $\tilde{R}^m(0^+)$  from the statics FRG fixed point, while in the depinning calculation  $-\tilde{\Delta}^m(0^+)$  takes a different value at the fixed point. In both problems the connected four-point function starts at order  $O(\epsilon^4)$ . However, in some cases the difference appears only to the next order in  $\epsilon$ . For instance, we can conclude that the results of [90] still hold here for the *static random field* to the lowest order in  $\epsilon$  at which they were computed there (of course, one expects differences at next order in  $\epsilon$ ). On the other hand, for the static random-bond case, the result for the connected four-point function will be different from depinning even at leading order in  $\epsilon$ . It can easily be obtained from the above formula following the lines of [90].

## VII. CONCLUSION

In this article we constructed the field theory for the statics of disordered elastic systems. It is based on the functional renormalization group, for which we checked explicitly renormalizability up to two loops. This continuum field theory is novel and highly unconventional: Not only is the

coupling constant a function, but more importantly this function and the resulting effective action of the theory are nonanalytic at zero temperature, which requires a nontrivial extension of the usual diagrammatic formulation.

In a first stage, we showed that two-loop diagrams and *in some cases even one-loop diagrams* are at first sight ambiguous at  $T=0$ . Left unaddressed, this finding by itself puts into question all previous studies of the problem. Indeed, nowhere in the literature was the problem addressed that even the one-loop corrections to the most basic object in the theory, the two-point function, are naively ambiguous in the  $T=0$  theory. Since the problem is controlled by a zero-temperature fixed point, there is no way to avoid this issue. An often invoked criticism states that the problems are due to the limit of  $n \rightarrow 0$  replicas. We would like to point out that even though we use replicas, we use them only as a tool in perturbative calculations, which could equally well be performed using supersymmetry or, at a much heavier cost, using disorder-averaged graphs. So replicas are certainly not at the root of any of the difficulties. Instead, the latter originate from the physics of the system—i.e., the occasional occurrence of quasidegenerate minima—resulting in ambiguities sensible to the preparation of the system. How to deal with this problem within a continuum field theory is an outstanding issue, and any progress in that direction is likely to shed light on other sectors of the theory of disordered systems and glasses.

The method we have proposed to lift the apparent ambiguities is based on two constraints: (a) that the theory be renormalizable—i.e., yields universal predictions—and (b) that it respects the potentiality of the problem—i.e., the fact that all forces are derivatives of a potential. Each of these physical requirements is sufficient to obtain the  $\beta$  function at two-loop order and the two-point function and roughness exponent to second order in  $\epsilon$ . Next, we have proposed several more general, more powerful, and mutually consistent methods to deal with these ambiguous graphs, which work even to higher number of loops and allow one to compute correlation functions with more than two points. We were then able to calculate from our theory the roughness exponents, as well as some universal amplitudes, for several universality classes to order  $O(\epsilon^2)$ . In all cases, the predictions improve the agreement with existing numerical and exact results, as compared to previous one-loop treatments. We also clarified the situation concerning the universality (precise dependence on boundary conditions, independence on small-scale details) of various quantities. Another remarkable finding is that the one-loop contribution to the four-point function is formally identical to the one obtained via the dynamical calculation at depinning. This hints at a general property that *all* one-loop diagrams are undistinguishable in the statics and at depinning. It would be extremely interesting to perform higher-precision numerical simulations of the statics and to determine not only exponents, but universal amplitudes and scaling functions, to test the predictions of our theory. We strongly encourage such studies.

Thus in this paper we have proposed an answer to the highly nontrivial issue of constructing a renormalizable field theory for disordered elastic systems. Contrarily to the

closely related field theory of depinning, which we were able to build from first principles, we have not yet found a first-principles derivation of the theory for the statics. However, we have found that the theory is so highly constrained and the results so encouraging that we strongly believe that our construction of the field is unique. It is, after all, often the case in physics that the proper field theory is first identified by recurrence to higher physical principles such as renormalizability or symmetries, as is exemplified by the Ginsburg-Landau theory of superconductivity, for which only later was a microscopic derivation found, or gauge theories in particle physics.

## ACKNOWLEDGMENTS

It is a pleasure to thank E. Brézin, W. Krauth, and A. Rosso for stimulating discussions. K.J.W. gratefully acknowledges financial support by the Deutsche Forschungsgemeinschaft (Heisenberg Grant No. Wi-1932/1-1), and additional support from the NSF under Grant No. PHY99-07949. P.L.D. thanks the KITP and K.J.W. thanks ENS for hospitality during part of this work.

## APPENDIX A: SYMMETRIZATION METHOD

### 1. Continuity of the renormalized disorder and summary of the method

The first observation is that one expects (if decomposition in  $p$ -replica terms is to mean anything) that one can write the (local disorder part of the) effective action as a sum over well-defined  $p$ -replica terms in the form

$$-\Gamma[u] = \sum_p \frac{1}{T^p} \Gamma_p[u] = \sum_p \frac{1}{p! T^p} \sum_{a_1, \dots, a_p} F^{(p)}(u_{a_1}, \dots, u_{a_p}), \quad (\text{A1})$$

where the functions  $F^{(p)}$  have full permutation symmetry. The idea of the symmetrization method is that we also expect, even at  $T=0$ , that these functions  $F^{(p)}$  should be *continuous* in their arguments when a number of them coincide.

This seems to be a rather weak and natural assumption. Physically, these functions can be interpreted as the  $p$ th connected cumulants of a renormalized disorder—i.e., a random potential  $V_R(u, x)$  in each environment. Discontinuity of the  $F^{(p)}$  would mean that the  $V_R(u, x)$  would not be a continuous function. This is not what one expects. Indeed, discontinuity singularities (the shocks) are expected to occur only in the force  $F_R(u, x) = -\nabla_u V_R(u, x)$  as is clear from the study of the Burgers equation (see, e.g., [54] for a discussion of the simple case: in the elastic manifold formulation the shocks corresponds to rare ground-state degeneracies). One thus expects  $V_R(u, x)$  to be a continuous function of  $u$ .

A further and more stringent assumption, discussed above, is the absence of a supercusp. A supercusp would mean  $R'(0^+) > 0$ . Thus we assume that the nonanalyticity in



the effective action starts as  $|u|^3$ . The usual interpretation<sup>7</sup> is that there is a finite density of shocks and just counting how many shocks there is in a interval between  $u$  and  $u'$  yields the  $|u - u'|^3$  nonanalyticity in  $R(u)$ .

Let us summarize the method before detailing actual calculations.

We thus define here the symmetrization method assuming no supercusp as a working hypothesis. We then *compute* corrections to the (local disorder part of the) effective action up to a given order in powers of  $R$ , with excluded vertices for any vector such that  $u_a \neq u_b$  for  $a \neq b$ , thus with no ambiguity. This yields, as in Sec. VB 1, sums over more than two replicas with exclusions. These exclusions are not permutation symmetric, so we first rewrite them in an explicitly permutation symmetric way which can be done with no ambiguity (see below). Thus we have a sum of terms of the form

$$\sum_{a_1, \dots, a_p; 2 \neq 2} f^s(u_{a_1}, \dots, u_{a_p}), \quad (\text{A2})$$

where  $2 \neq 2$  is a shorthand notation for  $a_i \neq a_j$  for all  $i \neq j$ —i.e., symmetrized exclusions. Each function  $f$  is fully permutation symmetric, as indicated by the  $s$  superscript. Next, the nontrivial part is that we *explicitly verify* that these *symmetrized* corrections can indeed be continued to coinciding points unambiguously—e.g., the limit  $f^s(u_1, u_1, u_3, \dots, u_{a_p})$  exists and is independent of the direction of approach. This in itself shows that the continuity discussed above seems to work. The existence of a four-replica term obliges us to also consider three coinciding points. This is done by considering  $f^{ss}(u_1, u_1, u_3, u_4)$ —i.e., symmetrizing the result of two coinciding points over  $u_1, u_3, u_4$  and then taking  $u_3 \rightarrow u_1$ . We check explicitly that this again gives a function which can be continued unambiguously. Thus, at first sight, it would appear as the ideal method to extract the functions  $F^{(p)}$  above to order  $R^3$ .

## 2. Calculations

Let us reconsider the diagrams of Fig. 13. We first transform them in sum with symmetrized constraints. We illustrate this on diagram  $\beta$  where the sum can be reorganized as

<sup>7</sup>One should be careful in these arguments, and consider the precise definition of  $R(u)$ . Indeed, one could argue that if there are many small shocks they could build a supercusp. For instance, consider the nontrivial  $d=0$  limit of the random-field model, when  $V(u)$  has at large  $u$  the statistics of a Brownian motion. Then, in some definitions of a coarse-grained disorder, e.g., such as used in [71] where this model was solved exactly,  $V_R(u)$  is a continuous one-dimensional Brownian motion, thus with a infinite number of small shocks and indeed a supercusp. However, in the present paper,  $V_R(u)$  is defined from the replicated effective action and not from the action, and should possess—in that case—a weaker singularity.

$$\begin{aligned} \beta &\sim \sum_{a \neq b, a \neq c} R''_{ab} R'''_{ab} R'''_{ac} \\ &= \sum_{ab; 2 \neq 2} R''_{ab} R'''_{ab}{}^2 + \sum_{abc; 2 \neq 2} R''_{ab} R'''_{ab} R'''_{ac}, \end{aligned} \quad (\text{A3})$$

with clearly no ambiguity. Performing similar rearrangement on all the graphs of class A yields the sum of the graphs:

$$\begin{aligned} \delta_A R &= 4 \sum_{ab; 2 \neq 2} R''_{ab} R'''_{ab}{}^2 + 2 \sum_{abc; 2 \neq 2} R''_{ab} R'''_{ab} R'''_{ac} \\ &\quad - \frac{1}{2} \sum_{abc; 2 \neq 2} R''_{ab} R'''_{ac} R'''_{bc} + 2 \sum_{abc; 2 \neq 2} R''_{ab} R'''_{ac}{}^2 \\ &\quad + \frac{1}{2} \sum_{abcd; 2 \neq 2} R''_{ab} R'''_{ac} R'''_{ad}. \end{aligned} \quad (\text{A4})$$

Now we use the property that has worked on all the examples needed here: namely, that a symmetric continuous function on  $\{(x_1, \dots, x_p); i \neq j \Rightarrow x_i \neq x_j\}$  is continuous on  $R^p$ . Writing for any  $f(x_1, \dots, x_p)$  symmetric and continuous,

$$\sum_{2 \neq 2} f = \sum_{a_1, \dots, a_p} \prod_{i < j} (1 - \delta_{a_i a_j}) f(x_{a_1}, \dots, x_{a_p}), \quad (\text{A5})$$

and expanding yields, for the three and four-replica sums,

$$\begin{aligned} \sum_{abc; 2 \neq 2} f_{abc} &= \sum_{abc} f_{abc} - 3 \sum_{ab} f_{aab} + 2 \sum_a f_{aaa} \\ \sum_{abcd; 2 \neq 2} f_{abcd} &= \sum_{abcd} f_{abcd} - 6 \sum_{abc} f_{aabc} + 3 \sum_{ab} f_{aabb} \\ &\quad + 8 \sum_{ab} f_{aaab} - 6 \sum_a f_{aaaa} \end{aligned} \quad (\text{A6})$$

in shorthand notation such that  $f_{abcd} = f(u_a, u_b, u_c, u_d)$ . This is just combinatorics.

For the three-replica sums the procedure is straightforward, as symmetrization makes manifest the continuity. One easily finds (we drop an uninteresting single-replica term)

$$\begin{aligned} \sum_{abc; 2 \neq 2} R''_{ab} R'''_{ab} R'''_{ac} &= \sum_{abc} R''_{ab} R'''_{ab} R'''_{ac} - \sum_{ab} R''_{ab} R'''_{ab}{}^2 \\ \sum_{abc; 2 \neq 2} R''_{ab} R'''_{ac}{}^2 &= \sum_{abc} R''_{ab} R'''_{ac}{}^2 - \sum_{ab} [R''_{ab} R'''_{ac}(0) +]^2 \\ &\quad + R''_{ab} R'''_{ab}{}^2 + R''(0) R'''_{ab}{}^2 \end{aligned}$$

$$\sum_{abc; 2 \neq 2} R''_{ab} R'''_{ac} R'''_{bc} = \sum_{abc} R''_{ab} R'''_{ac} R'''_{bc} - \sum_{ab} R''(0) R'''_{ab}{}^2,$$

where in the first line we have applied Eq. (A6) to  $f_{abc} = \text{sym}_{abc} R''_{ab} R'''_{ab} R'''_{ac}$  and so on (we define  $\text{sym}_{a_1 \dots a_p}$  as the sum over all permutations divided by  $p!$ ).

For the four-replica term we find that  $f_{abcd} = \text{sym}_{abcd} R''_{ab} R'''_{ac} R'''_{ad}$  has the following limits (in a symbolic form, omitting the free summations):

$$\begin{aligned} f_{aabc} &= \frac{1}{6} R''(0) R'''_{ab} R'''_{ac} - \frac{1}{6} R''_{ab} R'''_{ab} R'''_{bc} + \frac{1}{6} R''_{ac} R'''_{ac} R'''_{bc} \\ &+ \frac{1}{12} R''_{bc} R'''_{ab}{}^2 + \frac{1}{12} R''_{bc} R'''_{ac}{}^2, \\ f_{aabb} &= \frac{1}{3} R''(0) R'''_{ab}{}^2, \\ f_{aaab} &= \frac{1}{12} R''_{ab} R'''(0+)^2 + \frac{1}{4} R''_{ab} R'''_{ab}{}^2, \end{aligned}$$

where at each step we had to symmetrize before taking coinciding point limits (checking that this limit was unambiguous in each case).

The final result is found to be

$$\delta_A R_{ab} = [R''_{ab} - R''(0)](R'''_{ab})^2 - \frac{5}{3} R''_{ab} [R'''(0+)]^2. \quad (\text{A7})$$

The same procedure applied to the repeated counterterm confirms that it is unambiguous and given by Eq. (3.38). Thus, because of the ominous 5/3 coefficient above, rather than the expected 1, the theory, using this procedure, is not renormalizable.

Diagrams of class *B* and *C* behave properly. One finds with the same method their projections on the two-replica part:

$$\alpha' = \frac{1}{2} R'''_{ab} R''_{ab} R''_{ab}, \quad (\text{A8})$$

$$\beta' = \frac{1}{4} [2R'''(0)R''(0)R''_{ab} + R'''_{ab}R''(0)^2], \quad (\text{A9})$$

$$\gamma' = \beta', \quad (\text{A10})$$

$$\delta' = -2[R'''(0)R''(0)R''_{ab} + R'''_{ab}R''_{ab}R''(0)]. \quad (\text{A11})$$

Note the  $R'''(0)$ , which here is defined as  $R'''(0) = R'''(0+) = R'''(0-)$  since  $R'''(u)$ , can be continued at zero. One has, using the expressions given in Appendix C,

$$\alpha'' = R'''(0)(R''_{ab})^2 + 2R'''_{ab}R''(0)R''_{ab}, \quad (\text{A12})$$

$$\beta'' + \delta'' = -2[R'''(0)R''(0)R''_{ab} + R'''_{ab}R''_{ab}R''(0)], \quad (\text{A13})$$

$$\gamma'' + \lambda'' = R'''_{ab}R''(0)^2 + 2R'''(0)R''(0)R''_{ab}, \quad (\text{A14})$$

$$\nu'' + \eta'' = -\{R'''(0)(R''_{ab})^2 + R'''_{ab}[R''(0)]^2\}. \quad (\text{A15})$$

These graphs (more precisely their contribution to two-replica terms) sum exactly to zero:

$$\alpha'' + \beta'' + \gamma'' + \delta'' + \eta'' + \lambda'' + \nu'' = 0, \quad (\text{A16})$$

in agreement with the result of the ambiguous diagrammatics in the case of an analytic function.

To conclude, although promising at first sight, this method is not satisfactory. The projection defined here seems to fail to commute with further contractions. For instance, one can check that upon building diagrams *A* by contracting the subdiagram (a) in Fig. 2 onto a third vertex does give different answers if one first projects (a) or not. Since (a) is the divergent subdiagram, this spoils renormalizability. Since the initial assumptions of the method were rather weak and natural, it would be interesting to see whether this problem can be better understood in order to repair this method.

## APPENDIX B: DIRECT NONANALYTIC PERTURBATION THEORY

In this section we give some details on the method where one performs straight perturbation theory using a nonanalytic disorder correlator  $R_0(u)$  in the action. Expanding in  $R_0(u)$ , this involves computing Gaussian averages of nonanalytic functions: thus, we start by giving a short list of formulas useful for the field theory calculations of this section. One should keep in mind that these formulas are equally useful for computing averages of nonanalytic *observables* in a Gaussian (or more generally, analytic) theory.

### 1. Gaussian averages of nonanalytic functions: Formulas

We start by deriving some auxiliary functions, then give a list of expectation values for nonanalytic observables of a general Gaussian measure.

We need

$$\int_0^\infty dq (e^{iqx} + e^{-iqx}) e^{-\eta q} = \frac{2\eta}{\eta^2 + x^2}. \quad (\text{B1})$$

Integrating once over  $x$  starting at 0 yields

$$\frac{1}{i} \int_0^\infty \frac{dq}{q} (e^{iqx} - e^{-iqx}) e^{-\eta q} = 2 \arctan\left(\frac{x}{\eta}\right). \quad (\text{B2})$$

The right-hand side reduces in the limit of  $\eta \rightarrow 0$  to  $\pi \text{sgn}(x)$ , which gives a representation of  $\text{sgn}(x)$ :

$$\begin{aligned} \text{sgn}(x) &= \lim_{\eta \rightarrow 0} \frac{2}{\pi} \int_0^\infty \frac{dq}{q} \sin(qx) e^{-\eta q} \\ &= \lim_{\eta \rightarrow 0} \frac{1}{\pi} \int_{-\infty}^\infty \frac{dq}{q} \sin(qx) e^{-\eta|q|}. \end{aligned} \quad (\text{B3})$$

By integrating once more, we obtain

$$|x| = \lim_{\eta \rightarrow 0} \frac{2}{\pi} \int_0^\infty \frac{dq}{q^2} [1 - \cos(qx)] e^{-\eta q}. \quad (\text{B4})$$

This formula is easily generalized to higher odd powers of  $|x|$ , by integrating more often. The result is

$$|x|^{2n-1} = \lim_{\eta \rightarrow 0} \frac{2}{\pi} (-1)^n \Gamma(2n) \int_0^\infty \frac{dq}{q^{2n}} e^{-\eta q} \cos(qx) \Big|_n, \tag{B5}$$

where  $\cos(qx)|_n$  means that one has to subtract the first  $n$  Taylor coefficients of  $\cos(qx)$ , such that  $\cos(qx)|_n$  starts at order  $(qx)^{2n}$ :

$$\cos(qx)|_n := \sum_{\ell=n}^\infty \frac{[-(qx)^2]^\ell}{(2\ell)!}. \tag{B6}$$

We now study expectation values. We use the measure

$$\begin{pmatrix} \langle xx \rangle & \langle xy \rangle \\ \langle yx \rangle & \langle yy \rangle \end{pmatrix} = \begin{pmatrix} 1 & t \\ t & 1 \end{pmatrix}, \tag{B7}$$

from which the general case can be obtained by simple rescaling  $x \rightarrow x/\langle xx \rangle^{1/2}$ ,  $y \rightarrow y/\langle yy \rangle^{1/2}$ . Let us give an explicit example (we drop the convergence-generating factor  $e^{-\eta q}$  since it will turn out to be superfluous.)

$$\begin{aligned} \langle |x| \rangle &= \frac{1}{\pi} \int_0^\infty \frac{dq}{q^2} (2 - \langle e^{iqx} \rangle - \langle e^{-iqx} \rangle) \\ &= \frac{2}{\pi} \int_0^\infty \frac{dq}{q^2} (1 - e^{-q^2/2}) \\ &= \sqrt{\frac{2}{\pi}}. \end{aligned} \tag{B8}$$

A more interesting example is

---


$$\begin{aligned} \langle \text{sgn}(x) \text{sgn}(y) \rangle &= -\frac{1}{\pi^2} \int_0^\infty \frac{dq}{q} \int_0^\infty \frac{dp}{p} \sum_{\sigma, \tau = \pm 1} \sigma \tau \langle e^{iq\sigma x} e^{ip\tau y} \rangle \\ &= -\frac{1}{\pi^2} \int_0^\infty \frac{dq}{q} \int_0^\infty \frac{dp}{p} \sum_{\sigma, \tau = \pm 1} \sigma \tau e^{-(p^2+q^2)/2 - \sigma \tau p q t} \\ &= \frac{1}{2\pi^2} \int_{-\infty}^\infty \frac{dq}{q} \int_{-\infty}^\infty \frac{dp}{p} e^{-(p^2+q^2)/2} (e^{pqt} - e^{-pqt}) \\ &= \frac{1}{2\pi^2} \int_0^t ds \int_{-\infty}^\infty dq \int_{-\infty}^\infty dp e^{-(p^2+q^2)/2} (e^{pqs} + e^{-pqs}) \\ &= \frac{2}{\pi} \int_0^t ds \frac{1}{\sqrt{1-s^2}} = \frac{2}{\pi} \arcsin(t). \end{aligned} \tag{B9}$$

Another generally valid strategy is to use a path integral. We note the important formula

$$\begin{aligned} \langle f(x, y) \rangle &= \frac{1}{2\pi\sqrt{1-t^2}} \int_{-\infty}^\infty dx \int_{-\infty}^\infty dy f(x, y) \\ &\quad \times \exp\left[-\frac{x^2+y^2-2txy}{2(1-t^2)}\right]. \end{aligned} \tag{B10}$$

An immediate consequence is

$$\begin{aligned} \langle f(x) \delta(y) \rangle &= \frac{1}{2\pi\sqrt{1-t^2}} \int_{-\infty}^\infty dx f(x) \exp\left[-\frac{x^2}{2(1-t^2)}\right] \\ &= \frac{1}{2\pi} \int_{-\infty}^\infty dz f(z\sqrt{1-t^2}) \exp(-z^2) \\ &= \frac{1}{\sqrt{2\pi}} \langle f(x\sqrt{1-t^2}) \rangle. \end{aligned} \tag{B11}$$

The very existence of the path-integral representation (B10) also proves that Wick's theorem remains valid. Let us give an example which can be checked by using either Eq. (B10) or (B8):

$$\begin{aligned} \langle x^2 |y| \rangle &= \langle x^2 \rangle \langle |y| \rangle + 2 \langle xy \rangle \langle x \text{sgn}(y) \rangle \\ &= \langle x^2 \rangle \langle |y| \rangle + 2 \langle x, y \rangle^2 \langle \delta(y) \rangle \\ &= \sqrt{\frac{2}{\pi}} (1+t^2). \end{aligned} \tag{B12}$$

We finish our excursion by giving a list of useful formulas, which can be obtained by both methods:

$$\langle |xy| \rangle = \frac{2}{\pi} [\sqrt{1-t^2} + t \arcsin(t)], \tag{B13}$$

$$\langle xy|y| \rangle = 2 \sqrt{\frac{2}{\pi}} t, \tag{B14}$$

$$\langle xy|xy\rangle = \frac{2}{\pi} [3t\sqrt{1-t^2} + (1+2t^2)\arcsin(t)], \quad (\text{B15})$$

$$\langle |xy^3| \rangle = \frac{2}{\pi} [(2+t^2)\sqrt{1-t^2} + 3t\arcsin(t)]. \quad (\text{B16})$$

## 2. Perturbative calculation of the two-point function with a nonanalytic action

Let us consider the expansion of the two-point function

$$\langle u_x^a u_y^b \rangle = \frac{1}{T^2} \langle u_x^a u_y^b \mathcal{R} \rangle + \frac{1}{2T^4} \langle u_x^a u_y^b \mathcal{R} \mathcal{R} \rangle + O(\mathcal{R}^3) \quad (\text{B17})$$

in powers of the disorder<sup>8</sup> where  $\mathcal{R} = \frac{1}{2} \int_z \Sigma_{ef} R_0(u_z^{ef})$ , with  $u_z^{ef} = u_z^e - u_z^f$ . We want to evaluate these averages at  $T=0$  with a nonanalytic action  $R_0(u)$ . We restrict ourselves to  $a \neq b$ , since at  $T=0$  the result should be the same for  $a=b$ , and we drop the subscript 0 from now on. As mentioned above, the Wick theorem still applies: thus, we can first contract the external legs. The term linear in  $\mathcal{R}$  yields the dimensional reduction result (2.14): thus, we note  $\langle u_x^a u_y^b \rangle = \langle u_x^a u_y^b \rangle_{\text{DR}} + \langle u_x^a u_y^b \rangle'$  and we find

$$\begin{aligned} \langle u_x^a u_y^b \rangle' &= \frac{1}{T^2} \int_{zw} \left( G_{xz} G_{yw} \left\langle \sum_{cd} R'(u_z^{ac}) R'(u_w^{bd}) \right\rangle \right. \\ &\quad \left. - \frac{1}{2} G_{xz} G_{yz} \left\langle \sum_{cd} R''(u_z^{ab}) R(u_w^{cd}) \right\rangle \right) \quad (\text{B18}) \end{aligned}$$

up to  $O(\mathcal{R}^3)$  terms. For peace of mind one can introduce the restrictions  $c \neq a$ ,  $d \neq b$  in the first sum and  $c \neq d$  in the second, but this turns out to be immaterial at the end. We need only, in addition to Eq. (5.2),

$$\begin{aligned} R'(u) &= R''(0)u + \frac{1}{2} R'''(0^+) |u| + \frac{1}{6} R''''(0^+) u^3, \\ R''(u) &= R''(0) + R'''(0^+) |u| + \frac{1}{6} R''''(0^+) u^2, \quad (\text{B19}) \end{aligned}$$

since higher-order terms in  $u$  yield higher powers of  $T$ . Using Eq. (B13) to evaluate Gaussian averages, this yields

$$\begin{aligned} \langle u_x^a u_y^b \rangle' &= R'''(0^+) G_{zz}^2 \int_{zw} \left( G_{xz} G_{yw} \sum_{cd} \phi_1(t) \right. \\ &\quad \left. - \frac{1}{3} G_{xz} G_{yz} \sum_{cd} \phi_2(t') \right), \quad (\text{B20}) \end{aligned}$$

where we denote

$$t = \frac{G_{zw}}{2G_{zz}} (\delta_{ab} + \delta_{cd} - \delta_{ad} - \delta_{bc}), \quad (\text{B21})$$

$$t' = \frac{G_{zw}}{2G_{zz}} (\delta_{ac} + \delta_{bd} - \delta_{ad} - \delta_{bc}), \quad (\text{B22})$$

$$\phi_1(t) = \frac{2}{\pi} [3t\sqrt{1-t^2} + (1+2t^2)\arcsin(t)], \quad (\text{B23})$$

$$\phi_2(t') = \frac{2}{\pi} [(2+t'^2)\sqrt{1-t'^2} + 3t'\arcsin(t')]. \quad (\text{B24})$$

Note that the cross terms  $R''(0)R''''(0^+)$  involve analytic average<sup>9</sup> and yield zero (a remnant of dimensional reduction). Also, to this order, no terms with negative powers of  $T$  survive for  $n=0$  (see discussion below). Performing the combinatorics in the replica sums, we find, for  $n=0$ ,

$$\begin{aligned} \langle u_x^a u_y^b \rangle' &= R'''(0^+) G_{zz}^2 \int_{zw} \left[ G_{xz} G_{yw} \Phi_1 \left( \frac{G_{zw}}{G_{zz}} \right) \right. \\ &\quad \left. + G_{xz} G_{yz} \Phi_2 \left( \frac{G_{zw}}{G_{zz}} \right) \right], \quad (\text{B25}) \end{aligned}$$

$$\Phi_1(s) = 2\phi_1\left(\frac{s}{2}\right) - \phi_1(s), \quad (\text{B26})$$

$$\Phi_2(s) = -\frac{2}{3}\phi_2(s) + \frac{8}{3}\phi_2\left(\frac{s}{2}\right) - 2\phi_2(0). \quad (\text{B27})$$

It is important for the following to note that cancellation occur in the small-argument behavior of these functions: namely, one has  $\Phi_1(s) = -s^3/\pi + O(s^5)$  and  $\Phi_2(s) = s^4/(4\pi) + O(s^6)$ . In  $d=0$  it simplifies (setting  $G_{xy} = 1/m^2$  and restoring the subscript) to

$$\langle u^a u^b \rangle = -\frac{R_0''(0)}{m^4} - A \frac{R_0'''(0^+)^2}{m^8} + O(R_0^3/m^{12}), \quad (\text{B28})$$

with  $A = (24 - 27\sqrt{3} + 8\pi)/(3\pi)$ . As such, this formula and Eq. (B25) seem fine and it may even be possible to check them numerically in  $d=0$  for large  $m$  using a bare disorder with the proper nonanalytic correlator  $R_0(u)$ . To obtain the asymptotic  $m \rightarrow 0$  and large-scale behavior in any  $d$ , one must resum higher orders and use an RG procedure. The question is whether the above formula (B25) can be used in an RG treatment.

## 3. Discussion

We found that this procedure does not work and we now explain why. Let us rewrite the result (B25), including the dimensional reduction term:

$$C_{ab}(q) = \frac{-R_0''(0) - R_0'''(0^+)^2 [A_1(q) + A_2(0)]}{(q^2 + m^2)^2},$$

<sup>8</sup>These averages are connected but this is not needed here.

<sup>9</sup> $R''(0)$  can always be set formally to zero by a trivial additive random force contribution.

$$A_i(q) = \int d^d x e^{iqx} G(x)^2 \psi_i(x),$$

$$\psi_i(x) = - \left( \frac{G(0)}{G(x)} \right)^2 \Phi_i \left( \frac{G(x)}{G(0)} \right), \quad (\text{B29})$$

with  $i=1,2$ . One notes that if  $\psi_1(x)$  were a constant equal to unity, one would recover the result (6.5) obtained in Sec. VI. However, one easily sees that while  $\psi_1(x) \approx 0.346$  approaches a constant as  $x \ll a$  where  $a \sim 1/\Lambda$  is an ultraviolet cutoff, it decreases as  $\psi_1(x) \sim x^{2-d}$  at large  $x$ , as a result of the above-mentioned cancellations in the small-argument behavior of the functions  $\Phi_i(x)$ . Thus the infrared divergence responsible for all interesting anomalous dimensions in the two-point function as the nontrivial value of  $\zeta$  is destroyed, and the method fails. Even more, the theory would not even be renormalizable.

We have performed a similar calculation in the dynamical field theory formulation of the equilibrium problem in the limit  $T \rightarrow 0$ , using a nonanalytic action. There the method fails for very similar reasons. Only at the depinning threshold were we able to construct the dynamical theory as explained in [68,69]. One might suspect that one has to start with a somehow “normal-ordered” theory where self-contractions—i.e., terms proportional to  $G_{xx}$ —are removed, since they *never* appear in the  $T=0$  perturbation theory. We have not been able to find such a formulation.

Another problem with direct perturbation theory in a nonanalytic action is that there is *a priori* no guarantee that it has a well-defined  $T=0$  limit. Let us illustrate this in a simple example in  $d=0$ . The following correlation has been computed exactly by a completely different method [71] for the random-field model in  $d=0$  (Brownian motion plus quadratic energy landscape:  $\langle \cdots \rangle_0$  indicates averages over all  $u$ ):

$$\langle u_a^2 \rangle_\sigma = \left\langle u_a^2 \exp \left( \sum_{cd} \frac{\sigma}{2T^2} |u_c - u_d| - \frac{1}{2} m^2 \sum_c u_c^2 \right) \right\rangle_0$$

$$= C_2 \sigma^{2/3} m^{-8/3}, \quad (\text{B30})$$

a result which is also obtained by extrapolation from  $d=4$  using the FRG, as detailed in Sec. IV B 2.

On the other hand, the above perturbative method yields, expanding in  $\sigma$ ,

$$\langle u_a^2 \rangle_\sigma = \frac{T}{m^2} + \frac{\sigma}{\sqrt{T} m^3} \frac{1}{\pi} \sum_{c \neq d} (1+t^2) + O(\sigma^2), \quad (\text{B31})$$

with  $t = (\delta_{ac} - \delta_{ad})/\sqrt{2}$ . In the zero-temperature limit,  $\langle u_a^2 \rangle_\sigma \approx -\sigma/\sqrt{T} m^3 + O(\sigma^2)$ , which is ill behaved. The absence of a well-defined Taylor expansion in the zero-temperature limit is of course a sign that the correct result (B30) is simply nonanalytic in  $\sigma$ . Although this solvable example involves a correlator  $R_0(u)$  with a *supercusp*, it is possible that a similar problem occurs at higher orders (three or higher) in the expansion of the two-point function in the case of the usual cusp nonanalyticity. There have been conflicting claims in the literature about this question [47,54]—

i.e., the presence of fractional powers at higher orders of the expansion in a nonanalytic disorder—and it may be worth reexamining. It is however important to note that, since the  $\epsilon$  expansion proposed in the main text is not based on such a direct expansion, it *does not* yield fractional powers of  $\epsilon$ , contrarily to what was conjectured in [47].

Finally, let us point out some properties of nonanalytic observables. Let us study, e.g.,  $\langle |u_a^x| \rangle$ . Expansion in powers of  $\mathcal{R}$  yields a first-order term  $\sim 1/\sqrt{T}$ . This is the sign of nonanalytic behavior, and indeed it is easy to find that

$$\langle |u_a^x| \rangle = \frac{2}{\pi} \sqrt{\langle (u_a^x)^2 \rangle_{\text{DR}}} - \frac{2\sqrt{2}}{3\pi} R_0''(0^+) G(0)^2$$

$$\times \int_y [\sqrt{1-t^2}(2+t^2) + 3t \arcsin(t) - 2] + O(R^2), \quad (\text{B32})$$

where  $\langle (u_a^x)^2 \rangle_{\text{DR}} = -\int_q R_0(0)''/(q^2+m^2)^2$  and  $t = G(y)/\sqrt{2}G(0)$ . The first term is obtained by noting that  $R_0''(0)$  acts as a Gaussian random force, which can then be separated from the nonlinear force, and the last term, evaluated using the above formula, is the only one which survives at  $T=0$  to linear order in  $R_0$ . The formula (B32) is interesting as a starting point to compute universal ratio, such as  $\langle |u_a^x| \rangle^2 / \langle (u_a^x)^2 \rangle$  or  $\langle |u_a^x - u_a^y| \rangle^2 / \langle (u_a^x - u_b^y)^2 \rangle$ . Indeed, one notes that for  $d < 4$  the integral in the term proportional to  $R_0''(0^+)$  is infrared divergent at large  $y$ . This is left for future study.

### APPENDIX C: DIAGRAMS OF CLASS C

In this appendix we give the expression of each of the diagrams of class C represented in Fig. 13 in the excluded (nonambiguous) diagrammatics. One finds, including all combinatorial factors,

$$\delta'' = \beta'', \quad \lambda'' = \gamma'', \quad \nu'' = \eta'', \quad (\text{C1})$$

with

$$\alpha'' = -R_{ab}''' R_{ac}'' R_{bc}'', \quad (\text{C2})$$

$$\beta'' + \delta'' = 2R_{ab}''' R_{ab}'' R_{bc}'', \quad (\text{C3})$$

$$\gamma'' + \lambda'' = R_{ab}''' R_{ac}'' R_{ad}'', \quad (\text{C4})$$

$$\eta'' + \nu'' = R_{ac}''' (R_{ab}'')^2. \quad (\text{C5})$$

### APPENDIX D: SLOOP CALCULATION OF DIAGRAMS B AND C

Let us consider the expression  $\delta_B R$  for the B diagrams in the excluded diagrammatics (5.14). Let us start again from a single sloop (5.18) and (5.19) and contract this time between  $y$  and  $z$  twice to produce a diagram of type B. This yields

$$\begin{aligned}
 \text{Diagram} &= \frac{1}{2} R''(0) \sum_{a \neq b} R_{ab}''' R_{ab}'' \\
 &+ \frac{1}{2} R''(0) \sum_{a \neq b, b \neq c} R_{ab}''' R_{bc}'' + \frac{1}{2} \sum_{a \neq b, b \neq c} R_{ab}'' R_{bc}''' R_{bc}'' \\
 &+ \frac{1}{4} \sum_{a \neq b, a \neq c, c \neq d} R_{ab}'' R_{ac}''' R_{cd}'' \\
 &+ \frac{1}{4} \sum_{a \neq c, b \neq c, c \neq d} R_{bc}'' R_{ac}''' R_{cd}'' \equiv 0 \quad (D1)
 \end{aligned}$$

the terms  $R''(0)$  arising because the first vertex is not contracted in the process, so one must separate the (unambiguous) diagonal part to obtain excluded sums.

If one subtracts this identity from Eq. (5.14), one finds that there remain some improper three-replica terms (the improper four-replica term, however, cancels). This is because in the process of our last contractions we have generated new sloops, but since replicas were excluded, they have to be extracted with care.

Let us rewrite the two possible “double sloops” from unrestricted sums to restricted:

$$\begin{aligned}
 \text{Diagram} &= \frac{1}{2} \sum_{abcd} R_{ac}'' R_{ab}''' R_{ad}'' \\
 &= \frac{1}{2} \sum_{a \neq b, a \neq c, a \neq d} R_{ac}'' R_{ab}''' R_{ad}'' + \frac{1}{2} \sum_{a \neq b} R''(0)^2 R_{ab}''' \\
 &+ \sum_{a \neq b} R''(0) R_{ab}''' R_{ac}'' \quad (D2)
 \end{aligned}$$

$$\begin{aligned}
 \text{Diagram} &= \frac{1}{2} \sum_{abcd} R_{ac}'' R_{ab}''' R_{bd}'' \\
 &= \frac{1}{2} \sum_{a \neq b, a \neq c, b \neq d} R_{ac}'' R_{ab}''' R_{bd}'' + \frac{1}{2} \sum_{a \neq b} R''(0)^2 R_{ab}''' \\
 &+ \sum_{a \neq b} R''(0) R_{ab}''' R_{ac}'' \quad (D3)
 \end{aligned}$$

In the process we have set to zero the terms

$$\frac{1}{2} R'''(0) \sum_{acd} R_{ac}'' R_{ad}'' \rightarrow 0, \quad (D4)$$

$$\frac{1}{2} R'''(0) \sum_{acbd} R_{ac}'' R_{bd}'' \rightarrow 0, \quad (D5)$$

since they are proper three- and four-replica terms.

Defining now

$$\text{Diagram} := \frac{1}{2} \left[ \text{Diagram 1} + \text{Diagram 2} \right]. \quad (D6)$$

The simplest combination which allows to extract the two-replica part is

$$\begin{aligned}
 \text{Diagram} &- 2 \text{Diagram} + \text{Diagram} \\
 &= \frac{1}{2} \sum_{a,b} R_{ab}''' (R_{ab}'' - R_0'')^2. \quad (D7)
 \end{aligned}$$

We now turn to graphs  $C$ . The expression for  $\delta_C R$  is given as the sum of all contributions in Appendix C. Within the sloop method it gives immediately zero:  $\delta_C R = 0$ . This is because one can start by contracting the tadpole. Since this is a sloop, it can be set to zero:

$$\frac{1}{8T^5} G_{xx} \sum_{abcdef} R''(u_{ab}^x) R(u_{cd}^y) R(u_{ef}^z) \equiv 0. \quad (D8)$$

Upon further contractions, proceeding as in Sec. VB, one obtains exactly that the sum of all graphs  $C$  with excluded vertices is identically zero. Graphs  $C$  sum to zero since they are all descendants of a sloop.

### APPENDIX E: CALCULATION OF AN INTEGRAL

We will illustrate the universality of

$$X = \frac{2\epsilon(2I_A - I_1^2)}{(\epsilon I_1)^2} \quad (E1)$$

using a broad class of IR cutoff functions—namely, a propagator

$$\frac{1}{q^2 + m^2} \rightarrow \int dx \frac{g(x)}{q^2 + xm^2}. \quad (E2)$$

Here we denote  $\int_x A(x) \equiv \int dx g(x) A(x)$  and we normalize  $\int dx g(x) = 1$  (consistent with fixing the elastic coefficient to unity). We will show that  $X = 1 + O(\epsilon)$  independent of  $g(x)$ .

First, we write

$$\begin{aligned}
 I_1 &= \int_{x,x'} \int_q \frac{1}{(q^2 + xm^2)(q^2 + x'm^2)} \\
 &= \int_{x,x'} \int_{\alpha_1 > 0, \alpha_2 > 0} e^{-\alpha_1(q^2 + xm^2) + \alpha_2(q^2 + x'm^2)} \\
 &= \left( \int_q e^{-q^2} \right) \int_{x,x'} \int_0^\infty d\alpha_1 \int_0^\infty d\alpha_2 (\alpha_1 + \alpha_2)^{-d/2} \\
 &\quad \times e^{-m^2(\alpha_1 x + \alpha_2 x')}, \quad (E3)
 \end{aligned}$$

and using the parametrization  $\alpha = \alpha_1 + \alpha_2$  and  $\lambda \alpha = (\alpha_1 - \alpha_2)/2$ , one obtains

$$\begin{aligned}
 I_1 &= \left( \int_q e^{-q^2} \right) \int_{x,x'} \int_{-1/2}^{1/2} d\lambda \int_0^\infty d\alpha \alpha^{1-d/2} \\
 &\quad \times e^{-m^2 \alpha [(x+x')/2 + \lambda(x-x')]} \\
 &= m^{-\epsilon} \left( \int_q e^{-q^2} \right) \Gamma\left(\frac{\epsilon}{2}\right) \int_{x,x'} \int_{-1/2}^{1/2} d\lambda \\
 &\quad \times \left[ \frac{x+x'}{2} + \lambda(x-x') \right]^{-\epsilon/2}. \quad (E4)
 \end{aligned}$$

The hat diagram is

$$\begin{aligned}
 I_A &= \int_{x_i} \int_{q_1, q_2} \frac{1}{(q_1^2 + x_1 m^2)(q_2^2 + x_2 m^2)(q_2^2 + x_2' m^2)((q_1 + q_2)^2 + x_3 m^2)} \\
 &= \int_{x_i} \int_{\alpha, \beta_1, \beta_2, \gamma > 0} e^{-\alpha(q_1^2 + x_1 m^2) - \beta_1(q_2^2 + x_2 m^2) - \beta_2(q_2^2 + x_2' m^2) - \gamma[(q_1 + q_2)^2 + x_3 m^2]} \\
 &= \left( \int_q e^{-q^2} \right)^2 \int_{x_i} \int_{\alpha, \beta_1, \beta_2, \gamma > 0} e^{-m^2(x_1 \alpha + x_2 \beta_1 + x_2' \beta_2 + x_3 \gamma)} \left[ \text{Det} \begin{pmatrix} \alpha + \gamma & \gamma \\ \gamma & \beta_1 + \beta_2 + \gamma \end{pmatrix} \right]^{-d/2} \\
 &= \left( \int_q e^{-q^2} \right)^2 \int_{x_i} \int_{\alpha, \beta_1, \beta_2, \gamma > 0} \gamma^{3-d} e^{-m^2(x_1 \alpha + x_2 \beta_1 + x_2' \beta_2 + x_3 \gamma)} \gamma [\alpha + \beta_1 + \beta_2 + \alpha(\beta_1 + \beta_2)]^{-d/2} \\
 &= \left( \int_q e^{-q^2} \right)^2 \Gamma(4-d) m^{-2\epsilon} J, \tag{E5}
 \end{aligned}$$

where we split the divergent integral  $J$  in pieces, which are either finite or where the divergence can be calculated analytically:

$$J = \int_{x_i} \int_0^\infty d\alpha \int_0^\infty d\beta G(\alpha, \beta, x_i) = J_1 + J_2 + J_3, \tag{E6}$$

$$\begin{aligned}
 G(\alpha, \beta, x_i) &= (\alpha + \beta + \alpha\beta)^{-2+\epsilon/2} \int_{-1/2}^{1/2} d\lambda \\
 &\times \left\{ x_1 \alpha + \beta \left[ \frac{x_2 + x_2'}{2} + \lambda(x_2 - x_2') \right] + x_3 \right\}^{-\epsilon}, \tag{E7}
 \end{aligned}$$

$$J_1 = \int_{x_i} \int_0^\infty d\alpha \int_0^1 d\beta G(\alpha, \beta, x_i) = \ln 2 + O(\epsilon), \tag{E8}$$

$$\begin{aligned}
 J_2 &= \int_{x_i} \int_0^\infty d\alpha \int_1^\infty d\beta \left\{ G(\alpha, \beta, x_i) - \frac{1}{(1+\alpha)^{2-\epsilon/2} \beta^{1+\epsilon/2}} \right. \\
 &\times \left. \int_{-1/2}^{1/2} d\lambda \left[ \frac{x_2 + x_2'}{2} + \lambda(x_2 - x_2') \right]^{-\epsilon} \right\} \\
 &= -\ln 2 + O(\epsilon), \tag{E9}
 \end{aligned}$$

$$\begin{aligned}
 J_3 &= \int_0^\infty d\alpha \int_1^\infty d\beta \frac{1}{(1+\alpha)^{2-\epsilon/2} \beta^{1+\epsilon/2}} \int_{x_2, x_2'} \int_{-1/2}^{1/2} d\lambda \\
 &\times \left[ \frac{x_2 + x_2'}{2} + \lambda(x_2 - x_2') \right]^{-\epsilon}. \tag{E10}
 \end{aligned}$$

This gives the final result for the hat diagram,

$$\begin{aligned}
 I_A &= \left( \int_q e^{-q^2} \right)^2 \Gamma(4-d) m^{-2\epsilon} \left( \frac{2}{\epsilon} + 1 + O(\epsilon) \right) \\
 &\times \int_{x_2, x_2'} \int_{-1/2}^{1/2} d\lambda \left[ \frac{x_2 + x_2'}{2} + \lambda(x_2 - x_2') \right]^{-\epsilon} \\
 &= \left( \frac{1}{2\epsilon^2} + \frac{1}{4\epsilon} + O(\epsilon^0) \right) (\epsilon I_1)^2, \tag{E11}
 \end{aligned}$$

where we have used that in the one-loop integral (E4),

$$\begin{aligned}
 &\int_{x, x'} \int_{-1/2}^{1/2} d\lambda \left[ \frac{x + x'}{2} + \lambda(x - x') \right]^{-\epsilon/2} \\
 &= \left( 1 + \frac{1}{2} \alpha \epsilon + O(\epsilon^2) \right), \tag{E12}
 \end{aligned}$$

with  $\alpha$  depending on the regulating function  $g(x)$  and in the two-loop integral (E11):

$$\begin{aligned}
 &\int_{x, x'} \int_{-1/2}^{1/2} d\lambda \left[ \frac{x + x'}{2} + \lambda(x - x') \right]^{-\epsilon} \\
 &= [1 + \alpha \epsilon + O(\epsilon^2)] = \left( 1 + \frac{1}{2} \alpha \epsilon + O(\epsilon^2) \right)^2, \tag{E13}
 \end{aligned}$$

with the same  $\alpha$ .

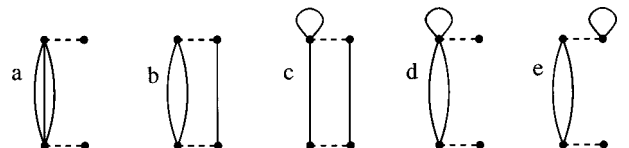


FIG. 15. Diagrams to order  $TR^2$  with excluded vertices.

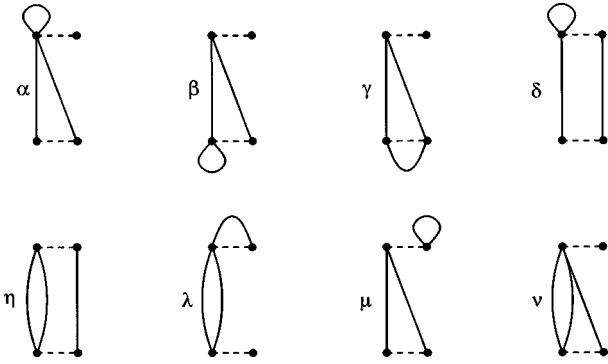


FIG. 16. Diagrams to order  $TR^2$  with nonexcluded vertices.

**APPENDIX F: SUMMARY OF ALL NONAMBIGUOUS DIAGRAMS, FINITE TEMPERATURE**

In this appendix we give all one- and two-loop diagrams including finite  $T$ , evaluated with the unambiguous diagrammatics, which have not been given in the text; see Figs. 15–18. We use the unambiguous vertex  $\sum_{a \neq b} R(u_a - u_b)$ , denote  $R_{ab} = R(u_a - u_b)$ ,  $R'_{ab} = R'(u_a - u_b)$ , etc.

The list of all UV-divergent diagrams up to two loops is given in Fig. 18. We write their contribution to the effective action as

$$\Gamma[u] \Big|_{u_x = u} = -\frac{1}{2T^2} R \tag{F1}$$

$$R = \sum_{ab} R_{ab} + \delta^{(1)}R + \delta^{(2)}R + \dots \tag{F2}$$

The total one-loop contribution is

$$\delta^{(1)}R = \left( \sum_{a \neq b} \frac{1}{2} (R''_{ab})^2 + \sum_{a \neq b, a \neq c} \frac{1}{2} R''_{ab} R''_{ac} \right) I_1 + \left( T \sum_{a \neq b} R''_{ab} \right) I_t. \tag{F3}$$

The total two-loop contribution is

$$\delta^{(2)}R = \delta_A^{(2)}R + \delta_B^{(2)}R + \delta_C^{(2)}R + \delta_T^{(2)}R, \tag{F4}$$

where  $\delta_A^{(2)}R$  is given Eq. (5.13),  $\delta_B^{(2)}R$  is given in Eq. (5.14), and

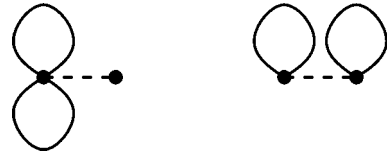


FIG. 17. Diagrams to order  $T^2R$  with excluded vertices.

$$\delta_C^{(2)}R = \left[ 2 \sum_{a \neq b, a \neq c} R'''_{ab} R''_{ab} R''_{ac} - \sum_{a, b, c, 2 \neq 2} R'''_{ab} R''_{ac} R''_{bc} + \sum_{a \neq b, a \neq c, a \neq d} R'''_{ab} R''_{ac} R''_{ad} + \sum_{a \neq b, a \neq c} R'''_{ab} (R''_{ac})^2 \right] I_t I_T, \tag{F5}$$

while the finite- $T$  diagrams are given by

$$\delta_T^{(2)}R = \left( \frac{1}{2} T^2 \sum_{a \neq b} R'''_{ab} \right) I_t^2 + \left( \frac{1}{6} T \sum_{a \neq b, a \neq c} R'''_{ab} R'''_{ac} + \frac{1}{2} T (R'''_{ab})^2 \right) I^4 + \left( T \sum_{a \neq b} R'''_{ab} R''_{ab} + T \sum_{a \neq b, a \neq c} R'''_{ab} R''_{ac} \right) I_1 I_t, \tag{F6}$$

$$I_4 = \int_{q_1, q_2} \frac{1}{q_1^2 q_2^2 (q_1 + q_2)^2}. \tag{F7}$$

For an *analytic*  $R$  one substitutes  $R_{ab} \rightarrow R_{ab}(1 - \delta_{ab})$  in the above formula and selects the two-replica terms:

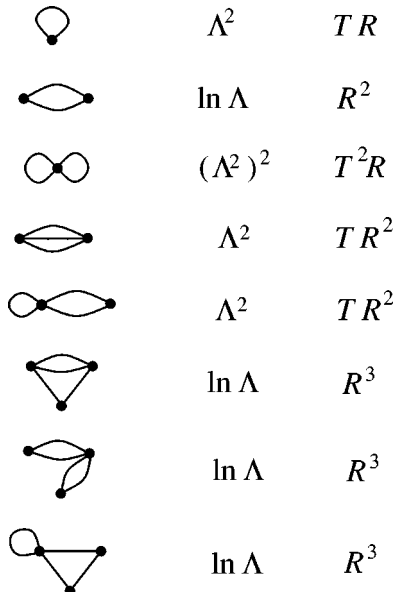


FIG. 18. Divergent unsplit diagrams to one and two loops.



$$\delta^{(1)}R = TR''I_t + \left[ \frac{1}{2}(R'')^2 - R''(0)R'' \right] I_1, \quad (\text{F8})$$

$$\delta_B^{(2)}R = \frac{1}{2}R''''[R'' - R''(0)]^2 I_1^2, \quad (\text{F9})$$

$$\delta_A^{(2)}R = [R'' - R''(0)](R''')^2 I_A, \quad (\text{F10})$$

$$\delta_C^{(2)}R = 0, \quad (\text{F11})$$

$$\delta_T^{(2)}R = \frac{1}{2}T^2 R'''' I_t^2 + \frac{1}{2}T(R''')^2 I_4 + \{TR''''[R'' - R''(0)] - TR''R''''(0)\} I_1 I_t. \quad (\text{F12})$$

Let us show that if one renounces to the projection onto two-replica terms, one can still obtain some formal renormalizability property, but at the cost of introducing an unmanageable series of terms with more than two replicas.

We show how to subtract divergences by adding counterterms of similar form. Let us discuss only  $T=0$ . To cancel the one-loop divergences we introduce the counterterm

$$\delta_c^{(1)}R + \left( \sum_{a \neq b} \frac{1}{2}(R''_{ab})^2 + \sum_{a \neq b, a \neq c} \frac{1}{2}R''_{ab}R''_{ac} \right) I_1^{\text{div}}. \quad (\text{F13})$$

The repeated counterterm is

$$\delta^{(1,1)}R = \left[ R''''_{ab}(R''_{ab})^2 + R''_{ab}(R''''_{ab})^2 + R''''_{ab}R''_{ab}R''_{ac} + R''_{ab}(R''''_{ac})^2 + R''''_{ab}R''_{ab}R''_{ac} + \frac{1}{2}R''''_{ab}R''_{ac}R''_{ad} + \frac{1}{2}R''''_{ab}R''_{ac}R''_{bd} + R''_{ab}R''''_{ab}R''_{ac} + \frac{1}{2}R''_{ab}R''''_{ac}R''_{ad} + \frac{1}{2}R''_{ab}R''''_{ac}R''_{ac} - \frac{1}{2}R''_{ab}R''''_{ac}R''_{bc} \right] I_1 I_1^{\text{div}}, \quad (\text{F14})$$

omitting all (excluded) sums. One checks that

$$2(\delta_B^{(2)}R + \delta_A^{(2)}R) \sim \delta^{(1,1)}R + O\left(\frac{1}{\epsilon}\right) \quad (\text{F15})$$

using that  $2I_A = I_1^2 + O(1/\epsilon)$ . Thus there is some renormalizability property for  $R$ . One can thus define formally a  $\beta$  function

$$-m \partial_m R = \epsilon R + \left[ \sum_{a \neq b} \frac{1}{2}(R''_{ab})^2 + \sum_{a \neq b, a \neq c} \frac{1}{2}R''_{ab}R''_{ac} \right] (\epsilon I_1) + \delta_A^{(2)}R \frac{\epsilon(I_A - \frac{1}{2}I_1^2)}{I_A}. \quad (\text{F16})$$

$R$ , however, includes a series of terms each with excluded sums over  $p$  replica. Thus to be consistent one should in principle include them from the start and pursue the method. It is not clear that it can be closed in any way.

- 
- [1] K. Johansson, *Commun. Math. Phys.* **209**, 437 (2000).  
[2] K. Johansson, e-print math.PR/9910146.  
[3] J. Baik, P. Deift, and K. Johansson, *J. Am. Math. Soc.* **12**, 1119 (1999).  
[4] M. Prähofer and H. Spohn, *Phys. Rev. Lett.* **84**, 4882 (2000).  
[5] M. Prähofer and H. Spohn, *Physica A* **279**, 342 (2000).  
[6] M. Kardar, G. Parisi, and Y.-C. Zhang, *Phys. Rev. Lett.* **56**, 889 (1986).  
[7] E. Frey and U. C. Täuber, *Phys. Rev. E* **50**, 1024 (1994).  
[8] M. Lässig, *Nucl. Phys. B* **448**, 559 (1995).  
[9] E. Frey, U. C. Täuber, and T. Hwa, *Phys. Rev. E* **53**, 4424 (1996).  
[10] K. J. Wiese, *Phys. Rev. E* **56**, 5013 (1997).  
[11] K. J. Wiese, *J. Stat. Phys.* **93**, 143 (1998).  
[12] E. Marinari, A. Pagnani, and G. Parisi, *J. Phys. A* **33**, 8181 (2000).  
[13] M. Prähofer and H. Spohn, *J. Stat. Phys.* **88**, 999 (1997).  
[14] J. Krug, *Adv. Phys.* **46**, 139 (1997).  
[15] M. Mezard, *J. Phys. IV* **8**, 27 (1997).  
[16] E. Medina, T. Hwa, M. Kardar, and Y. C. Zhang, *Phys. Rev. A* **39**, 3053 (1989).  
[17] T. Hwa and D. S. Fisher, *Phys. Rev. B* **49**, 3136 (1994).  
[18] R. Bundschuh and T. Hwa, *Discrete Appl. Math.* **104**, 113 (2000).  
[19] R. Bundschuh and T. Hwa, *Phys. Rev. Lett.* **83**, 1479 (1999).  
[20] T. Hwa and M. Lässig, *RECOMB 98*, pp. 109-116, 1998, e-print cond-mat/9712081.  
[21] T. Nattermann, in *Spin Glasses and Random Fields*, edited by A. P. Young (World Scientific, Singapore, 1997).  
[22] S. Lemerle, J. Ferré, C. Chappert, V. Mathet, T. Giamarchi, and P. Le Doussal, *Phys. Rev. Lett.* **80**, 849 (1998).  
[23] G. Gruner, *Rev. Mod. Phys.* **60**, 1129 (1988).  
[24] G. Blatter, M. V. Feigel'man, V. B. Geshkenbein, A. I. Larkin, and V. M. Vinokur, *Rev. Mod. Phys.* **66**, 1125 (1994).  
[25] T. Giamarchi and P. Le Doussal, in *Spin Glasses and Random Fields*, edited by A. P. Young (World Scientific, Singapore, 1997).  
[26] T. Giamarchi and P. Le Doussal, *Phys. Rev. B* **52**, 1242 (1995).  
[27] T. Giamarchi and P. Le Doussal, *Phys. Rev. Lett.* **72**, 1530 (1994).  
[28] T. Nattermann and S. Scheidl, *Adv. Phys.* **49**, 607 (2000).  
[29] A. Prevost, E. Rolley, and C. Guthmann, *Phys. Rev. B* **65**, 064517/1 (2002).  
[30] A. Prevost, Ph.D. thesis, Orsay, 1999.  
[31] D. Ertas and M. Kardar, *Phys. Rev. E* **49**, 2532 (1994).  
[32] M. Kardar, in *Fluctuating Geometries in Statistical Mechanics and Field Theory*, edited by F. David, P. Ginsparg, and J. Zinn-Justin, Volume LXII of Les Houches, école d'été de

- physique théorique 1994 (Elsevier Science, Amsterdam, 1996).
- [33] M. Kardar, Nucl. Phys. B **290**, 582 (1987).
- [34] E. Brunet and B. Derrida, Physica A **279**, 398 (2000).
- [35] E. Brunet and B. Derrida, Phys. Rev. E **61**, 6789 (2000).
- [36] M. Mézard and G. Parisi, J. Phys. I **1**, 809 (1991).
- [37] G. Parisi, e-print cond-mat/0205387.
- [38] M. Mézard, G. Parisi, and M. A. Virasoro, *Spin Glass Theory and Beyond* (World Scientific, Singapore, 1987).
- [39] M. Mezard, J. Phys. (France) **51**, 1831 (1990).
- [40] M. Weigt and R. Monasson, Europhys. Lett. **36**, 209 (1996).
- [41] M. Sales and H. Yoshino, e-print cond-mat/0203371.
- [42] B. Derrida and H. Spohn, J. Stat. Phys. **51**, 817 (1988).
- [43] J. Cook and B. Derrida, J. Stat. Phys. **57**, 89 (1989).
- [44] J. Cook and B. Derrida, Europhys. Lett. **10**, 195 (1989).
- [45] D. S. Fisher, Phys. Rev. B **31**, 7233 (1985).
- [46] D. S. Fisher, Phys. Rev. Lett. **56**, 1964 (1986).
- [47] L. Balents and D. S. Fisher, Phys. Rev. B **48**, 5949 (1993).
- [48] A. I. Larkin and Y. N. Ovchinnikov, J. Low Temp. Phys. **34**, 409 (1979).
- [49] K. B. Efetov and A. I. Larkin, Sov. Phys. JETP **45**, 1236 (1977).
- [50] A. Aharony, Y. Imry, and S. K. Ma, Phys. Rev. Lett. **37**, 1364 (1976).
- [51] G. Grinstein, Phys. Rev. Lett. **37**, 944 (1976).
- [52] G. Parisi and N. Sourlas, Phys. Rev. Lett. **43**, 744 (1979).
- [53] J. L. Cardy, Phys. Lett. **125B**, 470 (1983).
- [54] L. Balents, J. P. Bouchaud, and M. Mézard, J. Phys. I **6**, 1007 (1996).
- [55] T. Nattermann, S. Stepanow, L. H. Tang, and H. Leschhorn, J. Phys. II **2**, 1483 (1992).
- [56] H. Leschhorn, T. Nattermann, S. Stepanow, and L. H. Tang, Ann. Phys. (Leipzig) **6**, 1 (1997).
- [57] O. Narayan and D. S. Fisher, Phys. Rev. B **48**, 7030 (1993).
- [58] P. Chauve, T. Giamarchi, and P. Le Doussal, Europhys. Lett. **44**, 110 (1998).
- [59] P. Chauve, T. Giamarchi, and P. Le Doussal, Phys. Rev. B **62**, 6241 (2000).
- [60] H. Bucheli, O. S. Wagner, V. B. Geshkenbein, A. I. Larkin, and G. Blatter, Phys. Rev. B **57**, 7642 (1998).
- [61] O. S. Wagner, V. B. Geshkenbein, A. I. Larkin, and G. Blatter, Phys. Rev. B **59**, 11 551 (1999).
- [62] E. Brezin and C. De Dominicis, Europhys. Lett. **44**, 13 (1998).
- [63] D. E. Feldman, Phys. Rev. B **61**, 382 (2000).
- [64] D. E. Feldman, Phys. Rev. Lett. **88**, 177202 (2002).
- [65] P. Le Doussal and K. J. Wiese (unpublished).
- [66] D. A. Gorokhov, D. S. Fisher, and G. Blatter, Phys. Rev. B **66**, 214203 (2002).
- [67] L. Balents, Europhys. Lett. **24**, 489 (1993).
- [68] P. Chauve, P. Le Doussal, and K. J. Wiese, Phys. Rev. Lett. **86**, 1785 (2001).
- [69] P. Le Doussal, K. J. Wiese, and P. Chauve, Phys. Rev. B **66**, 174201 (2002).
- [70] P. Le Doussal and K. J. Wiese, Phys. Rev. E **67**, 016121 (2003).
- [71] P. Le Doussal and C. Monthus, Physica A **317**, 140 (2003).
- [72] P. Chauve and P. Le Doussal, Phys. Rev. E **64**, 051102 (2001).
- [73] Stefan Scheidl (private communication).
- [74] P. Le Doussal and K. J. Wiese, Phys. Rev. Lett. **89**, 125702 (2002); Phys. Rev. B **68**, 017402 (2003).
- [75] K. J. Wiese and P. Le Doussal (unpublished).
- [76] L. Balents and P. Le Doussal, Europhys. Lett. (to be published), e-print cond-mat/0205358.
- [77] L. Balents and P. Le Doussal (unpublished).
- [78] K. J. Wiese, Acta Phys. Slov. **52**, 341 (2002).
- [79] K. J. Wiese, Ann. I.H.P. Phys. Theor. **4**, 473 (2003).
- [80] J. Zinn-Justin, *Quantum Field Theory and Critical Phenomena* (Oxford University Press, Oxford, 1989).
- [81] C. Itzykson and J.-B. Zuber, *Quantum Field Theory* (MacGraw-Hill, Singapore, 1985).
- [82] U. Schulz, J. Villain, E. Brezin, and H. Orland, J. Stat. Phys. **51**, 1 (1988).
- [83] See, e.g., Appendix IV in [101].
- [84] P. Le Doussal and K. J. Wiese (unpublished).
- [85] A. A. Middleton, Phys. Rev. E **52**, R3337 (1995).
- [86] M. Kardar, D. A. Huse, C. L. Henley, and D. S. Fisher, Phys. Rev. Lett. **55**, 2923 (1985).
- [87] D. McNamara, A. A. Middleton, and Zeng Chen, Phys. Rev. B **60**, 10 062 (1999).
- [88] Noh Dong Jae and H. Rieger, Phys. Rev. Lett. **87**, 176102 (2001).
- [89] A. Rosso, W. Krauth, P. Le Doussal, J. Vannimenus, and K. J. Wiese, Phys. Rev. E **68**, 036128 (2003).
- [90] P. Le Doussal and K. J. Wiese, Phys. Rev. E **68**, 046118 (2003).
- [91] Stefan Scheidl and Yusuf Dincer, e-print cond-mat/0006048.
- [92] P. Chauve and P. Le Doussal (unpublished).
- [93] N. N. Bogoliubov and O. S. Parasiuk, Acta Math. **97**, 227 (1957).
- [94] K. Hepp, Commun. Math. Phys. **2**, 301 (1966).
- [95] W. Zimmermann, Commun. Math. Phys. **15**, 208 (1969).
- [96] M. C. Bergere and Y.-M. P. Lam, J. Math. Phys. **17**, 1546 (1976).
- [97] F. David, B. Duplantier, and E. Guitter, Nucl. Phys. B **394**, 555 (1993).
- [98] F. David, B. Duplantier, and E. Guitter, e-print cond-mat/9702136.
- [99] K. J. Wiese, *Polymerized Membranes, a Review*, Vol. 19 of *Phase Transitions and Critical Phenomena* (Academic, London, 1999).
- [100] J. C. Collins, *Renormalization* (Cambridge University Press, Cambridge, England, 1984).
- [101] D. Carpentier and P. Le Doussal, Phys. Rev. B **55**, 12 128 (1997).
- [102] D. Carpentier and P. Le Doussal, Phys. Rev. E **63**, 026110 (2001).
- [103] G. Schehr and P. Le Doussal, Phys. Rev. E **68**, 046101 (2003).